Universidade de Aveiro
2020

RUI MIGUEL FARINHA BENTO

ADSORPTION OF L-ASPARAGINASE ON SILICA-BASED SUPPORTED IONIC LIQUIDS

ADSORÇÃO DA L-ASPARAGINASE EM LÍQUIDOS IÓNICOS SUPORTADOS EM SÍLICA

2020

Universidade de Aveiro
2020

RUI MIGUEL FARINHA BENTO

ADSORPTION OF L-ASPARAGINASE ON SILICA-BASED SUPPORTED IONIC LIQUIDS

ADSORÇÃO DA L-ASPARAGINASE EM LÍQUIDOS IÓNICOS SUPORTADOS EM SÍLICA

Dissertação apresentada à Universidade de Aveiro para cumprimento dos requisitos necessários à obtenção do grau de Mestre em Biotecnologia realizada sob a orientação científica da Doutora Ana Paula Mora Tavares, Investigadora Auxiliar do Departamento de Química da Universidade de Aveiro, e coorientação da Doutora Márcia Carvalho Neves Investigadora Auxiliar do Departamento de Química da Universidade de Aveiro.

This work was financially supported by the NanoPurAsp R&D Project (POCI-01-0145-FEDER-031268, funded by FEDER, through COMPETE2020 - Programa Operacional Competitividade e Internacionalização (POCI), and by national funds (OE), through FCT/MCTES."

FCT Fundação para a Ciência e a Tecnologia
COMPETE 2020
PORTUGAL 2020
UNIÃO EUROPEIA
Fundo Europeu de Desenvolvimento Regional

o júri

presidente

Prof. Doutor João Filipe Colardelle da Luz Mano
Professor Catedrático, Departamento de Química, Universidade de Aveiro

Dra. Márcia Carvalho Neves
Investigadora Auxiliar, Departamento de Química, Universidade de Aveiro

Dra. Cláudia Gomes da Silva
Professora Auxiliar, Departamento de Engenharia Química, Faculdade de Engenharia da Universidade do Porto

agradecimentos

Em primeiro lugar gostaria de agradecer às minhas orientadoras Doutora Ana Paula e Doutora Márcia Neves pela oportunidade de poder trabalhar neste projeto, pela sua orientação e simpatia. Um enorme e especial obrigado por todo o apoio, horas despendidas e compreensão. Um obrigado também ao João Antunes, com quem tive o privilégio de trabalhar diariamente no laboratório, e à Mafalda, que mostrou sempre uma grande disponibilidade para ensinar e apoiar.

Um obrigado ao grupo de investigação, com quem tive oportunidade de aprender imenso e crescer tanto como estudante/investigador como pessoa. E como um laboratório é feito de pessoas, tive o prazer de partilhar de perto este ano de dissertação com pessoas espetaculares, nomeadamente, o Daniel, o Guilherme, o Alexandre e a Maria João, com quem sempre contei para qualquer situação, aquele apoio extra. Agradeço à Rita pela sua disponibilidade em ajudar e ensinar, sempre com um sorriso.

E um obrigado aos meus amigos, muitos deles de infância, Miguel, Carlitos, Nuno, Pedro, Alexandre, Rodrigo, Jorge, Inês, Rita e Mariana, que estiveram presentes em muitas etapas da minha vida não exceptuando esta, e que tenho o gosto de considerar amigos para a vida.

Por último, mas muito, muito importante, um obrigado gigante à minha família pelo apoio incondicional. Agradeço à minha mãe e ao meu pai, ao meu irmão, um chato, e à minha avozinha. Obrigado por estarem sempre por perto (obrigado por tudo). Vocês são especiais.

palavras-chave

L-asparaginase, líquidos iónicos suportados em sílica, imobilização de enzimas, adsorção.

resumo

A L-Asparaginase (L-ASNase) é uma enzima versátil que possui uma ampla gama de aplicações importantes, principalmente na indústria farmacêutica, onde é utilizada como um biofármaco anti leucémico, o que exige um elevado grau de pureza. Atualmente, a purificação da L-ASNase é convencionalmente alcançada utilizando cromatografia de troca iónica, uma técnica muito dispendiosa, o que encarece o produto final e torna inviável a sua utilização em grande escala. A procura de novos métodos para a sua purificação com um custo económico baixo, menos prejudicial ao ambiente e possíveis de aplicar a uma grande escala, é uma constante.

Esta dissertação tem como principal objetivo desenvolver uma plataforma alternativa de adsorção da L-ASNase utilizando líquidos iónicos suportados em sílica, com vista à purificação da enzima, e consequentemente diminuir o seu preço final. Este trabalho consistiu na síntese e caracterização de líquidos iónicos suportados em de sílica, nomeadamente, [Si][N_{3114}]Cl, [Si][N_{3116}]Cl, [Si][N_{3118}]Cl, [Si][N_{3222}]Cl, [Si][N_{3444}]Cl, [Si][N_{3666}]Cl e [Si][N_{3888}]Cl, e posterior aplicação destes materiais na adsorção da L-ASNase comercial. De forma a otimizar o procedimento experimental da imobilização da enzima foram realizados estudos sobre o efeito da concentração de L-ASNase, do pH e do tempo de contacto entre a enzima e os materiais. Os modelos de isotérmicas de equilíbrio de adsorção de Freundlich e de Langmuir foram aplicados aos dados experimentais para avaliar o tipo de adsorção da L-ASNase nos materiais. Além disto, estudou-se a estabilidade térmica da enzima e a sua reutilização. Por fim, foram realizados testes de adsorção da L-ASNase de um extrato celular de *Bacillus subtilis*, analisando a pureza do extrato final por atividade específica, SDS-PAGE e HPLC.

A caracterização dos líquidos iónicos suportados demonstrou que a sua síntese ocorreu com sucesso. No estudo de adsorção da enzima o modelo isotérmico que apresentou um melhor ajuste aos dados experimentais foi o modelo de Langmuir. Concluiu-se que para a adsorção da L-ASNase o material que apresenta melhores resultados é o [Si][N_{3222}]Cl, atingindo um $q_{máx}$ de 2.41 $U.mg^{-1}$. Para todos os materiais foi possível observar um aumento da atividade da enzima até cerca de 260% em comparação com a sílica ativada (controlo), e uma elevada reciclabilidade. Utilizando a L-ASNase do extrato celular, foi registado um aumento da atividade específica da enzima de 33% após a sua imobilização no [Si][N_{3222}]Cl. Este aumento da pureza após a adsorção do extrato foi confirmado pelos resultados do SDS-PAGE.

Este trabalho apresenta uma técnica promissora e simples de imobilização da L-ASNase e, consequentemente, de posterior purificação da mesma.

keywords

L-asparaginase, silica-based supported ionic liquids, enzyme immobilization, adsorption.

abstract

L-Asparaginase (L-ASNase) is a versatile enzyme that has important applications, mainly in the pharmaceutical industry, where it is used as an anti-leukemic biopharmaceutical, which requires a high degree of purity. Currently, this enzyme is conventionally purified through ion exchange chromatography, a very expensive technique, which makes the final product more expensive and makes its use on a large scale unviable. The investigation of new low-cost purification methods, less harmful to the environment and reliable when adapted on a large scale, is a constant.

The main objective of this dissertation is to develop an alternative L-ASNase adsorption platform using silica based supported ionic liquids, with a view to purifying the enzyme, and consequently reduce its final price. This work consisted of the synthesis and characterization of silica based supported ionic liquids, namely, [Si][N_{3114}]Cl, [Si][N_{3116}]Cl, [Si][N_{3118}]Cl, [Si][N_{3222}]Cl, [Si][N_{3444}]Cl, [Si][N_{3666}]Cl e [Si][N_{3888}]Cl, and subsequent application of these materials in the adsorption of commercial L-ASNase. In order to optimize the experimental procedure of the enzyme immobilization, studies on the effect of L-ASNase concentration, pH and contact time between the enzyme and the materials were carried out. The Freundlich and Langmuir models were applied to the experimental data to evaluate the type of adsorption of L-ASNase at the materials. In addition, the thermal stability of the enzyme and its reuse were studied. Finally, L-ASNase adsorption tests of Bacillus subtilis from a cell extract were performed, analysing the purity of the final extract by specific activity, SDS-PAGE and HPLC.

The characterization of the supported ionic liquids denoted a successful synthesis. In the enzyme adsorption study the isotherm model that presented a better fit to the experimental data was the Langmuir model. It was concluded that for the adsorption of L-ASNase the material that presents the best results is [Si] [N3222] Cl, reaching a $q_{máx}$ of 2.41 $U.mg^{-1}$. For all materials it was possible to observe an increase in enzyme activity of up to 260% compared to activated silica (control), and a high recyclability. Using the L-ASNase from the cell extract, a 33% increase in the specific activity of the enzyme was recorded after its immobilization in [Si][N_{3222}] Cl. This increase in purity after the adsorption of the extract was confirmed by the results of the SDS-PAGE. This work presents a promising and simple technique for immobilizing L-ASNase and, consequently, for its subsequent purification.

.

Contents

List of Tables

List of Figures

List of Abbreviations

ALL – Acute lymphoblastic leukemia

L-ASNase – L-asparaginase

L-ASN – L-asparagine

L-Asp – L-acid aspartic

ASNS – Asparagine synthetase

SmF – Submerged fermentation

FDA – Food and drug administration

PEG - Polyethylene glycol

MWCNT - Multi-walled carbon nanotubes

IL – Ionic liquid

SILP – Supported ionic liquid phase

SIL – Supported Ionic liquid-like phase

ATPS – Aqueous two-phase system

DEAE – Diethylaminoethyl

CNT - carbon nanotube

LAD - L-arabinitol 4-dehydrogenase

PZC – Point of zero charge

ATR-FTIR – Attenuated total reflectance – Fourier-transform infrared spectroscopy

IY – Immobilization yield

HPLC-DAD – High performance liquid chromatography with diode-array detector

BA – Bounding amount

S_{BET} – Brunauer-Emmett-Teller specific surface area

SDS-PAGE – Sodium dodecyl sulfate polyacrylamide gel electrophoresis

IP – Isoelectric point

1. Introduction

1.1 L-Asparaginase (L-ASNase)

L-asparaginase (L-ASNase) (EC 3.5.1.1), also called L-asparagine amidohydrolase, is an amidohydrolase, which catalyses the hydrolysis of L-asparagine (L-ASN) into L-aspartic acid (L-Asp) and ammonia.[1] The mechanism of the hydrolysis process of L-ASN by L-ASNase occurs in two steps by an intermediate: beta-acyl-enzyme (**Figure 1**). In the first step, the nucleophilic (Nuc) residue of the enzyme is activated by a powerful base, NH_2, which attacks the amide carbon atom of L-asparagine generating the intermediate beta-acyl-enzyme. Then, it acts on the ester carbon (R-C=O) made by a nucleophile activated by a water molecule giving the final product, L-Asp, with ammonia being released.[2] Other hydrolysis reactions catalysed by this enzyme are hydrolysis of L-glutamine and β-aspartyl peptide amide, however, the reaction yield is very low.[3]

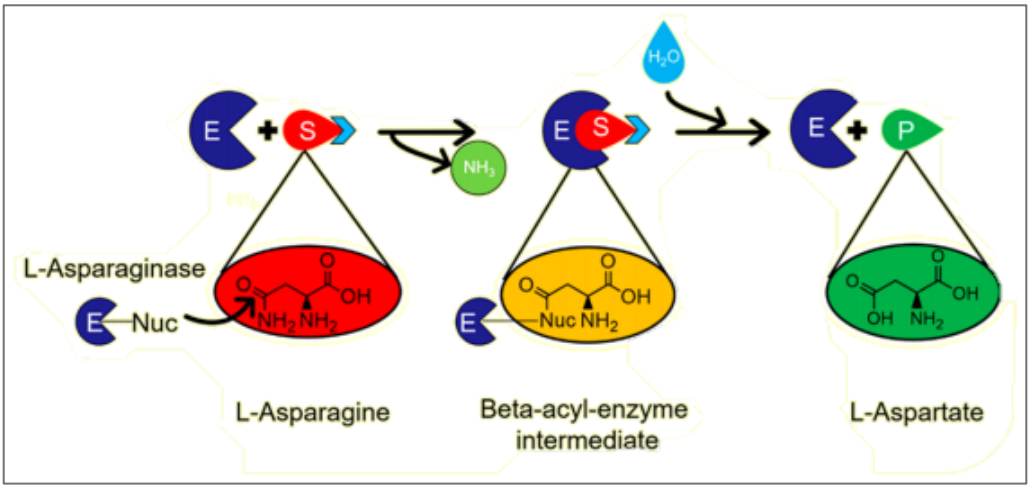

Figure 1: Mechanism of action of L-ASNase: E – enzyme; S – substrate; Nuc – nucleophilic residue (adapted from Ulu et al.)[4].

L-ASNase activity was first detected by Lang et al.[5] in beef tissues in 1904. Due to the type of reaction that L-ASNase performs, the enzyme has anticancer properties. This property was first reported by Kidd et al.[6] in 1953, who observed the antitumor properties of guinea pig serum. Later, in 1956 Neuman et al.[7] demonstrated the metabolic differences between normal and malignant cells, in vitro, in the presence and absence of the amino acid, asparagine. Based on insights from these studies, Broome et al.[8] linked the antitumor activity of guinea pig serum to asparagine depletion by the enzyme. L-ASNase was approved for

medical use in the United States in 1978[9] and, since then it is on the World Health Organization's List of Essential Medicines, the most effective and safe medicines needed in a health system.[10]

The bacterial-type L-ASNases are subdivided based on their location in the cell and on the activity into L-ASN and L-glutamine.[11] Both types of L-ASNase can be produced from the same microorganism, such as *Escherichia coli*. L-ASNase from *E. coli* produces two isoforms of enzyme, L-ASNase I (EC1), found in the cytoplasm and L-ASNase II (EC2), with periplasmic origin.[12] Both forms are characterized by enzymatic activity for both L-ASN and L-glutamine. EC1 has relatively low affinity to L-ASN and high specific activity towards L-glutamine, and EC2 displays higher specific action against L-ASN but a lower extent conversion of glutamine into glutamic acid.[13,14] EC2 precisely shows antitumor activity and is utilized as chemotherapeutics in Acute Lymphoblastic Leukemia (LAA).[15] This activity is related with the strains or culture conditions of microorganisms.[16] With the genome sequencing of *Bacillus subtilis*, it became possible to establish that the ansZ gene encoded a L-ASNase which showed 59% identity to the L-ASNase I from *Erwinia chrysanthemi* and 53% identity to the EC2.[17] Besides this, *B. subtilis* has another gene (ansA gene) that encodes type I L-ASNase.[18] Some reports describe EC1 as a constitutive enzyme and EC2 as secreted only as a response to exposure to low concentrations of nitrogen.[19] These findings provided a practical basis for the production of enzyme in large quantities for pre-clinical and clinical studies.[20]

1.1.1 Structure of L-ASNase

At the molecular level, L-ASNase usually exists as a tetramer but hexameric, dimeric, and monomeric forms are also found when isolated from different sources.[21] Most of the bacterial L-ASNases exhibit similar tertiary and quaternary structures and also have common biochemical properties.[22] The enzyme is active as a homotetramer. Each monomer consists of about 330 amino acid residues arranged to form a large N-terminal domain and a smaller C-terminal domain, that are connected by a flexible linker of approximately 20 residues.[11] The active site of the enzyme, located between the C- and N-terminal domains of two adjacent monomers, is composed by a rigid part and a flexible one; while the residues responsible for ligand binding form the rigid part of the active site, the flexible part of the active site regulates access to the binding pocket and provides the catalytic nucleophile Thr15, which is highly conserved for all L-ASNases.[23,24]

Molecular structures of L-ASNase from *E. coli* and *Erwinia sp.* are deeply investigated and their structural information is easily available.[24,25] The molecular native EC2 possess a molecular weight of 138-141kDa and contains four identical subunits with one active center each, as shown in **Figure 2**.[26] The molecular weight of the L-ASNase was found to be varied according to the source of enzyme.[24]

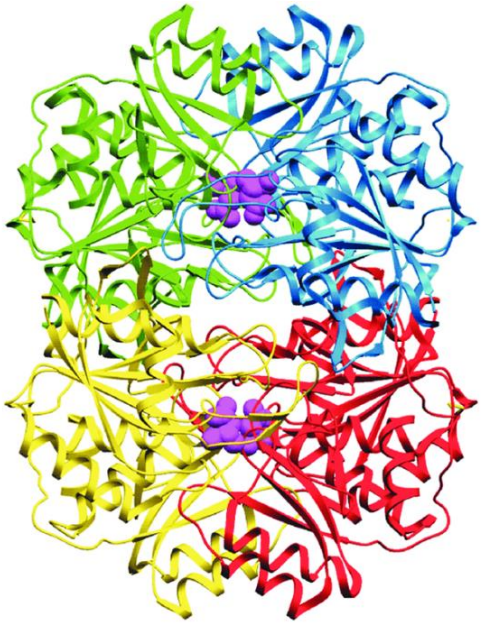

Figure 2: The *Escherichia coli* L-ASNase type II homotetramer. The active sites are represented by the violet balls.[27]

1.1.2 Production process of L-ASNase

A robust bioprocess is central for guaranteeing that the target quality profile of the final product meets specifications, which represents one of the biggest obstacles for the development of biopharmaceuticals, since small alterations in the process operating parameters, cell line, production methods and purification steps can affect critical quality attributes.[1] L-ASNase production is divided into upstream and downstream processing.[3]

Upstream process for industrial L-ASNase production presents some challenges, such as the search for new microorganisms able to produce it with less adverse effects.[3] Although the production of this enzyme is observed in animals and plants, the microorganisms are considered mainly source for L-ASNase synthesis.[28,29] Its production is mainly proceeded by submerged fermentation (SmF).[28] Experimental evidence has demonstrated that this production is greatly influenced by various factors such as type and concentration of carbon and nitrogen sources, pH, temperature, fermentation time, aeration and mainly the microbial agent.[28]

Thus, despite this enzyme can be isolated from several natural sources, the *E. coli* and *E. chrysanthemi* microorganisms have been more extensively studied because of their antineoplastic activity, substrate specificity and enzymatic properties, and are currently available for medical use.[30–32] Also, most of L-ASNases has low stability and catalytic activity, presenting only active in a narrow pH range.[33] The incidence of hypersensitivity is variable depending on three different formulations of L-ASNase used in clinical practice, with rates ranging from 20 to 30% in patients treated with native L-ASNase from *E. coli*.[31] Hypersensitivity reactions usually require the interruption of the treatment with *E. coli* L-ASNase and the substitution with the preparation from *E. chrysanthemi*.[31]

Therefore, the discovery of new producing microorganisms is of extreme importance for manufacturing L-ASNase with higher biological activity and less side effects. In recent years, different studies were developed aiming to find this enzyme with improved characteristics compared to L-ASNase from *E. coli*, with economically viable production as well as causing minimal collateral effects.[3] Searching from different L-ASN sources, specifically eukaryotic microorganisms, can lead to enzymes with less adverse effects and different features, which are advantageous for its application.[3] For instance, eukaryotic fungi have been investigated as L-ASNase source.[34] Fungal L-ASNase has acquired importance based on the fact that it is produced extracellularly, and it is a very easy to purify extracellular

enzyme.[21] Currently, fungal recombinant L-ASNase from *Aspergillus oryzae* and *Aspergillus niger* has already been used in food industry for reduction of acrylamide formation in some foods.[35]

Downstream processes present a large number of potentially critical process parameters that show interactions across unit operations and have to be investigated before scale-up.[1] Since 60–80% of the total production costs of biopharmaceuticals is usually associated with downstream processing, it has become really important the search for new efficient and cost-effective alternative techniques for the recovery and purification of drugs, with less number of downstream unit operations.[36] However, there are problems associated with the classical approach of purification like low yield and purity, difficulty in scale up and long processing hours, leading to a consequent increase of the process costs.[36] Thus, for industrial purposes, it would be important to develop novel and more efficient *in situ* integrated downstream processes that are inexpensive, rapid, high-yield, able to be scale-up, and above all, environmentally friendly.[37]

Most commercial applications of enzymes do not require highly purified enzyme preparations; L-ASNase as a biopharmaceutical requires high purity since this condition generates less toxic and allergic response in the patient.[38] Downstream processing includes all steps required for the enzyme purification, resulting in a purified protein product.[39] As a general guideline, the purification process can be described as a three-stage strategy that includes (i) capture, (ii) intermediate purification and (iii) polishing (**Figure 3**).[36,40]

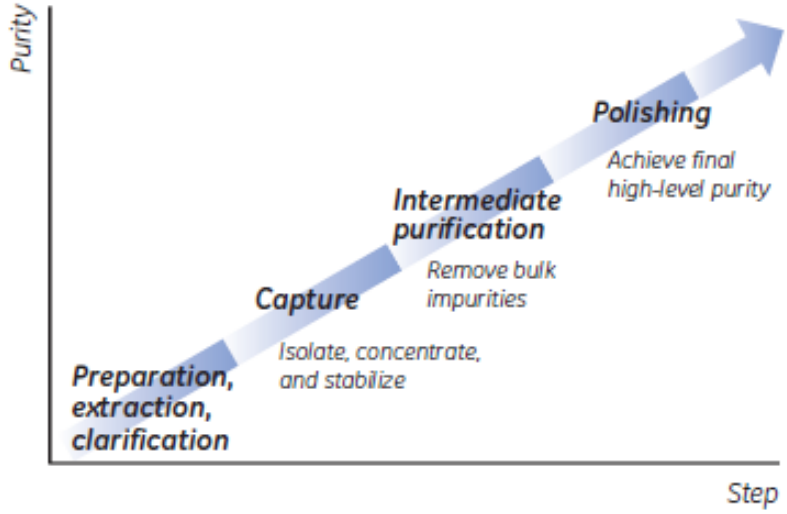

Figure 3: The stages purification strategy: Capture, Intermediate Purification, and Polishing (CIPP).[40]

Regarding injectable biopharmaceuticals, such as L-ASNase, the manufacturing process must be extremely thoughtful, since the presence of contaminants, may potentially lead to detrimental clinical consequences.[41] L-ASNase purification is complex due to the huge number of biomolecules released from intracellular media. Therefore, extracellular L-ASNase is considered more advantageous than the intracellular type for the downstream process, since the enzyme can accumulate in the culture broth under normal conditions, simplifying the extraction process.[1]

The integration of downstream unit operations is widely used for L-ASNase purification, through low resolution purification steps i.e., fractional precipitation[2], centrifugation[42] and membrane-based purification (dialysis) and high-resolution purification steps, namely, chromatographic processes.[43] However, chromatography is still widely preferred technology due to its scalability, robustness, selectivity, high clearance of impurities and easy validation compared to other purification processes.[1] Chromatographic processes are well established in the biotechnology and pharmaceutical industries. These techniques present their own characteristics such as hydrophobic interaction, ion exchange and gel filtration,[36] which is based on biomolecules hydrophobicity, charge and size, respectively.[1] Also, chromatographic steps are generally used to achieve a maximum purification and to polish the target compound.[36] In spite of that, gel filtration and ion-exchange chromatography are the most employed purification steps.[28]

The major requisition of L-ASNase is as an antileukemic drug that demands a very high level of purity for this enzyme.[21] Although only L-ASNases from *E. coli* and *E. chrysanthemi* are currently used for the treatment of ALL, isolation, and characterization of L-ASNases from other organisms have been extensively studied. As a result of this large number and variety of alternative L-ASNase proteoforms, a several methods have been reported and explored for purification of this enzyme produced from various sources.[21] These enzymes possess different biochemical characteristics, which, in turn greatly influence how they are purified.[44]

Purification involves multiple steps depending on the intracellular or the extracellular nature of the enzyme.[45] Most of the microbial asparaginases reported so far are intracellular in nature except for the few, which are extracellular.[21] For instance, purification methods used to obtain pure recombinant L-ASNase secreted into the extracellular medium will not be the same as those used to purify the enzyme produced intracellularly, there is no

standardised method for the purification of L-ASNase.[44] In either case, the proteins are often precipitated from the crude extract using techniques like ammonium sulphate (pre-purification step). The precipitated protein is then dialyzed and further subjected to column chromatography.[45] The choice of the column chromatography depends on several protein attributes, such as the isoelectric point (pI), hydrophobicity and molecular size of the L-ASNase.[44] Multiple steps of chromatography may be involved utilizing two or more types of column methods.[45] Its commercial manufacture conventionally uses downstream processes such as unit chemical lysis, protein precipitation, centrifugation, filtration, fluidised bed chromatography, and other chromatographic techniques (e.g. ion-exchange, gel filtration and immobilized metal affinity chromatography - IMAC). Recently, new strategies were developed regarding the purification of the enzyme, namely those based in aqueous two-phase system (ATPS) and aqueous micellar two-phase systems (AMTPS).[37,43,46]

The purification of native L-ASNases tends to be more laborious than that of their recombinant counterparts. The first L-ASNases obtained from *E. coli* and *Saccharomyces cerevisiae*, for instance, required the application of sonication and high pressure systems to disrupt the membrane and release the desired enzyme. In the case of L-ASNases produced by *E. coli*, the disruption method applied is very important, since this bacterium is able to produce two proteoforms of L-ASNase: EC2 with therapeutic application; therefore, separation of both L-ASNases is crucial. In addition, EC2 is firstly produced in the cytoplasm and subsequently directed to the periplasmic space for maturation. These methodologies, however, often lead to low recovery of L-ASNase, and multiple purification steps are required. In addition to the increased number of purification methods needed, a homogenous product is not always obtained.[44]

Expression of recombinant L-ASNases has significantly facilitated purification processes. Purification of recombinant L-ASNases has not only increased the amount and overall yield of the protein being expressed and purified but has also allowed a more homogeneous bioproduct to be obtained. In addition, the number of purification steps has decreased. Similar to native L-ASNases, gel filtration and ionic exchange chromatography are the most common methodologies employed following low-resolution purification steps of recombinant L-ASNases. Since recombinant enzymes are being produced, research has also been carried out regarding the purification of L-ASNases by affinity chromatography

using tags such as histidine and glutathione S-transferase. For these types of enzymes, less purification steps are required, a greater overall yield of purified product is obtained, and a more homogenous bioproduct is achieved. However, the use of affinity tags on L-ASNase is not recommended, since it may affect protein stability, biological activity, and toxicity. Once L-ASNase is often intended for clinical use to treat patients suffering from ALL, removal of the tag becomes necessary, therefore requiring an additional purification step that would likely cause an increase in manufacturing costs.[44] Some quantitative data concerning purification fold and overall yield (%) of the purification of L-ASNase from different organisms are reviewed in **Table 1**.

Table 1: Summary of relevant purification methods used to purify L-ASNases from different microorganisms.

Organism	Purification stage/ method	Yield (%) (final step)	Purification fold (final step)	Reference
Corynebacterium glutamicum	DEAE-Sephacel chromatography, Ammonium sulphate and Sephacryl S-200	12.5	98.0	[47]
Pseudomonas aeruginosa 50071	Sephadex G-100 gel filtration and CM Sephadex C50 chromatography	43.0	106.0	[48]
E. chrysanthemi	Diethylaminoethyl [DEAE]-cellulose chromatography	76.0	88.0	[49]
Bacillus sp.	DEAE ion-exchange chromatography	43.1	11.2	[50]
Streptomyces gulbargensis	Sephacryl S-200 gel filtration and CM Sephadex C-50 chromatography	32.0	82.1	[51]
Streptomyces sp.	DEAE-Cellulose and Sephadex G-50 chromatography	41.9	60.0	[52]

E. coli BL21 (DE3)	IL-ATPS	87.94 ± 0.03	20.1 ± 0.4	37
	Ammonium sulphate precipitation + IL-ATPS	≈ 90	173.8 ± 10.7	

L-ASNase pharmaceutical dosage in the market (intravenous/intramuscular solution) is available in four different formulations, as described in Table 2. In these pharmaceutical formulations, excipients have been used to stabilize the enzyme structure and reduce protein aggregation. Salts (phosphate buffer), sugars and polyols (sucrose, glucose and mannitol) have been reported to ensure L-ASNase stability during freeze-drying process and to enhance its shelf-life.[1] Despite of the groundbreaking medical innovation of the first L-ASNase therapy, most of the products currently in the market lack desirable pharmaceutical characteristics. Those include, but are not limited to, an extended blood serum half-life as well as reduced immunogenicity and toxicity.[1] The development of improved L-ASNases is not an easy task, given the microbiological source of the enzyme, which can result in immunogenicity. To face those challenges, researchers have nowadays a wide array of biomolecular and biochemical tools at their disposal to aid in the improvement of L-ASNase, tailoring the enzyme for its application.[1] **Figure 4** summarizes these issues about L-ASNase development as a biopharmaceutical.

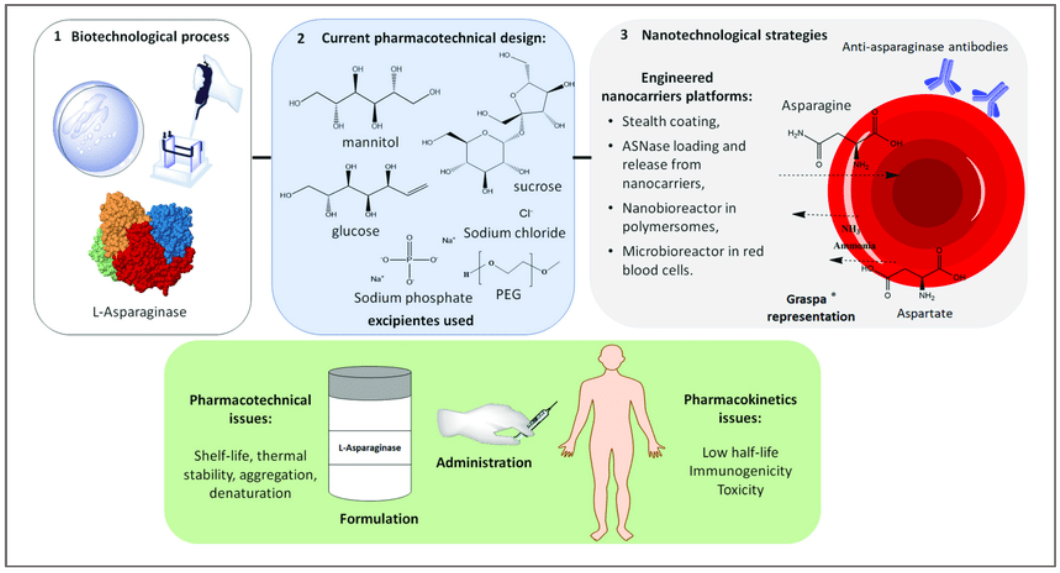

Figure 4: Recent pharmaceutical issues about L-ASNase development as a biopharmaceutical (adapted from Brumano et al.)[1].

In summary, the purification strategies depend on many factors: microbial source, recombinant or native L-ASNases, intra- or extracellular enzyme production, culture medium used, production scale, and recommended degree of purification.[44] Supported ionic liquids based on silica or polymers are already reported in the literature and have been mainly used in the separation of natural compounds from biomass.[53] Besides that, they have a high potential in the purification of proteins, however, this particular application has been scarcely considered.[54,55] So far, no studies have been found that demonstrate the use of silica based supported ionic liquids for the purification of enzymes, such as L-ASNase.

L-ASNase was initially marketed as a biopharmaceutical in 1978. After that, three more formulations from the *E. coli* and *E. chrysanthemi* bacterial species are approved by Food and Drug Administration (FDA). These formulations are commercially available under different trade names: I) native asparaginase from *E. coli* (Kidrolase®, EUSA Pharma; Elspar®, Ovation Pharmaceuticals; Crasnitin®, Bayer AG; Leunase®, Sanofi-Aventis; Asparaginase Medac®, Kyowa Hakko; among others), II) a PEGylated form of the native *E. coli* asparaginase, polyethylene glycol (PEG)-asparaginase (Oncaspar®, Sigma-Tau Pharmaceuticals, Inc), III) an enzyme from *E. chrysanthemi* (synonymous of *E. carotovora*) (Erwinase®, EUSA Pharma) and IV), a recombinant *E.coli* asparaginase preparation (Spectrila®, Medac GmbH). A PEGylated form of recombinant *E. chrysanthemi* L-ASNase is currently undergoing clinical evaluations.[11,31,56–58] Elspar® contains L-ASNase derived from *E. coli*. Oncaspar® is a modified version of Elspar® obtained through the covalent conjugation of *E. coli* L-ASNase with PEG, in order to increase the plasma half-life and decrease the immunogenicity and antigenicity of L-ASNase. Still, the intravenous administration of Oncaspar® (pegaspargase) has been recently related with an increased risk of allergic reactions. Erwinase® are obtained from *E. chrysanthemi* and is used alongside with chemotherapy or radiotherapy as a part of treatment protocols.[59] The characteristics of various L-ASNase preparations are summarized in **Table 2**.

Table 2: Main characteristics of commercial L-ASNase preparations (adapted from Chen et al.)[32].

L-ASNase type	Native *E. coli*	Pegylated form of native *E. coli*	*Erwinia chrysanthemi*	Recombinant *E. coli*
Trade name	Elspar® Leunase® Kidrolase® Crasnitin® ،sparaginase medac®	Oncaspar®	Erwinase®	Spectrila®
FDA approval	1978	1994	2011	2016[60]
Route*	IV, IM	IV, IM	IV, IM	IV
Half-life (d)	1.08-1.35 (IM)	5.5-5.7 (IM)	0.27 (IV) 0.65 (IM)	0.52-0.95 (IV)
Equivalent doses for complete ASN depletion for 2 weeks	6000-10,000 U/m^2 every 2-3 d	2500-3500 U/m^2 every 2 weeks	20,000-25,000 U/m^2 every 2-3 d	----------

* IM = intramuscular; IV = intravenous.

1.1.3 L-ASNase immobilization

One of the main problems in using enzymes out of their native niche is the lack of the physicochemical environment provided by the cells for efficient catalysis. The main challenges associated with the optimization of catalytic performance are related to the complexity of the protein three-dimensional structure and its conformational changes and structural dynamics during the biocatalytic process.[61] An alternative to solving this problem is found in the development of immobilization techniques.[61] An immobilized enzyme is an enzyme that is attached to the supporting material or matrix and thus confined to a phase different from the one for substrates and products.[62] The enzyme when immobilized is unable to move due to its linkage to the support or matrix, and its phase difference from

substrates and products.[63] The immobilization procedure results in protein structures that are more rigid and have different specific chemical, biocatalytic, mechanical, and kinetic properties from the respective features of the native enzyme.[61] Thus, immobilization has been used by numerous researchers as a tool to improve a variety of enzyme features, such as activity, selectivity, specificity, resistance to inhibitors, etc.[64] The commercial approved PEG-asparaginase is already an enzymatic immobilization process, reporting 18% of hypersensitivity reactions, compared with 32% for native L-ASNase.[4] In certain cases, some immobilization protocols have permitted the one-step immobilization and purification by a rigorous control of the support and/or immobilization conditions.[64] For instance, most of the chromatographic matrices for protein purification and immobilization base their enzyme adsorption capacity on the establishment of many weak enzyme–support interactions, in other words, the enzyme is only incorporated to the support if many enzyme–support interactions are accomplished.[64]

There are various enzyme immobilization methods, being categorized mainly as chemical, where covalent bonds between the enzyme and the support are established, and physical, where weak interactions are formed.[65] Traditionally, four main methods have been described in the literature, namely adsorption (physical), covalent bonding (chemical), entrapment/encapsulation (physical), and cross-linking (chemical).[65] These methods of immobilization and the nature of an enzyme supports are very important because the steadiness and long-term use of an enzyme depend on immobilization methods.[66] A general illustration of the differences between each methods of enzyme immobilization is presented in **Figure 5**.

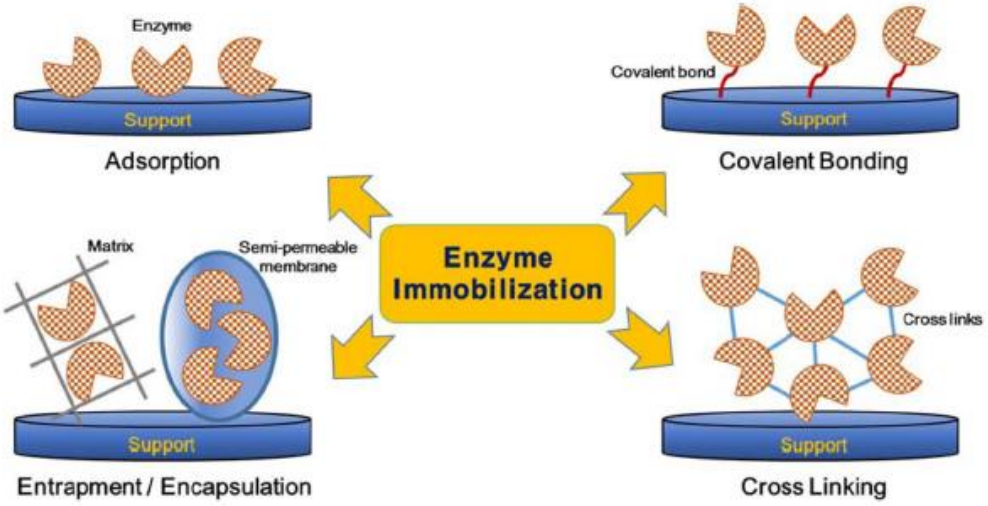

Figure 5: Schematic representation of different enzyme immobilization methods: Adsorption; Covalent bonding; Entrapment/Encapsulation; Cross-linking. (adapted from Nguyen et al.)[62].

However, no specific method and support is the best for all enzymes and their various applications. This is because of the extensively different chemical characteristics and composition of enzymes, the different properties of substrates and products, and the various uses of the product. Nevertheless, all of the methods may present a number of advantages and drawbacks as shown in **Table 3**.

Table 3: Preparation and characteristics of the different enzyme immobilization methods.[65]

Characteristic	Adsorption	Covalent binding	Entrapment/ Encapsulation	Cross-linking
Preparation	Easy	Difficult	Difficult/ Easy	Difficult
Enzyme activity	Low	High	High	Moderate
Substrate specificity	Unchangeable	Changeable	Unchangeable	Changeable
Binding force	Weak	Strong	Strong/ Moderate	Strong
Regeneration	Possible	Impossible	Impossible/ Possible	Impossible
Applicability	Low	Moderate	High/Moderate	Low
Cost	Low	High	Low	Moderate

So far, several supports were already described and investigated for L-ASNase immobilization in the literature, which can be divided by their chemical characteristics and origin, like organic (divide into natural, synthetic or nano), inorganic and hybrid materials.[4] An ideal support should be biocompatible, easily accessible, cheap, stable, and suitable for regeneration. Natural supports are the most common used for enzyme immobilization, being biocompatible, biodegradable, and inexpensive. Although synthetic polymers come from non-renewable petroleum resources, they have the advantage that their shape, form, porosity, pore diameter, polarity, hydrophobicity and surface functional groups can be manipulated

during their synthesis.[4] From all matrices, nanoparticles exhibit the highest surface areas and largest porosities, providing a high enzyme loading and facilitating the accessibility of the substrate to the active sites.[4] Another type of support, the inorganic supports, have few functional groups, limiting the enzyme attachment, but exhibit high chemical, physical, and biological resistance compared with organic ones. Moreover, inorganic materials have uniform pore sizes, large surface areas, and are easily functionalized.[67] Finally, the hybrid supports combines the properties of both natural and synthetic ones.[4] Some examples of supports and immobilization methods already used for L-ASNase immobilization are catalogued in **Table 4**.

Table 4: Examples of supports and methods used for L-ASNase immobilization.

Support nature	Immobilization method	Support	Reference
Natural	Albumin	Cross-linking	68
	Poly(DL-alanine) peptides	Covalent binding	69
	Dextran	Covalent binding	70
	Chitosan	Adsorption	71
	Agarose-glutaraldehyde	Covalent binding	72
	Fructose levan	Covalent binding	73
	Alginate, gelatin	Entrapment	74
	Silk fibroin	Covalent binding	75,76
	Fatty acids	Covalent Binding	77
	Bovine serum albumin	Cross-linking	78
Synthetic	PEG	Covalent binding	79
	Polyacrylamide	Entrapment	80
	Epoxy resin	Covalent binding	81
	Polyimide	Entrapment	82
Nano	Hydrogel-magnetic nanoparticles	Entrapment	83
	Polyaniline nanofiber	Covalent binding	84

	MWCNTs	Adsorption	[85]
Inorganic	Silica gel	Adsorption	[86,87]
	Activated carbon	Covalent binding	[88]
Hybrid	PEG-albumin	Chemical modification	[89,90]
	Calcium alginate-gelatin	Cross-linking	[91]

1.1.4 Adsorption method

Among many methods proposed for the protein immobilization, the most important and useful is the immobilization by adsorption. Adsorption makes use of the interactions generated between the surface of support particles and enzyme based on weak bonds such as van der Waals forces, electrostatic and hydrophobic interaction.[62,92] These interactions are rather weak and, what is important, typically there are no changes in the native structure of the enzymes.[1] This prevents the active sites of the enzyme from disturbing and allows the enzyme to retain its activity.[92] Enzyme is dissolved in solution and the solid support is placed in contact with the enzyme solution for a fixed period of time under suitable conditions.[62] The unadsorbed enzyme molecules are then removed from the surface by washing with buffer. Immobilization by adsorption is a simple and economical technique which is reagent-free, low cost and is usually non-destructive toward enzyme activity since it does not involve any functionalization of the support.[62] However, enzyme desorption/leaching is a common problem, because enzymes are loosely bound to the support by weak physical bonding so that changes in temperature, pH or ionic strength may result in this drawback.[62,93]

For the successful adsorption of the enzyme to occur, certain conditions must be met, among which an enzyme-support affinity is the most important. This is assured by the presence of the specific active groups on the surface of the support material, which enable the generation of the enzyme–support interactions. However, if absent, the interactions can be tuned by applying intermediate agents.[92] A wide range of available compounds can be successfully used as valuable supports for enzyme adsorption. The criteria of the choice suitable for a given enzyme and its application include: the cost, availability, stability (or reactivity if necessary) in specific conditions, and the type of reactor.[92]

1.2 Applications of L-ASNase

1.2.1. Antileukemic drug

Cancer is a generic term to describe a large group of diseases that are capable to affect almost any part of the body.[94] It begins with an induced change in a single normal cell which makes it "neoplastic".[95] Tumours mature from benign to malign lesions by gaining multiple mutations over time.[96] Cancer is anticipated to be the leading cause of death in every country of the world in the 21st century.[97] Its incidence and mortality are growing rapidly for many reasons, including ageing population and changes in the prevalence and distributions of the main risk factors for cancer, multiple of which are related with socioeconomic growth.[97]

Leukemia is a type of cancer of the early blood-forming cells.[98] Most often, it is a cancer of the white blood cells, but some of them start in other blood cell types. There are several types of leukemia, which are divided based mainly on whether the leukemia is acute (fast growing) or chronic (slower growing), and whether it starts in myeloid cells or lymphoid cells.[98] In particular, Acute Lymphoblastic Leukemia (ALL) is a malignant transformation and proliferation of lymphoid progenitor cells in the bone marrow, blood and extramedullary sites.[99] ALL is the most common type of childhood cancer, however, about 4 out of every 10 cases occur in adults,[100] and it is expected to affect over 53,000 people worldwide by 2020.[1] **Figure 6** shows the number of cancer cases in 2018 worldwide, by different types of cancer, where leukemia corresponds to more than one in four cases.

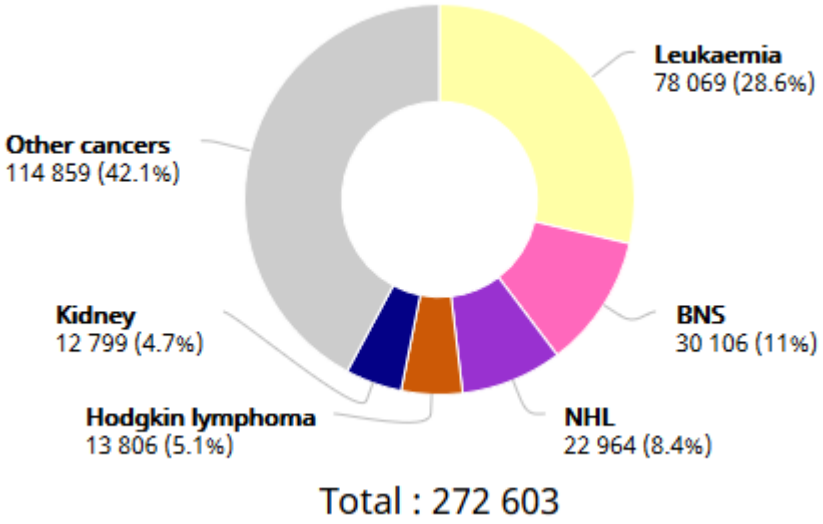

Figure 6: Estimated number of new cancer cases in 2018 worldwide (both sexes, ages 0-19) (adapted from Bray et al.)[101].

The hallmark of ALL is chromosomal abnormalities and genetic alterations involved in differentiation and proliferation of lymphoid precursor cells.[99] The term "Acute" means that the leukemia can progress quickly, and if not treated, would probably be fatal within a few months. "Lymphocytic" means that it develops from early (immature) forms of lymphocytes, a type of white blood cell.[98] Other types of cancer that start in lymphocytes are known as lymphomas (either non-Hodgkin lymphoma or Hodgkin lymphoma). While leukemias such as ALL mainly affect the bone marrow and the blood, lymphomas mainly affect the lymph nodes or other organs (but it may also involve the bone marrow). Usually, if at least 20% of the bone marrow is made up of cancerous lymphocytes (called lymphoblasts), the disease is considered leukemia.[98]

Different types and progress of leukemia have different treatment options and outlooks. Therefore, there are several methods of treatment, such as chemotherapy, immunotherapy, radiation therapy, bone marrow transplantation or the combination of different treatments. The main treatment for ALL in adults is typically long-term chemotherapy.[98]

L-ASNase is an antileukemic biopharmaceutical of current high-cost and is considered one of the most important oncologic drugs, as it is used in pharmaceutical industry since it is vital in the first line of ALL treatment, as well as malignant diseases of the lymphoid system and certain non-Hodgkin's.[1,36,102,103] This enzyme is commercially available in vials containing 10,000 IU of asparaginase in 80 mg of mannitol.[104] As a case in point, the wholesale cost in the developing world in 2015 was about US$52.88 per 10,000 IU vial.[105] Recent studies have also reported the L-ASNase contribution to the reduction of cancer metastasis.[1] Further developments might be expected as a result of the application of L-ASNase to reduce cancer invasion, circulation of tumor cells and metastasis as recently reported for a mouse model of breast cancer by Knott et al.[106] The development of L-ASNase as antileukemic biopharmaceutical is characterized in **Table 5**.

Table 5: Development of L-ASNase as antileukemic drug (adapted from Batool et al.)[21].

Year	Advancement
1953	Kidd[6]: discovery of antileukemic effect of guinea pig serum
1963	Broome[8]: identification of L-ASNase as antileukemic agent in guinea pig serum
1964-1967	Suppression of tumor cell growth by *E. coli*-derived L-ASNase; isolation and purification of active *E. coli* isoform
1966	Dolowy[107]: first clinical use of L-ASNase
1968	Wade[108]: isolation of L-ASNase from *E. chrysanthemi*
1978	Native *E. coli* asparaginase approved by FDA for use to treat ALL
1981	Kamisaki[109]: initial development of pegylated *E. coli*-derived L-ASNase
1994	Pegylated *E. coli* asparaginase (Oncaspar®) approved by FDA for use to treat ALL
2006	Pegylated *E. coli* L-ASNase approved by FDA for first-line use to treat ALL
2011	Asparaginase *E. chrysanthemi* approved by FDA for use in patients with hypersensitivity to *E. coli*-derived L-ASNase

L-ASNase as a chemotherapeutic agent represented a landmark in the field of medicine due to the nearly 90% increase in survival rates since its introduction into pediatric treatments protocols and due to its selectivity against the tumour cells.[1] This is an enzyme of prime therapeutic importance that contributes to 40% of the total worldwide enzyme demands.[110] It contributes to one-third of global requirements as anti-leukemic and anti-lymphoma agents.[110] In addition, it is known that a reduction in the supply of L-ASNase drug would reduce the chances of curing of approximately 5000 child-juvenile patients.[1] In this way, the chemotherapeutic potential of this enzyme has been one of the most eminent discoveries of modern times.[19]

L-Asparagine (L-ASN) is a nonessential amino acid required for the biosynthesis of proteins. The precursor of asparagine is oxaloacetate. Transaminase transfers an amino group from glutamate to oxaloacetate to produce aspartate and 2-KG.[111] Asparagine synthetase (ASNS) carries an amino group from glutamine to aspartate.[111] In eukaryotic

cells, ASNS does not use other substrates; it is therefore referred to as glutamine dependent. Asparagine usually enters the Krebs cycle as oxaloacetate.[111] ASNS catalyses the synthesis of asparagine and glutamate from aspartate and glutamine in an ATP-dependent amidotransferase reaction.[112] ASNS is present in most mammalian organs, and an elevated ASNS protein expression is associated with resistance to L-ASNase therapy in childhood ALL.[112] Tumour cells, more specifically lymphatic tumour cells, require huge amounts of L-ASN to keep up with their fast growth.[59] In this context, L-ASN is an essential amino acid for the growth of tumour cells and the growth of normal cells is not dependent on L-ASN since it can be synthesized in enough amounts for themselves. A scheme summarizing the main action mechanism of L-ASNase to attack tumour cells is presented in **Figure 7**.[59]

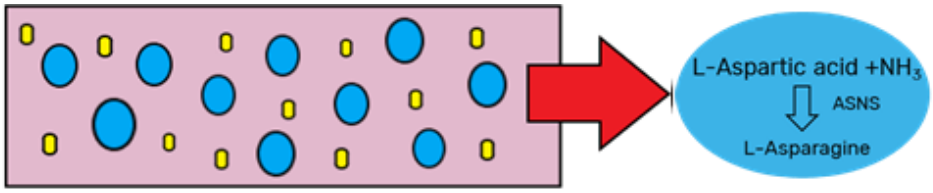

(A) Normal cells synthetize amino acid L-ASN with the help of the enzyme ASNS;

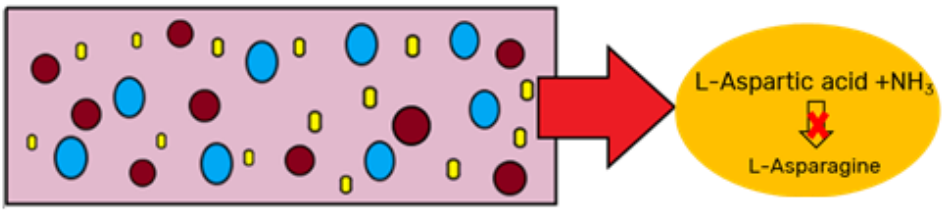

(B) Cancer cells are unable to synthetize amino acid L-ASN due to absence of ASNS and they depend on uptake of extracellular L-ASN for their survival;

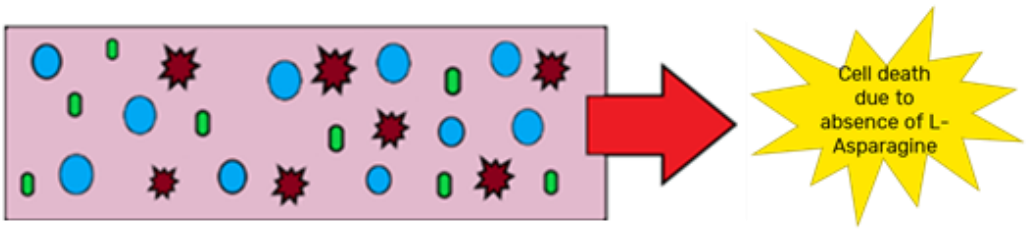

(C) L-ASNase decreases the concentration of extracellular L-ASN. Tumour cells selectively die due to the absence of protein synthesis and normal cells survive due to ASNS.

Figure 7: Antineoplastic action of L-ASNase: ● normal cell; ● cancer cell; ● L-Asparagine; ● L-ASNase (adapted from Shrivastava et al.)[59].

The underlying principle behind the L-ASNase anti-cancer mechanism of action is based on the fact that leukemic cells are relatively unable to synthesize L-ASN required for protein synthesis because they express low levels of ASNS, having a depletion of this amino acid from bloodstream.[113] To meet this demand, they depend on the uptake of extracellular L-ASN for their survival. Normally, they obtain the amino acid both from blood serum as well as synthesizing the amino acid themselves in limited amounts.[113] The administration of the enzyme, L-ASNase, quenches this free source of L-ASN, decreasing the concentration of extracellular amino acid. Since they lack the enzyme ASNS, tumour cells are unable to synthesize enough L-ASN for their maintenance and accelerated malignant growth which compromises their cellular functions and leads to cell death.[1] However, depending on the L-ASNase source, the medical use of L-ASNase still faces some challenges as several types of side effects such as allergic reactions occur due to its high immunogenicity as well as clinically important toxicities, such as pancreatitis, thrombotic events, mucositis, nausea, etc.[114–116] Another issue is that glutaminase activity generated by these enzymes can cause secondary effects such as allergic reaction, nausea, pancreatitis, diabetes and coagulation abnormalities.[19] A therapeutic response by patients with the L-ASNase agents commercially available rarely occurs without some evidence of toxicity.[1]

1.2.2. Food industry

L-ASNase has become one of the main attentions of food processing industries as a promising acrylamide mitigating agent when foods are processed in high temperatures.[117] Acrylamide (C_3H_5NO) is also recognized as 2-propenamide, acrylic amide, ethylene carboxamide, propenamide, propanoic acid amide or acrylic acid amide, presenting 71.08 g mol^{-1} of molecular mass.[118] Acrylamide is a neurotoxin and has been categorized as a carcinogenic to the humans.[21] The formation of this organic compound has been quite studied in the past and it was demonstrated the occurrence of acrylamide in regular starch-based foods that were baked, roasted or fried.[119] Essentially, foods that are processed or cooked at high temperature like potato products, coffee, bakery products, roasted almonds, olives dry fruits are the prominent sources of acrylamide.[119] Researchers demonstrated that acrylamide is produced as a result of the Maillard reaction (**Figure 8**) from L-ASN and

reducing sugars.[120] In fact, L-ASN and reducing sugars are used in a conjugation reaction resulting in the formation of N-glycosylasparagine. When treated at high temperature, a decarboxylated Schiff base is formed that may decompose directly to form acrylamide or hydrolyse to form 3-aminopropionamide, also a precursor of acrylamide.[120,121]

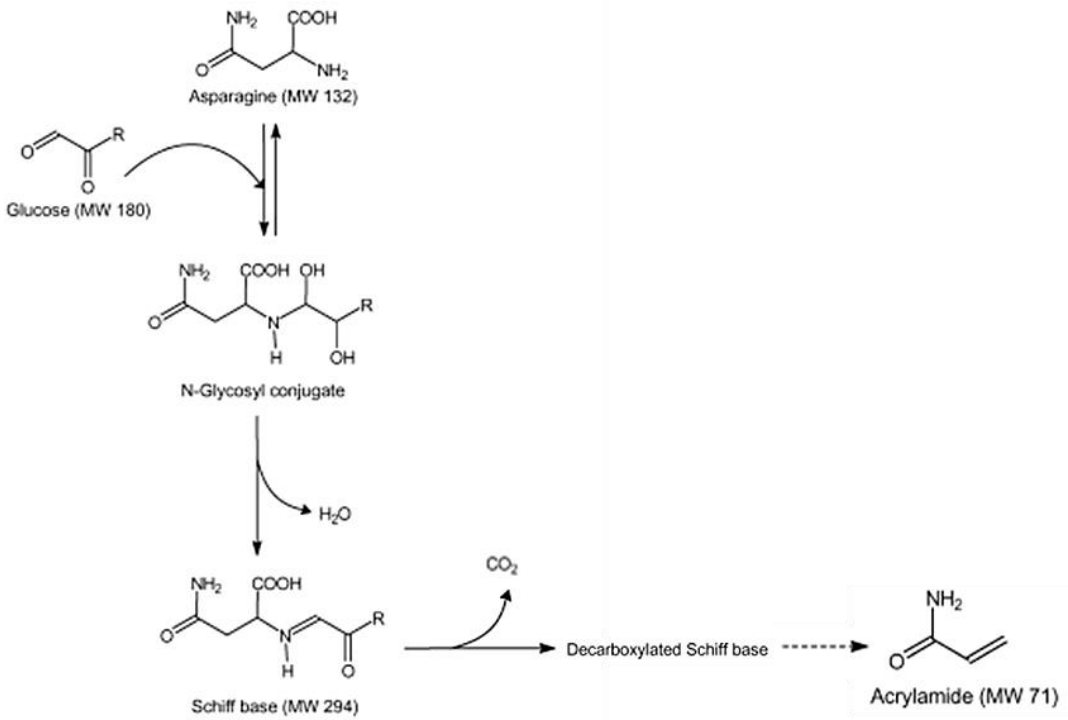

Figure 8: Mechanism of acrylamide formation in food processing (adapted from Gökmen et al.)[122]

The removal of acrylamide is important because it is a neurotoxin, classified as potentially carcinogenic to humans.[123] Therefore, L-ASNase pre-treatment of food before heat treatment could be a suitable solution supported by several researchers for the reduction of free L-ASN and consequently the imminent risk of synthesis of acrylamide. Different tests were made, concluding that L-ASNase pre-treatment resulted on an acrylamide reduction of at least 90% in foods, such as crackers, french fries, potato, gingerbread, among others.[119,124] Regarding this, L-ASNase from *Aspergillus oryzae* and *A. niger* are often used in baking industries. These enzymes have an optimal temperature of 40-60ºC and a pH of 6.0-7.0 and since the baking temperatures go up to 120ºC, it is appropriate to have stable and active enzymes over a wide range of temperature and pH.[125] Although, complete removal of acrylamide is not possible due to other L-ASN-independent formation.[120] Other studies

allowed to know that L-ASNase pre-treatment does not only leave sensorial properties of the final food products unaffected, but also improves the flavour by increasing the percentage of glutamic acid on the food.[119]

1.2.3 Biosensors

L-ASNase biosensors can be a promising technology for the detection of L-ASN in physiological fluids at levels as low as nano-levels, either in leukemia or food industry.[21] Spectroscopy techniques such as X-ray Powder Diffraction (XRD), X-ray photoelectron spectroscopy (XPS), scanning electron microscope (SEM) and transmission electron microscopy (TEM) are currently used for L-ASNase analysis.[21,126] One of the main studies aimed at the development of L-ASNase-based biosensors was made by Erdogan et al.[82], who developed polyimide based amperometric biosensor for determination of L-ASN in serum samples. Polyimides are very interesting due to their excellent thermal, chemical, electrical, and mechanical properties. Therefore, a polyimide membrane was assessed as carrier for L-ASN biosensor.[4] The schematic diagram of this process was illustrated in **Figure 9**. The results evidenced that proposed biosensors showed a wide linear detection range, acceptable reproducibility, high sensitivity, long-term stability, and low detection limit.

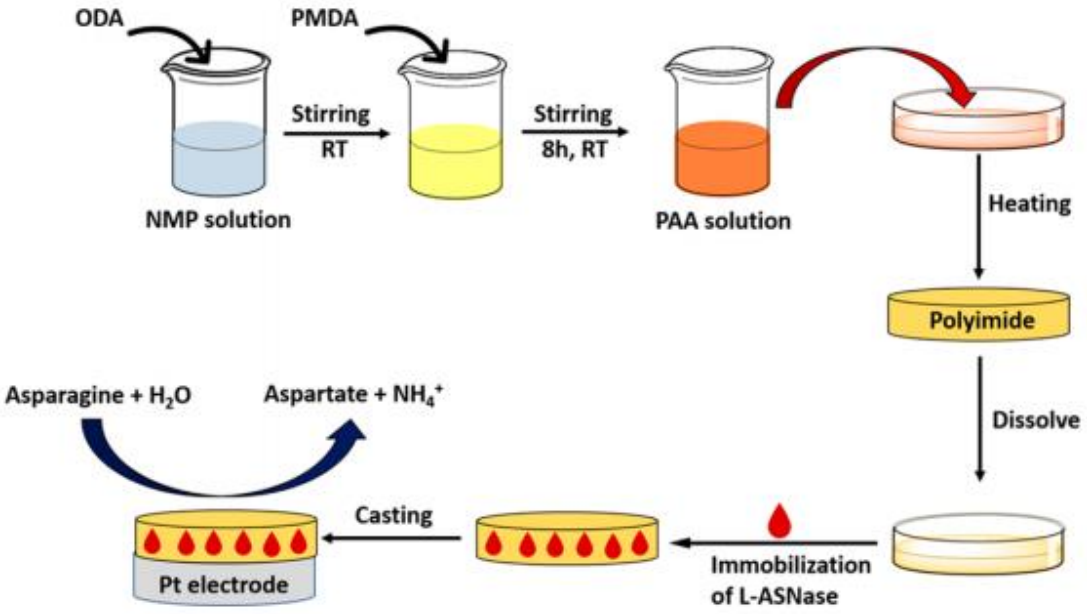

Figure 9: Schematic diagram of L-ASNase/polyimide/platinum (Pt) electrode (adapted from Ulu et al.).[4] First, dried 4-4'-oxydianiline (ODA) powder was dissolved in freshly distilled NMP (N-methyl-2-pyrrolidinone). After the diamine was totally dissolved, an equimolar amount of pyromellitic dianhydride (PMDA) was added to the solution with stirring to obtain a viscous poly(amic acid) (PAA). The PAA solution was then spread on a Petri dish and the PAA was imidized by heating in a forced-air oven.[82]

In another study, based on the deamination of L-ASN by L-ASNase and the formation of ammonia, an enzymatic method has been developed by Tagami and Mastsuda[127] for the measurement of the enzyme's activity and L-ASN with an ammonia gas-sensing electrode. One more study carried by Verma et al.[128] have used garlic tissue electrode for the determination of L-ASN, where garlic tissue cells were responsible for conversion of the amino acid into ammonia using an ammonium gas electrode as detector. Also, Verma et al.[129] developed a whole-cell based fiber optic biosensor using a L-ASNase-producing coliform bacterial and phenol red indicator, which can monitor L-ASN content in food samples.

In conclusion, several spectroscopy techniques are currently used for the analysis of L-ASN, however, their high cost and tiresome procedures make them less favourable. Therefore, biosensor technology can become a reliable, cheap and user-friendly solution. The mechanism of action of the biosensor depends on L-ASNase activity, ammonium ions produced from the hydrolysis of L-ASN causing a change in pH and, thus, changes of colour and absorption.[21]

1.3 Supported Ionic Liquids

1.3.1 Ionic liquids

Ionic liquids (ILs) are composed of organic cations (e.g. imidazolium, pyrrolidinium, pyridinium, ammonium, and phosphonium) and organic or inorganic anions (e.g. chloride, bromide, acetate, nitrate, and ethyl sulfate).[130] In **Figure 10** are displayed some of the chemical structures of cations and anions present in the most common ILs. The main difference between ILs and simple molten salts is that the former is composed of bulky and asymmetrical ions, that only loosely fit together, prevents them from easy crystallization and makes them in the liquid state at or near room temperature.[130]

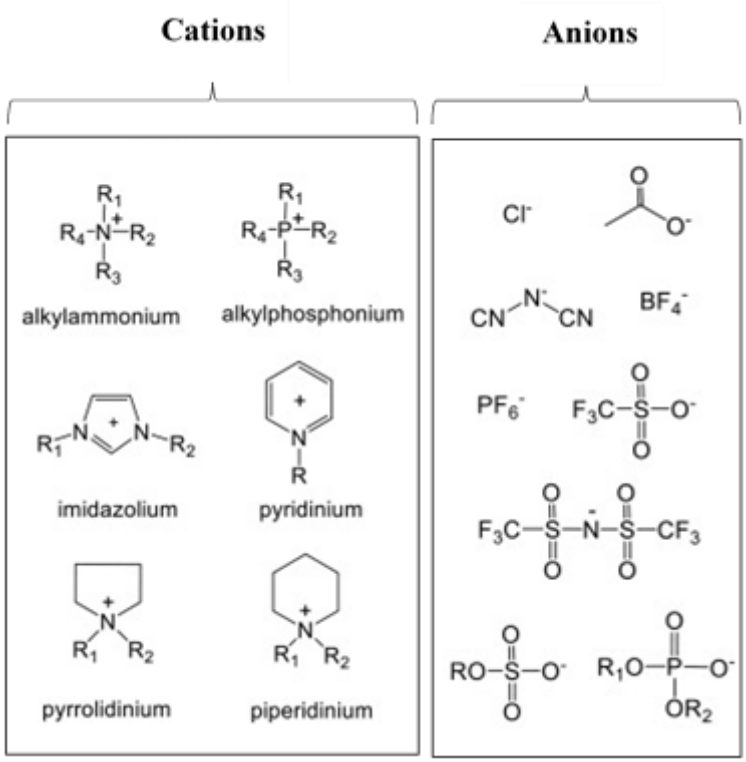

Figure 10: Chemical structure of most commonly used cations and anions forming ILs (adapted from Zhao et al.)[131].

ILs are characterized by a highly pre-organized and homogeneous liquid structure.[132] Because of the great variety of cation/anion pairs and the diversity in the side chains of the cations, an almost unlimited IL combinations can be produced and tailored according to the

specific requirements of the given application.[133] Therefore, ILs are frequently described as tunable or "designer solvents".[130,134] Task-specific ILs can be developed by the manipulation of their physicochemical properties, namely, solubility and reactivity, by an appropriate choice of the ions contained in the IL.[132] Thus, it is possible to provide a long list of ILs with different polarity, hydrophobicity and viscosity, among others.[134,135]

Nowadays, ILs are widely recognized solvents due to their extended list of excellent properties, and their success comes mainly from their distinctive and exceptional characteristics.[134] As an example, they can selectively interact with different types of solutes and solvents, have excellent chemical, thermal and electrochemical stabilities, are not flammable, have negligible volatility and have an excellent solvation ability for a wide range of compounds and materials.[136] Compared to water and other traditional molecular liquids, ILs are single-component systems in which the ions likely play independent roles in determining the liquid behaviour.[130] Thus, the favourable properties displayed by these salts allowed significant advances in several application domains, making them promising candidates as an alternative to organic solvents for chemical synthesis[137], catalysis[138–140], separation[141,142] and extraction.[143]

However, the exceptional performance of bulk ILs may be hindered when they are applied in the liquid state, due to problems mainly associated with the ILs high viscosity, low diffusion coefficients, difficulties in product purification and solvent recycling, and high cost derived from the large quantities of ILs required.[53] Immobilized ILs allow to overcome these shortcomings, justifying the more recent interest and accomplishments achieved with this concept. Due to the known remarkable advantages obtained by the immobilization of ILs onto supports, numerous applications in distinct fields, ranging from chemical to biological sciences, have been developed.[53]

1.3.2. Immobilization of ILs, types of supports and applications

Supported ionic liquids combine the unique properties of pure liquid-state ILs with the convenient recovery features of supports, resulting in functionalized materials.[144,145] These materials are obtained by the immobilization of ILs in a suitable solid support.[53]

Depending on the nature of the interactions established between the IL and the support material, two principal categories can be distinguished.[146] The first one is the non-covalent method based on simple physical confinement (physisorption) of the IL to the surface of a high surface area support, the so-called class of supported ionic liquid phase (SILP).[146] In this case, only weak interactions such as van der Waals forces and hydrogen bonding interactions between the IL and the surface of the support are present, and the IL is distributed over the surface of the support obtaining a multilayer film.[146] Physical confined systems can be easily achieved using relatively simple impregnation techniques of the IL dissolved in a suitable organic solvent or water, the addition of the support, and, finally, solvent evaporation under vacuum. Other methods are post-impregnation and the "ship-in-a-bottle" method.[53,147] The second one is the covalent grafting (chemisorption) of ILs to different functional groups present in the surface of support material, which is defined as supported ionic liquid (SIL) concept, the type of supported ionic liquid used in this work.[146] In these materials, strong interactions like covalent bonding between the support and the IL are present.[147,148] The grafting of functionalized IL fragments can be obtained using traditional sol-gel synthesis and often involves multistep reactions in which pre-functionalized solid supports react with ILs containing specific functional groups, without subsequent impregnation.[53,147] Usually, systems obtained by this method are present as a monolayer, although covalently linked multilayers or brushes can also be obtained.[149] **Figure 11** represents both strategies for incorporating LIs into the material pores: chemisorption (A) and physisorption (B).

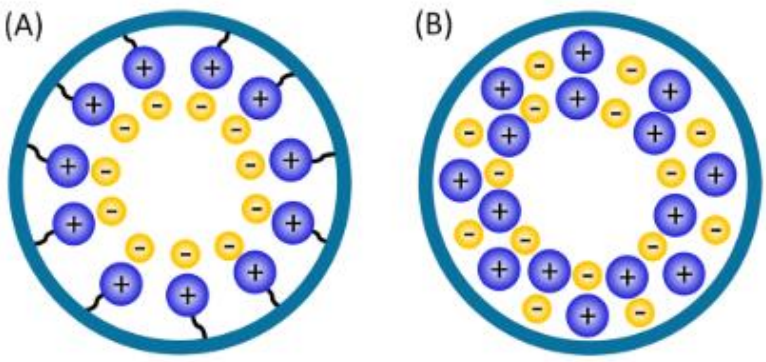

Figure 11: Incorporation of ILs into the pore structure of materials by two different strategies: (A) covalent grafting of monolayer IL on the pore wall and (B) physical confinement of multilayers of ILs into nanopores (adapted from Zhang et al.)[130].

As expected, the main disadvantage of the physical adsorption approach is the potential problem of ILs leaching or detachment from the support surface due to weak interactions between the support and the IL, especially when the supported ionic liquids are used in the solvents that can solve the ILs.[145] Therefore, the covalent approach is more suitable under this condition.[145] Nevertheless, this concept presents significant advantages, such as: (1) the multilayers of ILs achievable by physisorption allow to retain, in some extent, the specific bulk physicochemical characteristics of ILs to the heterogeneous material; (2) the ILs can be removed, allowing the ILs and material recycling; and (3) the properties of confined ILs can be easily modulated for a given application.[53]

On the other hand, the immobilization of ILs on materials by covalent anchoring is a highly attractive strategy to circumvent the leaching of ILs, thus minimizing the amount needed.[130] In these materials, specific properties observed in the IL bulk state may no longer be present in the prepared support.[130] Despite this condition, the IL chemical structure and specific functional groups are still present, which may contribute to improve the target material properties and application performance. This method exhibits, however, some limitations and drawbacks, such as: (1) the more challenging preparation since at least one reaction step is required; (2) the low density of ions resulting from the assembly of a monolayer of IL onto a support, which may limit the performance of catalysis; and (3) the pre-treatment requirement of inert materials .[53,150]

1.4 Silica based supported ionic liquids

1.4.1 Support materials

As described in the previous section, for the synthesis of supported ionic liquid materials, ILs can be attached on the surface of a solid material by physisorption or chemisorption. This immobilization may be performed in different solid matrices, including silica (silica gel, mesoporous silica or silica nanoparticles), carbon nanotubes (CNTs), polymers, crystalline materials, and inorganic materials.[53,146]

Both for immobilization and purification, an appropriate selection of the support and of the protocol are critical.[64] The choice of the support material is important since the

structure and properties of confined ILs are significantly influenced by the pore structure and the chemical nature of the support, which determines the nature and extent of the IL-pore wall interactions;[53,147] however, Zhang et al.[130] observed changes in the structure and properties of the support materials and ILs after confinement. There are various parameters that define a support: internal geometry (e.g., flat surfaces or thin fibers), specific surface area, superficial activation degree, mechanical resistance, pore diameter, etc.[64] In some instances, several positive properties of a support for enzyme immobilization may be also positive for enzyme purification, but typically they have a critical difference in their objective, which may cause the optimal properties for each support to be different. While for enzyme purification an easy release of the enzyme from the support is mandatory to avoid enzyme inactivation, enzyme immobilization requires a strong enzyme–support attachment.[64] Thereby, the undesired release of the enzyme during operation needs to be avoided for enzyme immobilization, whereas a too strong enzyme–support interaction may be unsuitable for enzyme purification.[64]

During the applications of SILs, both the IL structures (or types) and the IL loading on the supports could affect the surface properties of the supports, such as wettability, lubricating features and separation efficiency, and further affect the performance in their applications.[132,145,147] The use of nanoconfined ILs can overcome the major drawbacks of bulk ILs, such as high cost, high viscosity, and slow gas diffusivity. [130]

1.4.2 Silica as support for enzyme immobilization

The prerequisite for the successful immobilization of an enzyme by adsorption on a support is the existence of specific functional groups on the surface of both the enzyme and the support. These give rise to the interactions sufficiently strong for the enzyme-support binding (adsorption) to occur. When such groups are absent, the support is subjected to a chemical modification.[92] Among all materials that can act as the support, silica-based materials correspond to the most widely used supports for IL immobilization since silica is a low-cost and inert material, easily chemically modified, biocompatibility, and has a high specific surface area, mechanical strength and thermal stability.[149,151] In point of fact, modifications of the morphological features of silica like pore size, pore geometry and

surface area have been used to develop better supports for enzyme immobilization because porous materials provide a better structure for entrapping or covalently binding enzymes.[152] Nevertheless, even though silica-based materials are inexpensive and easily accessible, these materials have not been used for L-ASNase immobilization, because biocompatible supports have been preferred for this method.[4]

The chemistry of silica surface depends on the content in silanol (Si-OH) and siloxane groups (Si-O-Si). Usually, Si-OH dominates the properties of the silica surface and corresponds to the group required to perform chemical modifications with ILs.[53] Nevertheless, immobilization of ILs cannot be easily accomplished only using native silica, it is frequently required to modify the silica, adding more functional groups with the objective of improving selectivity and capability of attachment.[153] Once the IL is immobilized onto a surface, it loses its liquid state; however, properties such as the designer ability and tunability of ILs are maintained.[154] The first step to anchor ILs to silica surface is to activate the silica particles using an acidic aqueous solution (typically nitric acid or hydrochloric acid) to enhance the content of acidic silanol groups on the silica surface and to eliminate impurities.[155] Then, according to the literature, the next task is to carry out the reaction in toluene between these activated silica particles with one silane-coupling agent like 3-chloropropyltrimethoxysilane (compound frequently used as the support modifier for adsorption of enzymes), leading to chloropropyl silica ([Si][C_3]Cl).[151,155] Afterwards, it can react with a cation source, resulting in the formation of IL-based supported silica with chloride as the counter ion.[151,155] The technique described above was used in this work.

1.4.3 SILs and enzymes - Biocatalysis

As mentioned above, the properties of ILs can be properly tailored, thus resulting in ILs that have catalytic properties and that can ultimately behave both as catalysts and solvents.[53] Compared to conventional reagents, the use of these enzyme preparations in ILs can dramatically increase the solvent tolerance, enhance activity as well as stability, and improve enantioselectivity.[156] Consequently, numerous strategies have been used successfully for activation and stabilization of enzymes in non-aqueous ILs media. [156]

Until now, supported ionic liquids have been widely applied in almost all of fields involving ILs and have brought about drastic expansion of the IL area. In the last years, these materials have been used as green media and functional materials for supports of catalysts, surface modifying agents, stationary phases in separation technologies, and electrodes in electrochemistry.[86,87] The potential application of ILs in biocatalysis was initially proposed in 2000 and combines the advantages of ILs with those of heterogeneous support materials.[88,89] Materials based on supported ionic liquids present many advantages over classical gas-liquid or liquid-liquid systems, namely, an efficient catalyst immobilization in a confined environment.[53] Due to an increase in the number of accessible active sites of the catalyst and decrease of mass transfer restrictions, supported ionic liquids allow a more efficient use of the catalyst and a significant reduction of the amount of IL required.[53] This will decrease the economic cost and potential environmental pressure in a large-scale process. In addition, the growing concerns about their toxicological and ecotoxicological properties can be overcome, at least partly and if properly designed, by the use of supported ionic liquids.[145] **Figure 12** depicts a schematic representation of SIL-based biocatalysis.

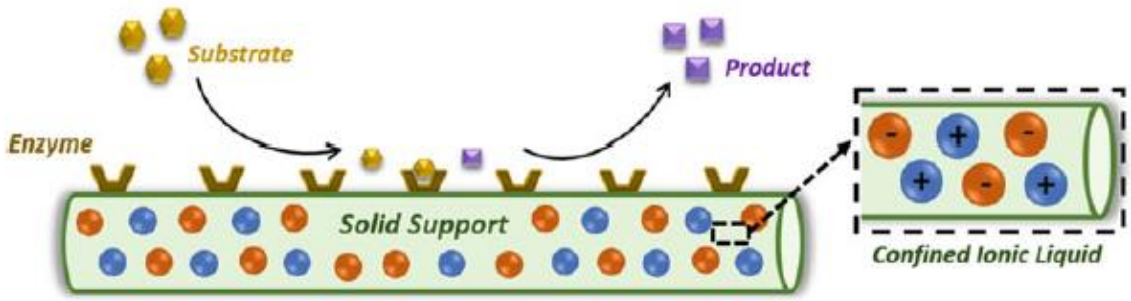

Figure 12: Scheme of a SIL-based biocatalytic with the detail of the confined IL in the solid support (green) (adapted from Pedro et al.)[53].

Enzyme-supported ionic liquids biocatalytic systems have been successfully applied with various enzymes, which may be immobilized in a wide range of support materials, including silica gel.[53] Giacalone et al.[149] showed that with *Candida antarctica* lipase B the biological activity may be enhanced by supporting the enzyme onto a SIL, although a higher concentration of IL-like fragments decreases the enzyme activity. In this study,

immobilization of lipase B was carried out by using poly(styrene-co-divinylbenzene) support, macroporous resin, with low and high degrees of functionalization. The resins were modified by reaction with 1-dodecyl-2-methylimidazol. Lipase B was then immobilized by adsorption from an aqueous solution of the enzyme onto the SIL bearing either chloride (Cl^-) or bis(trifluoromethanesulfonyl)imide (NTf_2^-) as the counterion. A significant enhancement of the enzyme activity was observed for the enzyme supported on SILs. Under microwave irradiation, a 28-fold increase was seen for lipase B supported on the SIL containing the hydrophobic NTf_2^- counter anion with low degree of functionalization. Use of resins with higher IL loading gave lower activity.[149] It is concluded that in the field of biocatalysis, the amount of IL, its distribution on the solid surface, and the nature of the counterion are of crucial importance to preserve and improve the enzymes catalytic performance.[149]

The supported ionic liquid concept allows custom-making of solid materials, resulting in uniform and well-defined surface topologies with definite properties and a controlled chemical reactivity.[132] Different support will form different interaction with ILs and catalysts, and then induce different catalytic activity. Therefore, some factors are necessary to consider during the choice of supports. For instance, supports should possess large specific surface area, highly ordered pore structure. Both the Brunauer, Emmett and Teller (BET) surface area and pore morphology of supports can provide different reservoirs for catalyst species, affecting the catalyst loading. Additionally, the interactions among support, ILs and catalyst determine the catalytic performance.[157] Considering this, silica is used as support because SiO_2 materials show high affinity to enzymes, have been successfully applied for enzyme immobilization and recyclable catalysts.[152,158] As an example, Singh et al.[159] reported the covalent immobilization of a L-arabinitol 4-dehydrogenase (LAD) onto various resins including SiO_2 nanoparticles. These nanoparticles were activated by glutaraldehyde to immobilize the enzyme through covalent bonding. Using purified recombinant LAD, they obtained an efficiently immobilized, exceptionally stable enzyme. Recombinant LAD enzyme was immobilized onto SiO_2 nanoparticles with immobilization efficiency of 94.7%. This result indicated that the immobilization procedure was highly efficient and that this was properly aligned on the support through multiple covalent bonds. Upon immobilization, the enzyme could be used for many cycles of oxidation without any significant reduction in activity. Even after 10 cycles, the LAD

immobilized on SiO_2 nanoparticles retained up to 94 % of its initial activity. Besides that, immobilized LAD exhibited improved thermal stability compared to that of the free enzyme. Thus, the high stability and reusability of immobilized LAD make it very attractive for industrial applications, that could be effectively utilized in the biotechnological production of L-xylulose from L-arabinitol.

1.5. Objectives

Based on the exposed, the goal of this master thesis is to develop a novel platform for the purification of L-ASNase from a real cell extract of *Bacillus subtilis* using supported ionic liquids based on silica. Firstly, the conditions for the immobilization of L-ASNase onto these materials are optimized using aqueous solutions of commercial L-ASNase. Supported ionic liquids have several beneficial properties for this purpose, such as high potential in the purification of proteins. With this approach is expected to overcome the drawbacks associated with the classical methodologies for L-ASNase purification and reduce its costs. However, due to the restrictions caused by SARS-CoV-2, only the immobilization of the L-ASNase extract onto supported ionic liquids was achieved, not reaching its purification, the final step intended at the beginning of this work.

Furthermore, other objectives of this work are to synthetize different SILs and characterize them by using multiple techniques. Then, study the adsorption performance of these materials to L-ASNase through the isotherms studies using aqueous solutions of the commercial enzyme. Finally, the immobilization procedure was monitored by determining the specific activity before and after the L-ASNase immobilization, and by performing SDS-PAGE and HPLC analysis.

The bacterium used in this study for L-ASNase production was a recombinant *Bacillus Subtilis*. This microorganism was successfully genetically modified with the insertion of *Vibrio fischeri* gene (ansB) able to produce L-ASNase type II. The production step was carried out by another master student from the same research group.

2. Experimental section

2.1 Materials

The experimental part of this work is divided in three main tasks: (i) synthesis of SILs and its characterization, (ii) immobilization of pure commercial L-ASNase onto SILs and (iii) immobilization of L-ASNase from a cell extract preparation onto SILs. All the materials used in both parts are listed in **Table 6**, along with the information of their degree of purity and its respective supplier.

Table 6: Materials used for the synthesis of SILs and preparation of solutions, with the respective degree of purity and supplier.

Reagent	**Purity**	**Supplier**
Albumine bovine / fraction V	98%	Acros Organics
Asparagine	99%	Acros Organics
Bromophenol blue	Pure	Merck
Citric acid 1-hydrate ($C_6H_8O_7 \cdot H_2O$)	99.5-102%	Panreac
Coomassie Brilliant Blue G-250	Ultrapure	Amresco
Dimethyloctylamine	95%	Sigma-Aldrich
Disodium phosphate heptahydrate ($Na_2HPO_4 \cdot 7H_2O$)	98.0-102%	Sigma-Aldrich
Dithiothreitol (DTT)	99.0%	Acros Organics
Ethanol	HPLC grade	Fischer Scientific
Glycerol	99.0%	Acros Organics
Hydrochloric Acid	37%	Sigma-Aldrich
L-Asparaginase*	>96.0%	Prospec
Methanol	HPLC grade	CHEM-LAB
Nessler reagent	Pure	Sigma-Aldrich
N,N-dimethylbutylamine	99%	Sigma-Aldrich

N,N-dimethylhexilamine	98%	Sigma-Aldrich
Silica Gel (60Å)	-	Merck
Sodium carbonate (Na_2CO_3)	99.0%	Vencilab
Sodium dodecyl sulfate (SDS)	99.0%	Acros Organics
Sodium hydrogen carbonate ($NaHCO_3$)	99.5%	Merk
Sodium hydroxide – pellets	98,0%	Fisher
Tributylamine	99%	Acros Organics
Trichloroacetic acid (TCA)	Analitic	Prolabo
Triethylamine	HPLC grade	Fisher Chemical
Trihexylamine	96%	Sigma-Aldrich
Trioctylamine	<98%	Fluka
Tris(hydroxymethyl)aminomethane ($(HOCH_2)_3CNH_2$	99.0%	Alfa Aesar
Toluene	99.8%	Carlos Erba
3-chloropropyltrimethoxysilane	98%	Acros Organics

* purified from *E. coli* ASI.357

2.2 Synthesis of supported ionic liquids

The first step for the synthesis of SILs consisted in the treatment of silica gel, with pore size of 60 Å (0.2-0.5 mm), with hydrochloric acid (HCl) for 24h. This pre-treatment allowed the activation of the silica, with the increase of -OH groups at silica surface, prior to its functionalization with ILs. Before it can be used, the silica must be washed with water until the pH increases and equals the pH of the distilled water, and it was dried at 55ºC for 24h. Then 5.0 g of the activated silica was dispersed in 60 mL of toluene and placed in a round bottom flask with a reflux condenser and 5 mL of 3-chloropropyltrimethoxysilane was added. The suspension prepared was refluxed under magnetic stirring at around 100ºC for 24h. Subsequently, the pale yellow solid resulting from this reaction is filtrated and washed with several solvents and mixtures in the following order: 100 mL of toluene, 200 mL of ethanol:water 1:1 (v/v), 500 mL of water and lastly 100 mL of methanol. The material produced was dried in an oven at 50ºC for 24h and denominated [Si][C_3]Cl. For the second part of the functionalization, 5.0 g of [Si][C_3]Cl, 50 mL of toluene and 5 mL of a cation source, for example, N,N-dimethylbutylamine, were put in a round bottom flask and refluxed under magnetic stirring for 24h. Thereupon the material was filtrated and washed with 100 mL of toluene, 350 mL of methanol, 350 mL of water, 150 mL of methanol and finally dried at 50ºC for 24h. The SIL obtained was N,N-dimethylbutylamine-based supported silica with chloride as the counter ion ([Si][N_{3114}]Cl), and the preparation route is shown in **Figure 13**.

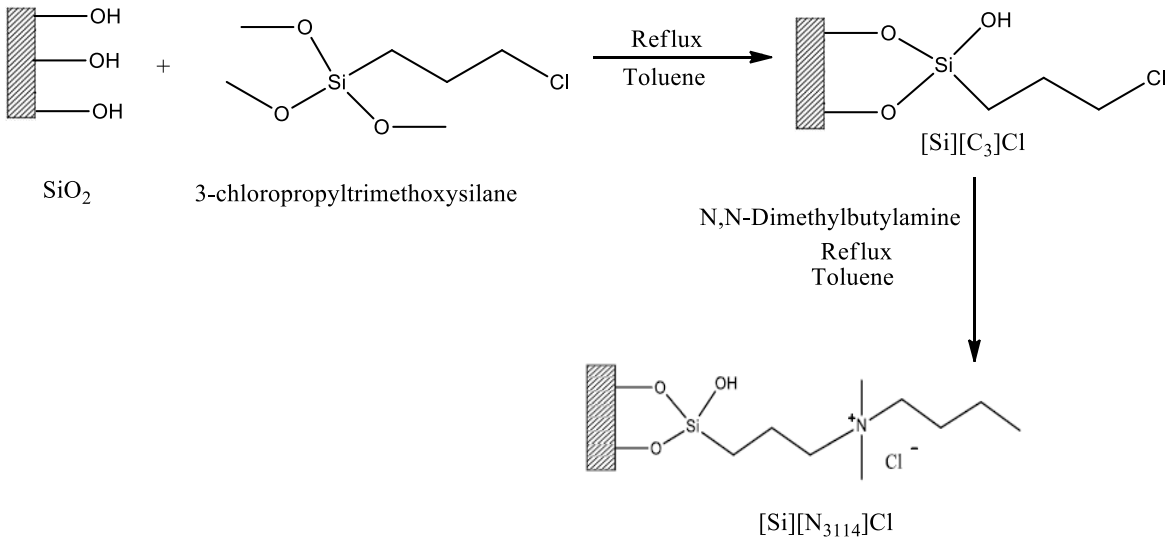

Figure 13: Scheme for the synthesis of SILs.

The synthesis was repeated using different cation sources, namely N,N-dimethylhexilamine, dimethyloctylamine, triethylamine, tributylamine, trihexilamine and trioctylamine, and all the resulting SILs are displayed in **Table 7**.

Table 7: SILs synthesized and corresponding abbreviation, cation source and number of mols used in the corresponding synthesis.

SIL abbreviation	Structure of materials	Cation source	n (mol)
[Si][C$_3$]Cl	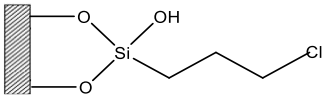	-	-
[Si][N$_{3114}$]Cl	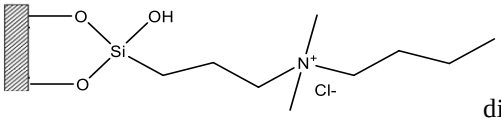	N,N-dimethylbutylamine	0.035
[Si][N$_{3116}$]Cl	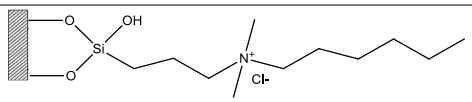	N,N-dimethylhexilamine	0.028
[Si][N$_{3118}$]Cl	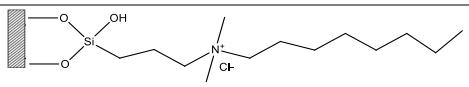	Dimethyloctylamine	0.023
[Si][N$_{3222}$]Cl	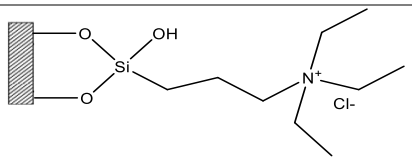	Triethylamine	0.036
[Si][N$_{3444}$]Cl	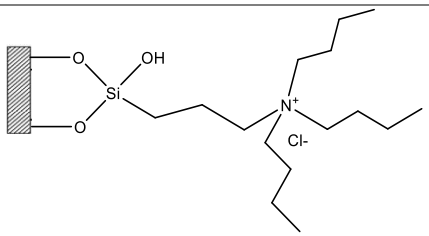	Tributylamine	0.021
[Si][N$_{3666}$]Cl	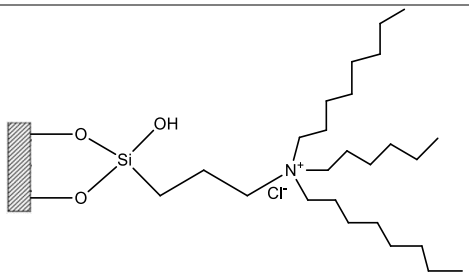	Trihexilamine	0.014

[Si][N_{3888}]Cl	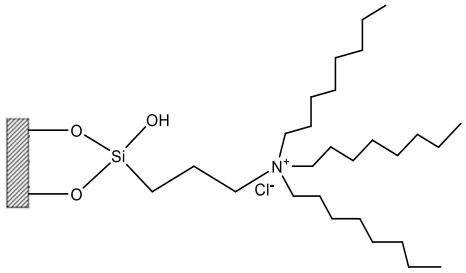	Trioctylamine	0.011

As depicted, the volume added of cation source was 5 mL for all of the SILs, and since they all have different molecular weight and densities (**Table 8**) the molar amount added in the synthesis of different SILs was different, which is also shown in **Table 7**.

Table 8: Volume (V), molecular weight (M), density (d), purity (% (w/w)) and number of moles (n) of the cation source used in the synthesis of the corresponding SIL.

SIL	V (ml)	M (g/mol)	d (g/ml)	%(w/w)	n (mol)
[Si][N_{3114}]Cl	5.0	101.19	0.721	0.99	0.035
[Si][N_{3116}]Cl	5.0	129.24	0.744	0.98	0.028
[Si][N_{3118}]Cl	5.0	157.30	0.765	0.95	0.023
[Si][N_{3222}]Cl	5.0	101.19	0.726	0.99	0.036
[Si][N_{3444}]Cl	5.0	185.35	0.778	0.99	0.021
[Si][N_{3666}]Cl	5.0	269.51	0.794	0.96	0.014
[Si][N_{3888}]Cl	5.0	353.67	0.811	0.98	0.011

2.3 Characterization of the supported ionic liquids

All the prepared SILs were chemically and surface characterized by elemental analysis, FTIR spectroscopy and point zero charge (PZC).

2.3.1 Elemental analysis

The content (weight percentage) of carbon, hydrogen and nitrogen of the SILs were determined by elemental analysis using the equipment TruSpec 630-200-200, with a sample of ~2 mg, combustion furnace temperature of 1075ºC and after burner temperature of 850ºC.

The detection method for carbon and hydrogen was infrared absorption and for nitrogen was used thermal conductivity.

2.3.2 Attenuated total reflectance – Fourier-transform infrared spectroscopy (ATR-FTIR)

Infrared spectroscopy was assessed by ATR-FTIR analysis. This technique was executed using a spectrophotometer of FTIR (Perkin Elmer FT-IR System Spectrum BX) and a solid sample of each SIL, at 25ºC and between 4000-400 cm^{-1}. The samples were scanned 128 times in a resolution of 8.0 cm^{-1} and interval of 2.0 cm^{-1}.

2.3.3 Point of zero charge (PZC)

The PZC of all SILs was determined by the measurements of zeta potential of aqueous suspensions of the materials in a wide range of pH values. To adjust the pH of the SILs suspensions, aqueous solutions of NaOH and HCl 0.01M were used. These results were acquired by the equipment Malvern Zetasizer Nano ZS (Malvern Instruments Ltd. Malvern) at room temperature (25ºC) and using an appropriate cell to perform this experiment.

2.4 L-ASNase activity measurement

There are several quantification techniques used for the measurement of the L-ASNase activity. The most widely applied method for L-ASNase quantification is the colorimetric Nessler method, which quantifies ammonia. This method was used according to Magri et al.,[160] and consists of the reaction of Nessler's reagent (composed of dipotassium tetraiodomercurate (II), an alkaline solution) with the ammonia released during the L-Asp hydrolysis by L-ASNase (nesslerization), as expressed in equation (1). This reaction produces a characteristic yellow reaction mixture that can be quantified by spectrophotometry. The yellow color intensity of the solution is proportional to the initial ammonia concentration, allowing an indirect measurement of the enzymatic activity.[160] L-ASNase activity was measured with aqueous solutions by UV-Vis spectroscopy, using microplate spectrophotometer.[161,162]

$$NH_3 + 2(HgI_4)^{2-} + 3OH^- \rightarrow OHg_2(NH_2)I + 7I^- + 2H_2O \qquad (1)$$

Product colour- yellow

The experimental procedure comprises the addition of 50 µL of free L-ASNase or 1 mL of L-ASNase with each SIL (immobilized enzyme) to 500 µL of Tris-HCl buffer (pH 8.6, 50 mM), 50 µL of 189 mM L-ASN solution and 450 µL of deionized water and incubated at 37 ºC for 30 min under stirring. Then, the enzymatic reaction was interrupted by adding 250 µL of TCA (1.5 M) to the mixtures. Afterwards, the ammonia amount released after the hydrolysis of L-ASNase was measured by adding 100 µL of each sample with 250 µL of Nessler's reagent and 2.15 mL of deionized water. The control solution was prepared with 100 µL deionized water.

After incubation during 30 min, the absorbance was determined at 436 nm, and the free L-ASNase activity (U mL^{-1}) and immobilized L-ASNase activity (U mg^{-1}) in enzyme unit (U) were calculated according to equations (2) and (3), respectively.

One unit of free L-ASNase activity (U) is described as the quantity of enzyme that produces 1 µmol of ammonia per minute (equation (2)).

$$\text{ASNase activity (U mL}^{-1}) = \frac{[NH4^+] \times \text{Volume of enzimatic reaction } (V_R) \times \text{Volume of Nessler method } (V_{Nessler})}{\text{Volume of reacted soluction } (V_T) \times \text{ Incubation time } (t_r) \times \text{Volume of enzyme } (V_E)} \quad (2)$$

where $[NH_4^+]$ is the ammonia concentration in solution (μmol mL^{-1}), V_R is the total volume of the solution where the enzymatic reaction occurs (mL), $V_{Nessler}$ is the total volume of the solution for quantification of ammonia with Nessler (mL), V_T is the V_R transferred to the tube with Nessler and distilled water (mL), t_r is the reaction time (min) and V_E is the total volume of L-ASNase sample (mL).

One unit of immobilized L-ASNase (U) is described as the quantity of enzyme that produces 1 μmol of ammonia per minute and per mass of support at 37 °C (equation (3)).

$$\text{ASNase activity (U mg}^{-1}) = \frac{[NH4^+] \times \text{Volume of enzimatic reaction } (V_R) \times \text{Volume of Nessler method } (V_{Nessler})}{\text{Volume of reacted soluction } (V_T) \times \text{ Incubation time } (t_r) \times \text{Mass of material } (m_S)} \quad (3)$$

where m_S is the mass (mg) of support.

2.4.1 Effect of SILs on the Nessler method

The effect of SILs on the Nessler method was evaluated in order to select the SILs with negative reaction when in contact with Nessler's regent, to subsequently properly determine the recovered activity of L-ASNase. For this study, 10.0 mg of each SIL was added to 250 μL of Nessler's reagent and 2.15 mL of deionized water. A control was also prepared without SIL material. After incubation during 30 min, the absorbance was determined at 436 nm, since one of the products from the Nessler reaction absorbs in the visible region.[162]

2.5 Optimization of L-ASNase immobilization conditions

In this study, the immobilization of commercial L-ASNase was evaluated through adsorption onto SILs. Initially, the different immobilization conditions were optimized (contact time, medium pH, and L-ASNase/SIL ratio) to improve the enzyme loading and enzyme activity.

L-ASNase immobilization was performed by adding 10.0 mg of each SIL to 1 mL of an L-ASNase solution (8.6×10^{-2} mg mL^{-1}) in an appropriate buffer solution under stirring for 1 h at room temperature. Specific conditions of each optimization are detailed below.

The immobilization yield (IY, %), determined in each condition, is the difference between the enzyme activity (calculated as previously described) of the free enzyme before L-ASNase immobilization and the activity of the free enzyme remaining in the supernatant after immobilization, divided by the free enzyme activity before immobilization, as demonstrated in equation (4).

$$\text{IY}\ (\%) = \frac{\text{free enzyme activity}\left(\frac{\text{U}}{\text{mL}}\right) - \text{supernatant activity}\left(\frac{\text{U}}{\text{mL}}\right)}{\text{free enzyme activity}\left(\frac{\text{U}}{\text{mL}}\right)} \times 100 \qquad (4)$$

2.5.1 Optimization of L-ASNase concentration

The enzyme concentration was optimized by performing the immobilization at different concentrations of L-ASNase: from 1.0×10^{-2} to 1.4×10^{-1} mg mL^{-1}, pH 8.0 and 30 min of contact time. To measure the immobilized enzyme activity (U mg^{-1}) and IY (%), the method described in section 2.4 was used according to equations (3) and (4), respectively.

2.5.2 Optimization of the pH of the enzymatic medium

The pH was evaluated at 0.6×10^{-2} mg mL^{-1} of L-ASNase by using citrate/phosphate buffer (50 mM) for pH 5.0, 6.0, 7.0 and 8.0. To measure the immobilization enzyme activity (U mg^{-1}) and IY (%), the method described in section 2.4 was used according to equations (3) and (4), respectively.

2.5.3 Optimization of L-ASNase incubation time

The contact time was optimized at 0.6×10^{-2} mg mL^{-1} of L-ASNase and pH 8 by performing the immobilization in different intervals of time: from 30 to 120 min at room temperature. To measure the immobilization enzyme activity (U mg^{-1}) and IY (%), the method described in section 2.4 was used according to equations (3) and (4), respectively.

2.6 Thermal stability of free and immobilized L-ASNase

The stability of the L-ASNase to temperature was determined by incubating the free and immobilized enzyme (without its substrate) for different time intervals (0 to 165 min) at different temperatures (60 and 80 ºC). Samples of the enzyme solution and of immobilized L-ASNase on SILs were kept in a temperature-controlled water bath. After the end of the incubation periods, a sample was taken, the substrate L-ASN was added and the enzymatic activity was immediately determined according to the above described methods.

2.7 Adsorption isotherms studies

Adsorption is the aggregation of matter from a gas or liquid to the surface of an adsorbent, it depends on the existence of a force field at the surface of the solid.[163] There are two classes of adsorption, physical and chemical adsorption (chemisorption) according to the nature of the surface forces.[164] In the physical adsorption the forces mainly involved are dispersion-repulsion forces (van der Waals forces) complemented by various electrostatic contributions which are crucial for polar adsorbents. The forces of chemisorption are stronger and involve electron transfer or electron sharing, forming a chemical bond. Therefore, chemisorption is highly specific, and the adsorption energies are typically greater than those for physical adsorption.[163] Chemisorption is limited to a monolayer coverage of the surface while, in physical adsorption, multilayer adsorption is possible.[163] The capacity for physical adsorption matches the specific micropore volume. Van der Waals are dominant in non-polar adsorbents and the affinity is determined by size and polarizability of the sorbate and dimensions of the pore. Non-polar adsorbents are often described as hydrophobic since they have low affinity for water and higher affinity for organic molecules.[163]

The challenge in the field of adsorption is to find the most promising type of adsorbent. Thus, the isotherms models can help the pursue to find the more appropriate ones and to find reasonable explanation for the mechanisms behind the adsorption process.[165,166] Adsorption isotherms are quantitative models used to characterize the retention or mobility of a substance from an aqueous media to a solid phase at a constant temperature and time of contact.[167,168] The adsorption equilibrium is reached when an adsorbate containing phase has been in contact with the adsorbent for enough time, which means the adsorbate concentration in the solution is in a dynamic balance with the solid interface.[168]

In the literature a wide variety of isotherm adsorption models have been applied, they can be classified as irreversible isotherms and one-parameter isotherms, two-parameter isotherms, three-parameter isotherms and more than three-parameter isotherms. Although adsorption isotherms are less helpful in elucidating adsorption mechanisms than adsorption kinetics they are very helpful to describe the relationship between the adsorbate concentration in solution and the adsorbent at a constant temperature and to design adsorption systems.[168] The models commonly used for adsorption isotherms are Langmuir and Freundlich isotherms, they differ from each other because Langmuir model assumes a

totally homogeneous adsorption surface whereas Freundlich isotherm is suitable for a heterogenous surface.[169,170]

2.7.1 Data analysis of the results

The adsorption equilibrium behaviour of the L-ASNase was determined by Langmuir and Freundlich isotherms. The Langmuir isotherm model can be effectively applied to multiple adsorption processes, being the best-known isotherm describing sorption. The parameters of this model were calculated by non-linearized fitting of equation (5) to the experimental data:

$$q = \frac{q_{max} * K * C}{1 + K * C} \quad (5)$$

where q is the amount of adsorbed active L-ASNase per milligram of SIL (U mg^{-1}), q_{max} is the maximum adsorption capacity of active L-ASNase (U mg^{-1}), K is the Langmuir equilibrium adsorption constant (mL mg^{-1}) associated to the strength of affinity between the L-ASNase and the SIL surface[171] and C is the L-ASNase concentration (mg mL^{-1}). This equation assumes that a fixed number of accessible sites are available on the adsorbent surface and they all have the same energy, it also assumes that the adsorption is reversible, that once an adsorbate lodges in a site no further adsorption can occur in that spot, there is no interaction between adsorbate species and the adsorbent gets saturated once a monolayer is formed on the surface.[167,172,173]

The Freundlich isotherm is commonly used for the adsorption of organic components in solution or highly interactive species on activated carbon and molecular sieves.[174,175] Is an exponential equation and it presumes that the concentration of adsorbate on the surface increases as the adsorbate concentration increases, assuming that multiple layers could occur instead of a single layer.[172] The parameters of the Freundlich model were determined by the non-linear fitting of the equation (6) to the experimental data:

$$q_e = K_F \times C^{1/n} \quad (6)$$

where K_F (mg mg^{-1}) is the Freundlich binding constant related to L-ASNase adsorption per weight of SIL, and *n* is an empirical parameter, which measures the intensity of adsorption in Freundlich adsorption isotherms.[171,176]

The modelled data for the adsorption of L-ASNase onto SILs and activated silica resulting from these adjustments, i.e., the parameters of the isotherms equations (5) and (6) and the correlation coefficients (R^2) were determined using the CurveExpert_v_nova software. L-ASNase concentrations from 1.0×10^{-2} to 1.4×10^{-1} mg mL^{-1} were applied in the equilibrium studies. The equilibrium time was fixed at 60 min and pH 8.0.

2.8 Cell extract preparation

The cell extract preparation stage was carried out in another work by the same research group. The enzyme extract production was carried out using a SmF. Firstly, a pre-inoculum was manufactured by adding 5 mL of Luria Bertani (LB) broth, 5 µL of Erythromycin (1 mg mL^{-1}) and 1 µL of the microorganism (*Bacillus subtilis*) into a falcon tube. The mixture was incubated overnight at 37ºC at 250 rpm. Subsequently, 50 mL of LB broth, 50 µL of Erythromycin (1 mg mL^{-1}) and a pre inoculum volume was added to an Erlenmeyer to start the inoculum.

After, the inoculum is incubated at 37ºC and 250 rpm. Then, an aqueous solution of xylose (50%) is added to the inoculum (final xylose concentration in the inoculum is 0.5% (w/v), according the final concentration studied), to induce the production of L-ASNase. The mixture was incubated during 8-36h at 30ºC and 210 rpm. All the materials and solutions were previously sterilized in autoclave and all the procedure was performed in a laminar flow chamber.

Since the production of L-ASNase is intracellular, a cellular lysis was carried out after the fermentation process. The total fermentation volume was transferred to a falcon tube and centrifugated for 20 min at 5000 rpm. The supernatant was discarded, and the cells were resuspended in 5 mL of phosphate-buffered saline (PBS). Following this, the solution

was taken to ultrasound and each sample was treated with 90 cycles of 5s of pulse and 10s of inactivity. To conclude this process, the mixture was centrifugated during 10 min at 4000 rpm, and the supernatant containing L-ASNase was analysed.

2.8.1 Total protein concentration

The protein concentration of L-ASNase extract was determined by direct spectrophotometric by the measuring absorbance at 280 nm (A_{280}). This method is based on the inherent absorbance of UV light by the aromatic amino acids tryptophan and tyrosine, as well as by cystine (disulfide-bonded cysteine residues).[177] The measured absorbance of a protein sample solution is used to calculate the concentration by comparison with a calibration curve prepared from measurements with standard protein solutions, in this case bovine serum albumin (BSA). From the total protein concentration and enzyme extract activity, it is possible to calculate the specific enzyme activity (U mg^{-1}), the number of enzyme units per mL divided by the concentration of total protein in mg mL^{-1}, which is indirectly determined by equation (7):

$$\text{Specific activity (U mg}^{-1}) = \frac{\text{Enzymatic activity } (\frac{\text{U}}{\text{mL}})}{\text{Total protein } (\frac{\text{mg}}{\text{mL}})} \quad (7)$$

2.8.2 Protein profile of L-ASNase samples

The proteins profiles of the commercial L-ASNase and enzyme extract were determined by SDS-PAGE (sodium dodecyl sulfate-polyacrylamide gel electrophoresis). The samples were diluted at a 1:1 (v/v) ratio in a sample buffer composed by 2.5 mL of 0.5 M Tris-HCl pH 6.8, 4.0 mL of 10 % (w/v) SDS solution, 2.0 mg of bromophenol blue, 2.0 mL of glycerol and 310 mg of DTT (added at the moment). After this dilution, the samples were heated for 5 min at 95 ºC, to break up the quaternary structure and deconstruct part of the tertiary structure by reducing the disulfide bonds and denaturing the proteins.

The diluted samples were loaded and run on a polyacrylamide gel (stacking: 4 % and resolving: 20 %). To stain the proteins the gels were impregnated with BlueSafe and stirred in an orbital shaker at 50 rpm for 40 minutes at room temperature. GRS Protein Marker MultiColour (grisp Research Solutions) was used as molecular weight standards while lyophilized and purified L-ASNase from *E. coli* (P1321-10000; 10 000 IU) was used as a pure L-ASNase standard.

2.8.3 Purity of the L-ASNase extract after immobilization

To determine the L-ASNase purity in the L-ASNase extract after immobilization size-exclusion high-performance liquid chromatography (SE-HPLC) was applied. A calibration curve was determined for this purpose using commercial purified L-ASNase from *E. coli* (P1321-10000; 10 000 IU). A phosphate buffer solution (1000 mL), used as mobile phase, was prepared using 47 mL of a Solution A (27.8 g of NaH_2PO_4), 203 mL of a Solution B (53.65 g $Na_2HPO_4.7H_2O$) and 17.5 g of NaCl. Each sample was diluted at a 1:9 (v/v) ratio in the phosphate buffer and then injected on a *Chromaster HPLC system* (*VWR Hitachi*). The SE-HPLC was performed on an analytical column *Shodex Protein KW-802.5* (8 mm x 300 mm). The mobile phase, a 50 mM phosphate buffer + NaCl 0.3 M, ran isocratically with a flow rate of 0.5 mL/min and the injection volume was 25 µL. The column oven and autosampler temperatures were kept at 25ºC and at 10ºC, respectively. The wavelength was set at 280 nm using a DAD detector. The obtained chromatograms were treated and analysed using the PeakFit version 4 software.

The L-ASNase purity was calculated based on equation (8). The purity (% L-ASNase Purity) was determined by the ratio between the peak area of L-ASNase and the area of all peaks of the chromatogram, corresponding to other proteins present in the samples (A_{Total}).

$$\%\text{Purity} = \frac{A_{L-ASNase}}{A_{Total}} \times 100 \quad (8)$$

3. Results and Discussion

3.1. Synthesis and characterization of SIL's

3.1.1 Elemental analysis

Elemental analysis of the SIL was carried out to quantitatively determine the carbon, hydrogen, and nitrogen contents of the prepared SILs, whose results are provided in **Table 9**.

Table 9: Content of carbon, hydrogen and nitrogen (in weight percentage, w%) for the synthetized SILs.

Material	%C	%H	%N
[Si][C_3]Cl	4.637	1.394	0.000
[Si][N_{3114}]Cl	7.719	1.840	0.767
[Si][N_{3116}]Cl	10.715	2.324	0.986
[Si][N_{3118}]Cl	10.923	2.334	0.788
[Si][N_{3222}]Cl	7.289	1.509	0.263
[Si][N_{3444}]Cl	5.741	1.336	0.148
[Si]N_{3666}]Cl	6.551	1.522	0.087
[Si][N_{3888}]Cl	6.899	1.335	0.071

From the elemental analysis it can be conclude that all the SILs samples contain in their composition nitrogen. The carbon and nitrogen contents (w%) range from 4.64 to 10.92% and from 0.07 to 0.99%, respectively. It should be noted that no nitrogen was detected in **[Si][C_3]Cl**, the intermediate material of the two-step reaction, supporting the absence of IL organic moieties. On the other hand, the presence of nitrogen, carbon and hydrogen demonstrate that the studied ILs were successfully covalently attached to the silica surface, because, as predicted the **[Si][C_3]Cl** don't present a nitrogen content but after the introduction of the cation source a nitrogen content is observed.

The percentage of nitrogen in SILs decreases as the length of alkyl chains increases. A likely reason for the decrease percentage of nitrogen is the fact that the volume used of

each amine was kept the same, 5 mL, and as explained in **Table 8** their densities are not the same and the molar mass increases has the length of the alkyl chain increases, so the molar amount of each amine introduced in the synthesis decreased with the increase of the molar weight. Therefore, the extend of the functionalization is lower in the SILs with bigger alkyl chain.

The bonding amount (BA) of ILs onto SILs was determined from the elemental analysis data obtained for each SIL. For these calculations, the specific surface area (S_{BET}) of the initial silica (435 m^2 g^{-1}) was used. This value was obtained in another work carried out in the research group. Thus, it was possible to combine the surface area of silica available to the functionalization with ionic liquids with the percentage of carbon found in [Si][C_3]Cl and nitrogen in each SIL to calculate the BA in mol m^{-2} to the silica by using the following equations:

$$BA = \frac{\frac{\%C}{3 \times M(C)}}{S_{BET}} \quad (9)$$

The equation (9) is used for the calculation of the bonding amount of [Si][C_3]Cl, %C was presented in **Table 9**, M(C) is the molar weight of carbon, which is 12 g mol^{-1}, and is multiplicated by three to represent the three carbons present in the molecule, and S_{BET} is the surface area of silica.

$$BA = \frac{\frac{\%N}{1 \times M(N)}}{S_{BET}} \quad (10)$$

The equation (10) is used for all SILs since the corresponding IL only have one atom of nitrogen in their structure. The %N is presented in **Table 9**, where M(N) is the molar weight of nitrogen (14 g mol^{-1}) and S_{BET} is the surface area of silica. These results are shown in **Table 10**.

Table 10: Amount of IL bounded to the silica matrix (μmol m^{-2}).

Material	Bonding amount (μmol/m^2)
[Si][C_3]Cl	2.96
[Si][N_{3114}]Cl	1.26
[Si][N_{3116}]Cl	1.62
[Si][N_{3118}]Cl	1.29
[Si][N_{3222}]Cl	0.43
[Si][N_{3444}]Cl	0.24
[Si]N_{3666}]Cl	0.14
[Si][N_{3888}]Cl	0.12

From these results we can conclude that after introducing the cation source not all the amines reacted with the amount of **[Si][C_3]Cl** existed on the surface of silica, meaning that every SIL material not only have the IL anchored to the surface but also have some [Si][C_3]Cl, without having reacted with the amine.

The SILs with a higher functionalization degree with the IL are the **[Si][C_{3114}]Cl, [Si][C_{3116}]Cl** and **[Si][C_{3118}]Cl** with values of 1.26, 1.62 and 1.29 μmol m^{-2} of bonding amount, respectively. On the other hand, **[Si][N_{3222}]Cl**, **[Si][N_{3444}]Cl**, **[Si][N_{3666}]Cl** and **[Si][N_{3888}]Cl** are poorly functionalized with the corresponding ILs, with values of 0.43, 0.24, 0.14 and 0.12 μmol m^{-2}, respectively. An explanation could be because the number of moles of tributylamine, trihexilamine and trioctylamine used in the synthesis was less than the number of mols used of N,N-dimethylbutylamine, but this explanation is not consistent with the behaviour observed for triethylamine, for example.

In order to increase the functionalization degree, the molar amount of amines introduced in the second step of the synthesis should be kept the same, which means changing the volume added of each amine. In this work, the added volume of the amine was changed only in the synthesis of **[Si][N_{3222}]Cl**, in which the volumes of 1.0, 2.0, 7.5 and 10.0 mL were also used (**Table 11**).

Table 11: Volume (mL) and number of mols (n) of triethylamine used in the several synthesis of **[Si][N_{3222}]Cl** materials and the content of carbon, hydrogen and nitrogen (w%) and bounding amount (µmol m^{-2}) for the synthetized [Si][N_{3222}]Cl SILs.

Cation source	V (mL)	n (mol)	%C	%H	%N	Bounding amount (µmol/m^2)
Triethylamine	1.0	0.007	6.838	1.682	0.220	0.36
	2.0	0.014	7.175	1.583	0.322	0.53
	5.0	0.036	7.289	1.509	0.263	0.43
	7.5	0.053	6.81	1.75	0.32	0.53
	10.0	0.071	6.95	1.76	0.40	0.65

The variation in the volume of amine for the synthesis of **[Si][N_{3222}]Cl** aimed to understand whether the increase in the volume of cation source would result in an increase in IL functional groups in this SIL. From the results obtained in **Table 11**, it can be concluded that, for the tested SIL, there was a small increase in the functionalization of the material, but that it is not proportional to the volume of amine used in its synthesis. The results do not follow a trend, and this SIL has a low level of functionalization for all conditions tested, achieving only a maximum value of 0.65 µmol m^{-2} using 10.0 mL of triethylamine. Therefore, for all tests performed in this work a volume of 5 mL of each amine was used.

3.1.2 Attenuated total reflectance – Fourier-transform infrared spectroscopy ATR - FTIR

Infrared spectroscopy is a useful technique for the identification of chemical modifications and to identify the surface composition which is important to understand the adsorption process. FTIR-ATR spectra of silica, [Si][C_3]Cl and SILs ([Si][N_{3116}]Cl and [Si][N_{3222}]Cl), was acquired and is given in **Figure 14**.

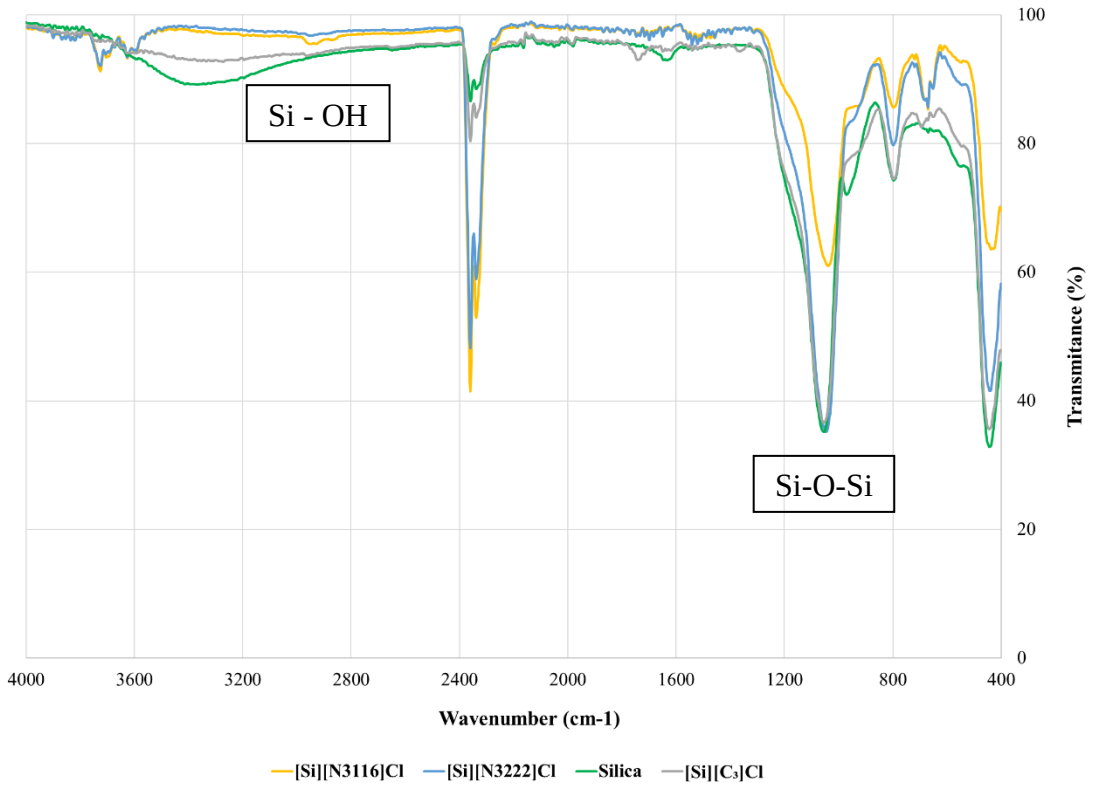

Figure 14: FTIR-ATR spectrum of the silica, [Si][C_3][Cl], [Si][N_{3116}]Cl and [Si][N_{3222}]Cl.

The broad absorption band around 1100 cm^{-1} and around 800 cm^{-1} was attributed to Si-O-Si asymmetric and symmetric vibration, respectively. This bond is presented in the matrix of the silica.[178] The absorption band at around 3000 cm^{-1} corresponds to the silane, Si-OH group.[179] For these two SILs this peak is weaker than the one found in silica, indicating the successful bonding of the ionic liquid because it means they reacted effectively. All the aliphatic carbons should appear around 2900 and 3000 cm^{-1}, but it is not possible to distinguish between them because of the presence of water.[180]

3.1.3 Point of zero charge

Zeta potential measurements were used to study the surface charge of the functionalized silica-based materials. Data of the zeta potential as a function of pH for the all synthesized SILs, silica and [Si][C_3]Cl are displayed in the **Figure 15**.

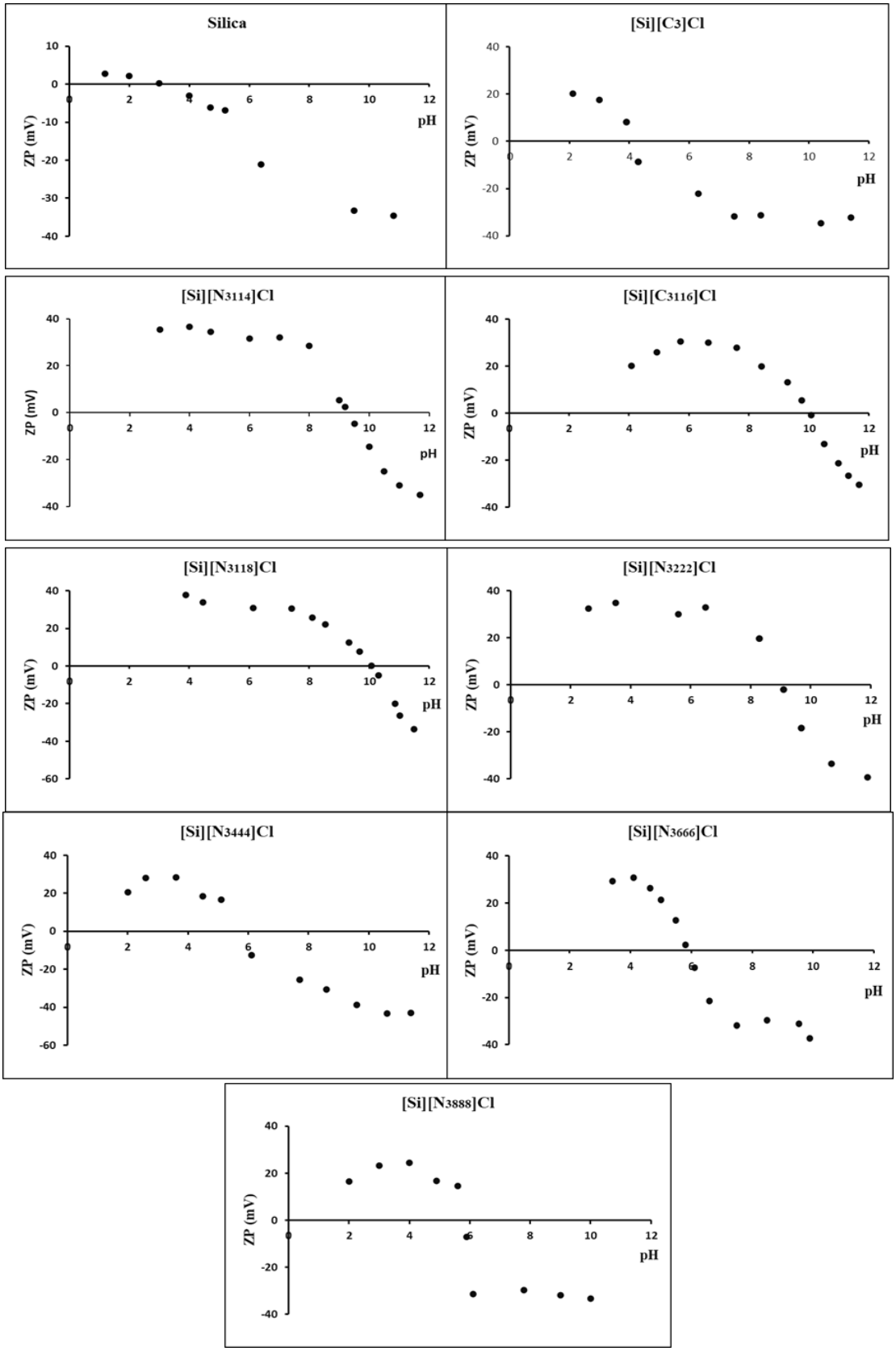

Figure 15: Zeta potential as a function of pH for silica, [Si][C_3]Cl and all the synthetized SILs ([Si][N_{3114}]Cl, [Si][N_{3116}]Cl, [Si][N_{3118}]Cl, [Si][N_{3222}]Cl, [Si][N_{3444}]Cl, [Si][N_{3666}]Cl and [Si][N_{3888}]Cl).

From these data, it was determined the point of zero charge (PZC), which is the pH value at which a solid particle in suspension exhibits zero net electrical charge on its surface. **Table 12** provides the PZC values of the prepared SILs, silica and [Si][C_3]Cl.

Table 12: PZC of silica, [Si][C_3]Cl and all the synthetized SILs ([Si][N_{3114}]Cl, [Si][N_{3116}]Cl, [Si][N_{3118}]Cl, [Si][N_{3222}]Cl, [Si][N_{3444}]Cl, [Si][N_{3666}]Cl and [Si][N_{3888}]Cl).

Sample	PZC
Silica	3.4
[Si][C_3]Cl	4.2
[Si][N_{3114}]Cl	9.3
[Si][N_{3116}]Cl	10.0
[Si][N_{3118}]Cl	10.1
[Si][N_{3222}]Cl	9.0
[Si][N_{3444}]Cl	6.0
[Si][N_{3666}]Cl	5.9
[Si][N_{3888}]Cl	5.5

The electrical state of an adsorbent's surface in solution can be characterized by the point of zero charge, that is defined as the solution conditions under which the surface charge density is equal to zero. This technique is frequently used to quantify surface charge and can be used to anticipate the coulombic interaction (opposite charges on the adsorbate and adsorbent induce coulombic attraction) between particle and ions.[167,181]

Amongst many physicochemical parameters used to characterize the solid-liquid interface, the zeta potential is crucial to explain the adsorption mechanism from an electrostatic adsorption point of view.[182]

From these results it can observed that the value of PZC for silica conforms to what is found in the literature.[183] The PZC of all of the SILs synthesized is higher when comparing with starting silica and [Si][C_3]Cl ranging from 5.5 ([Si][N_{3888}]Cl) to 10.1 ([Si][N_{3118}]Cl), confirming the presence of a cation in SILs (most positively charged surfaces) and the successful silica functionalization. From a structure point of view these results are in agreement with the successfully functionalization of the silica, because the cations are present and on the surface of the silica.[151] The difference between the PZC values of SILs might be due to the differences of functionalization since the lower values of PZC correspond to the SILs with lower bonding amounts, therefore, with less cations on the surface.

3.2 Effect of SILs on the Nessler method

The Nessler method was used to determine the recovered activity of L-ASNase in this work. Therefore, it was necessary to confirm if the SILs used could interfered with Nessler reagent to ensure a correct determination of L-ASNase activity. SILs were in contact with Nessler reagent for 30 min, since is the incubation time of Nessler method, and the macroscopic aspect of the mixtures was observed. In all investigated SILs the reaction mixture was clear, without turbidity and/or precipitate formation, which indicates that no material interferes on the L-ASNase activity determination, since no yellow solution was obtained (negative reaction). Therefore, all these materials were selected for the following tests (**Figure 16**).

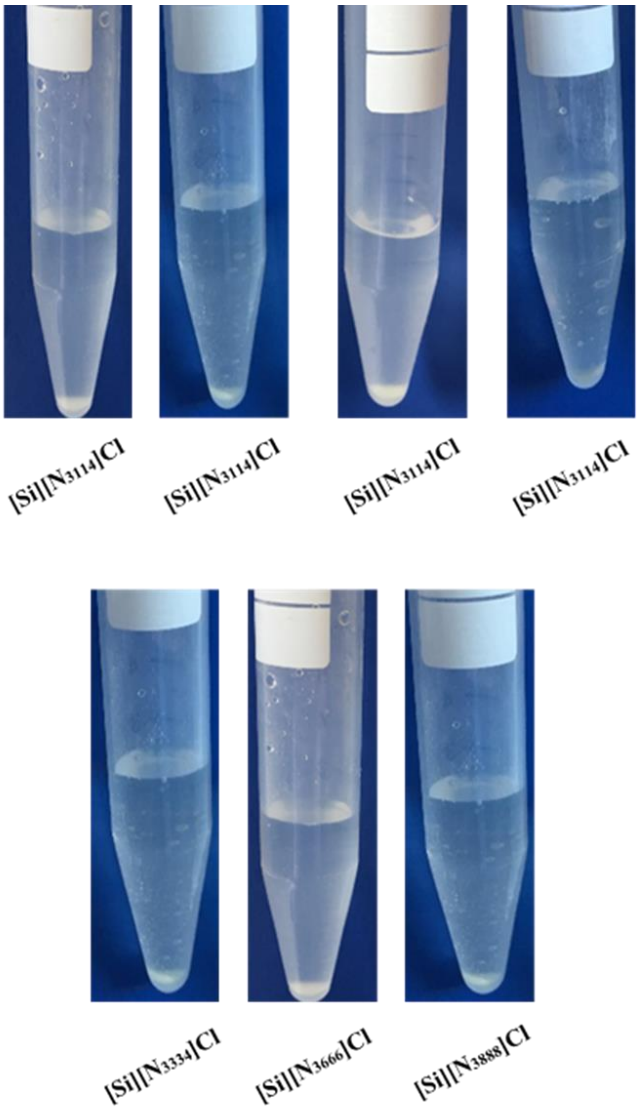

Figure 16: Investigation on the effect of each SILs on the Nessler method.

3.3 Optimization of L-ASNase immobilization conditions

3.3.1 Effect of L-ASNase concentration

The immobilization of L-ASNase onto SILs is expected to be influenced by L-ASNase concentration. In this sense, initial tests were conducted using six L-ASNase concentrations ranging from 1.0×10^{-2} to 8.0×10^{-2} mg mL^{-1}, at pH 8.0 and 30 min of contact time (**Figure 17**).

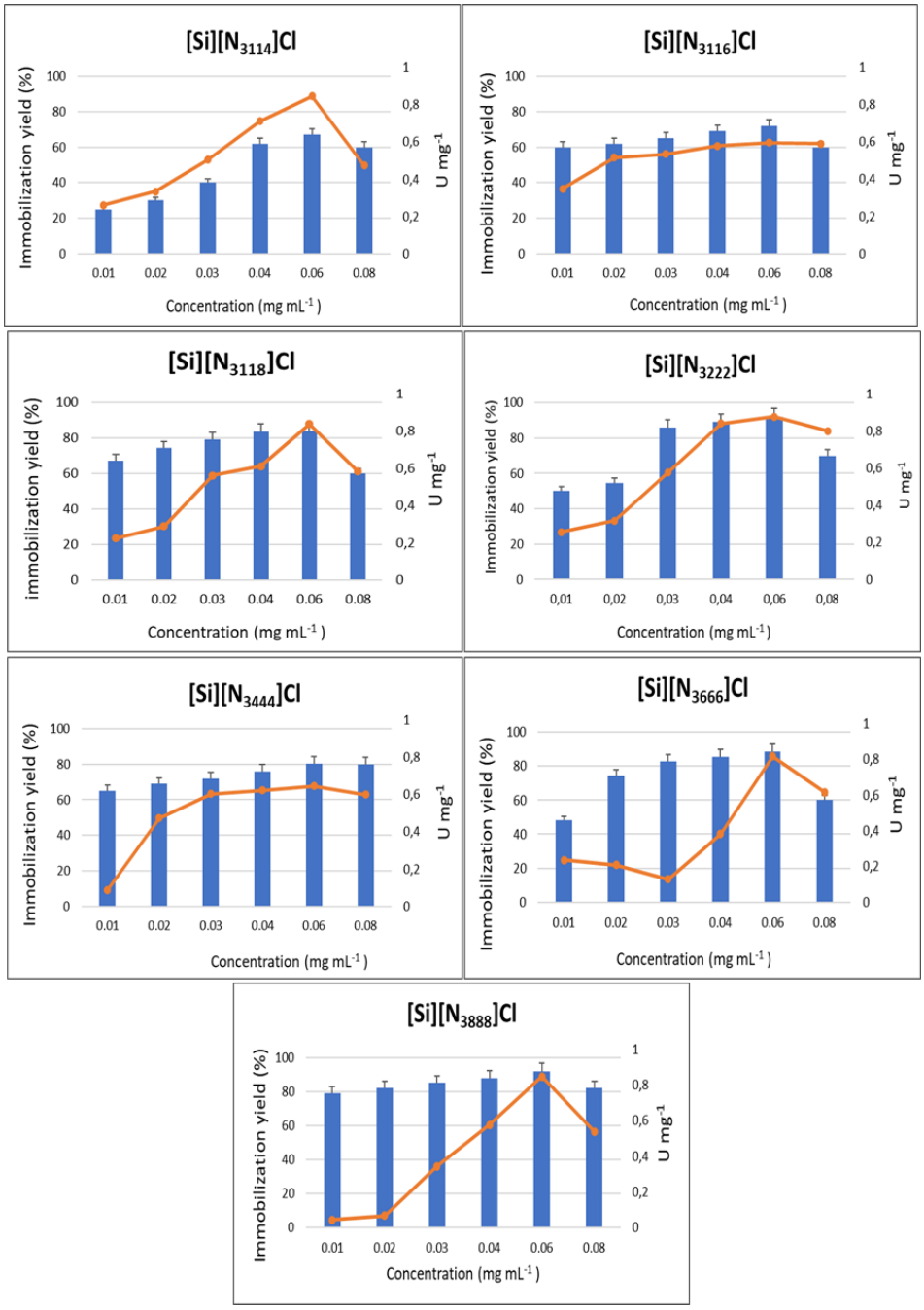

Figure 17: Effect of enzyme concentration on the immobilization yield (columns) and immobilized L-ASNase activity (symbols, line) with the immobilization of L-ASNase onto 10 mg of SILs at pH 8.0 for 30 min.

The efficacy of the immobilization was analysed through the balance between the IY and immobilized L-ASNase activity, whose results are given in **Figure 17**. The effect of enzyme concentration on the immobilization method showed a similar comportment for IY in all tested SILs. There is an increment in the IY with the increase of the L-ASNase content up to 6.0×10^{-2} mg mL^{-1}, and a slight reduce to the enzyme concentration of 8.0×10^{-2} mg mL^{-1}. Furthermore, an improvement in the immobilized L-ASNase activity was observed with the increase of the enzyme concentration from 1.0×10^{-2} to 6.0×10^{-2} mg mL^{-1}. This behaviour may be associated to a higher amount of L-ASNase molecules available to adsorb onto SILs surface, forming an enzyme layer, covering the SIL surface. However, the increment in the enzyme concentration up to 6.0×10^{-2} mg mL^{-1} shows a negative effect on the enzyme activity when compared with the concentration of 8.0×10^{-2} mg mL^{-1}, suggesting that the SILs surface attained its maximum adsorption capacity for this concentration, which is evaluated and explained below in the study of adsorption isotherms. So, considering the results obtained, the concentration of L-ASNase of **6.0×10^{-2} mg mL^{-1}** was chosen for the following assays.

3.3.2 Effect of pH

To attain the maximum IY and immobilized L-ASNase activity values, the influence of other key conditions, namely pH and contact time was then assessed.

L-ASNase is generally active across a wide pH range with optimum activity between pH 6.0 and 9.5, which gives a perception of the pHs where L-ASNase is most active, however, these values may not be where the immobilized enzyme exhibits the most activity.[2,119] The immobilization of ASNase onto SILs is expected to be influenced by pH, since it determines the surface charge of the enzyme and of the support. Thus, the tests were conducted varying the pH between 5.0 to 8.0 during the immobilization of 0.6×10^{-2} mg mL^{-}

[1] of L-ASNase onto SILs for 30 min taking into account the isoelectric point (IP) of L-ASNase and the data reported previously for the PZC of each SIL (**Figure 18**).

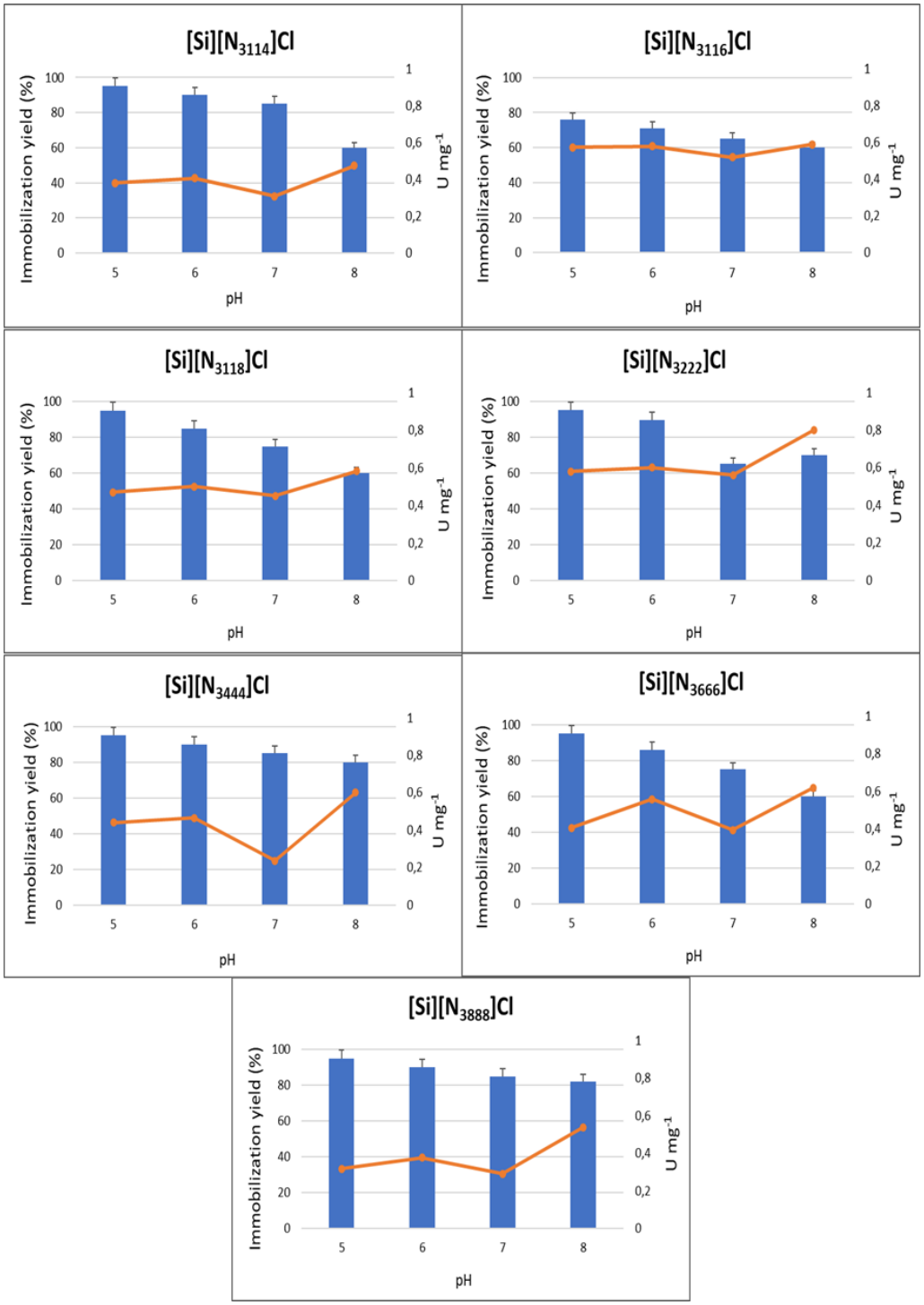

Figure 18: Effect of pH on the immobilization yield (columns) and immobilized L-ASNase activity (symbols, line) with the immobilization of 0.6×10^{-2} mg mL^{-1} of L-ASNase onto 10 mg of SILs for 30 min of contact time.

The effect of pH on the immobilization method showed a relatively similar behaviour for immobilized L-ASNase activity and IY in all tested SILs. According to **Figure 18**, the enzyme adsorption onto SILs was higher for pH 5.0, decreasing with the transition to more alkaline pHs. However, with regard to immobilized enzyme activity, L-ASNase exhibited more activity in all SILs at pH 8.0. An explanation for this behaviour may be the fact that the largest number of immobilized L-ASNase molecules can originate layers of enzyme that cause a decrease in the activity of the mixture.

It is known that the IP of the used L-ASNase is around 5.2.[184] In addition, the PZC of the SILs used in this work is greater than 5.5. Therefore, for values above pH 6 both enzyme and support are negatively charged, suggesting that electrostatic interactions are not expected to be responsible for the enzyme immobilization, which is in line with the decrease in IY with the increase of pH. Thus, from these results, the **pH 8** was selected for the following assays, since the L-ASNase activity is higher at this pH, and the differences in IY are not significant.

3.3.2 Effect of contact time

After the evaluation of the best L-ASNase concentration of 0.6×10^{-2} mg mL^{-1} and the optimal pH of 8.0, the adsorption of ASNase onto SILs was assessed for five contact times, between 30 to 120 min. **Figure 19** shows the effect of contact time on the IY and immobilized enzyme activity.

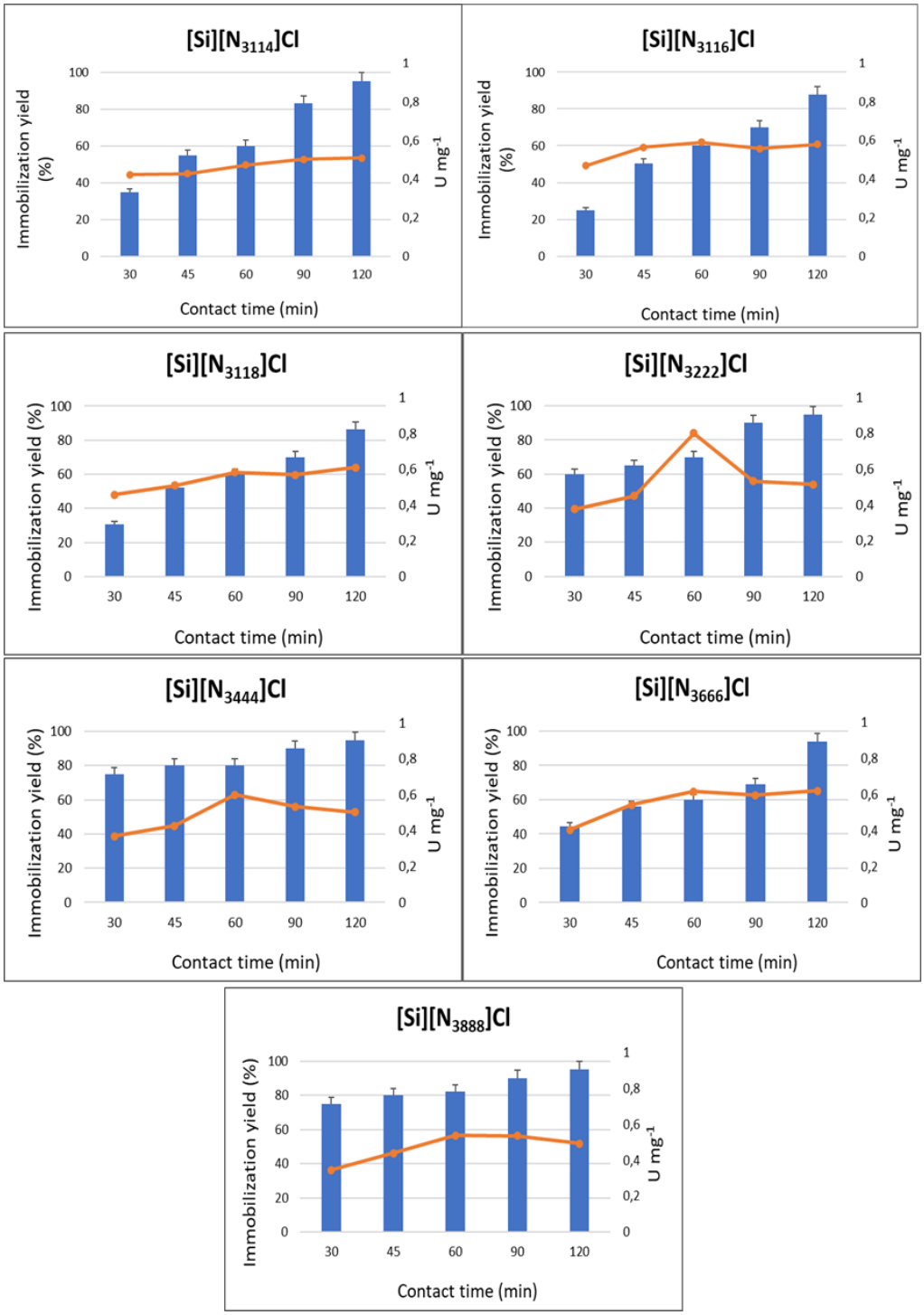

Figure 19: Effect of contact time on the immobilization yield (columns) and immobilized L-ASNase activity (symbols, line) with the immobilization of 0.6×10^{-2} mg mL^{-1} of L-ASNase onto 10 mg of SILs at pH 8.0.

Overall, there is an increase in the IY with time. For an immobilization time of 60 min, an IY above 60% was observed for all SILs, while this value was only achieved using the [Si][N_{3888}]Cl with lower contact times, 30 and 45 min. After 120 min of contact time between the enzyme and the SILs, an IY of 90% was reached for all SILs, except for [Si][N_{3118}]Cl. However, there is a decrease in the immobilized enzyme activity after contact times above 60 min, the time where the highest values of enzyme activity were found for all SILs. In fact, with lower amounts of immobilized enzyme, it will be more able to react by avoiding mass transfer restrictions that may occur with a higher enzyme loading. As more enzyme is immobilized, a multi-layered stacking of adsorbed L-ASNase or an uncontrolled enzyme packing during the immobilization procedure may occur, blocking the access of substrate molecules to the active site of L-ASNase. Therefore, **60 min** of contact time was selected for further experiments.

Considering the results gathered, the optimal conditions for the L-ASNase adsorption onto the SILs were a L-ASNase concentration of **6.0×10^{-2} mg mL^{-1}** at **pH 8.0** during a contact time of **60 min**. These conditions were used for all tests performed throughout this work.

In order to compare the results obtained with others in the literature, it should be noted that no scientific articles were found reporting the immobilization of L-ASNase using silica based SILs materials. However, a correlation was made with L-ASNase immobilization studies with other supports. Resorting to the literature (**Table 13**), the L-ASNase immobilization on other supports has been reported.

Table 13: Comparison of IY values reported in the literature on L-ASNase immobilization with those obtained in this work.

Immobilization method	Support	L-ASNase source	Results	Ref.
Adsorption	-COOH functionalized CNTs	*Aspergillus versicolor*	54.4% IY	[185]

Covalent binding	Silica gel	*Bacillus sp.* R 36	62.1% IY	[88]
Covalent binding	Activated silica	*Bacillus sp.* R 36	73.5% IY	[88]
Entrapment	-COOH functionalized CNTs; calcium alginate	*Escherichia coli*	97.0% IY	[186]
Adsorption	-COOH functionalized CNTs	*Escherichia coli*	>90.0% IY	[85]
Covalent binding	Silica gel	Thermophilic fungi	86.8% IY	[86]
Adsorption	Silica gel	*Vicia faba*	74.6% IY	[87]
Adsorption	[Si][N_{3222}][Cl]*	*Bacillus subtilis*	95.0% IY	This work

* Conditions used: L-ASNase concentration of 6.0×10^{-2} mg mL^{-1} at pH 8.0 during a contact time of 120 min.

Haroun et al.[185] tested oxidized multi-walled carbon nanotubes (MWCNTs) as a support for an *Aspergillus versicolor* L-ASNase reporting higher IY values using a physical adsorption technique than with the covalent binding of the enzyme to the support, with a maximum IY attained about 54.4%. In addition, immobilized L-ASNase activity exhibited maximum activity at 40ºC and alkaline pH (pH 8).[185] Moharam et al.[88] studied antitumor activity as well as immobilization parameters of *Bacillus subtilis R36* L-ASNase by covalent bonding with different supports. The authors described an efficiently L-ASNase immobilization with activated carbon and silica gel achieving a IY of 73.5 and 62.1%, respectively.[88] The immobilization of L-ASNase by entrapment was already reported in literature. Ulu et al.[186] described the use of a novel calcium-alginate/carboxylated multi-walled carbon nanotube hybrid bead (Ca-ALG/MWCNT-COOH) for the entrapment of L-ASNase reaching a high IY (97%) on these hybrid beads. The immobilized enzyme showed

maximum activity at 45 °C and pH 8.5 in this work. A recent study on L-ASNase immobilization on CNTs and carried out with physical adsorption in functionalized and then encapsulated CNTs. The adsorbed L-ASNase retains 90% of the initial enzyme activity at the optimized conditions (pH 8.0, 60 min of contact time, and 1.5×10^{-3} g mL^{-1} of L-ASNase).[85] Silica gel, activated carbon, celite, and tricalcium phosphate were used as support for immobilization of L-ASNase by Sundaramoorthi et al.[86] and El-Sayed et al.[87] Sundaramoorthi et al. produced L-ASNase from fungal isolates. They immobilized L-ASNase on these different supports via covalent binding and the highest immobilized activity and IY (87%) were obtained with silica gel support. On the other hand, El-Sayed et al. assessed immobilization, properties, and antitumor activity of L-ASNase of *Vicia faba*. They used simple adsorption as the L-ASNase immobilization method, and the best support was silica gel with a specific activity of 2.75 U mg^{-1} protein and IY of 74.6%. The immobilized enzyme retained activity in the alkaline pH range compared to the free enzyme, concluding that the stability of the immobilized L-ASNase was higher than that of the free L-ASNase at the alkaline pH range.

Comparing with the literature, it is noted that the IY achieved in this work using the SILs as a support were very high, showing that these materials can be a good support for the immobilization of this enzyme. Although this is simply a physical adsorption process and the same enzyme was used, the results of this work were similar or better than those previously reported. SILs provided a relatively high enzyme loading by this method, highlighting the easy accessibility of enzyme's active sites by the substrate.

3.4 Thermal stability of free and immobilized L-ASNase

For the following assays on the thermal stability of commercial L-ASNase, the conditions previously optimized for L-ASNase immobilization were used. Free enzyme and the best and the worst SIL according to the enzyme adsorption test, **[Si][N_{3222}]Cl** and **[Si][N_{3116}]**, respectively, were used. The temperature impact on L-ASNase stability was studied, taking into account that in the literature is reported that this enzyme is thermostable.[187,188] The thermal stability of L-ASNase as a function of the time of the reaction is represented in **Figure 20**.

The stability of the L-ASNase was expressed as a percentage of residual activity compared to the initial activity of the untreated enzyme activity, incubated at room temperature (25ºC), which considered as a control (100%).

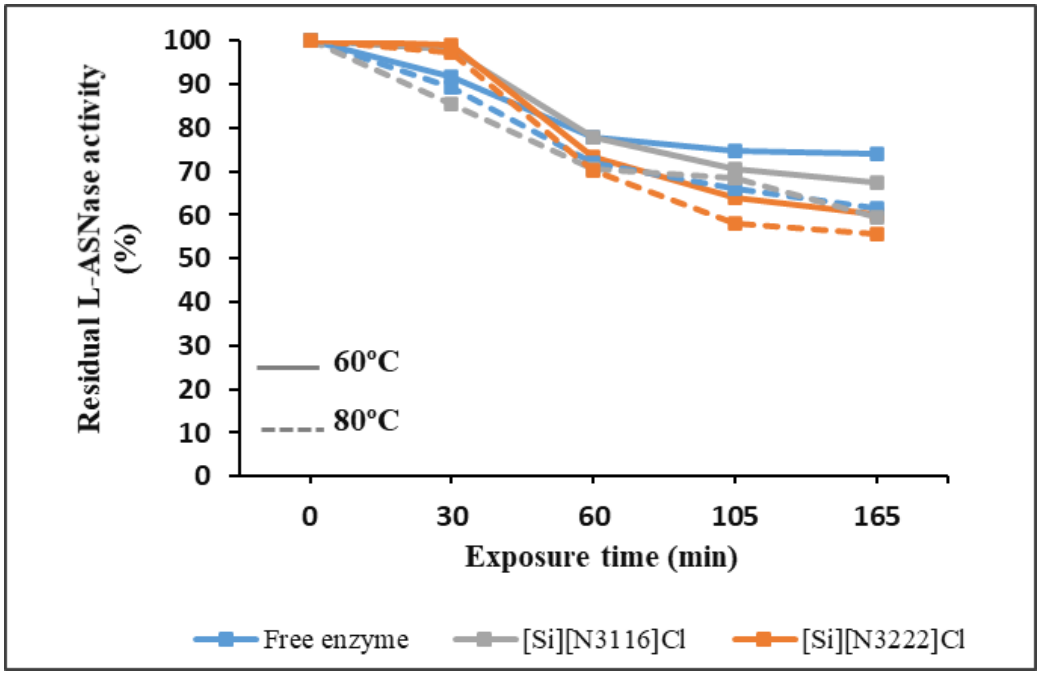

Figure 20: Thermal stability at 60ºC (solid line) and 80ºC (dashed line) of L-ASNase as a function of the time of the reaction. Room temperature (25ºC) was considered as a control (100%).

The effect of temperature on the stability of free and immobilized L-ASNase showed maximum retained enzyme activity at 60 °C. More than 98% of the initial activity was retained by the immobilized enzyme after 30 min of incubation at 60 ºC. On the other hand, enzyme exposure to higher temperatures and to an incubation time of more than 30 min led to observed decrease in retained L-ASNase activity. For both the free enzyme and the immobilized enzyme the results are similar, about 25% of L-ASNase activity was lost after incubation at two temperatures for 60 min, while a rapid decrease in the enzyme activity was observed after incubation for more than this time. It is noted that for immobilized L-ASNase on [Si][N_{3222}]Cl the residual activity decreased by 60 and 55% for an exposure time of 165 min after incubation at 60 and 80 ºC, respectively. It can be concluded from the previous results that the higher thermal stability behaviour of the enzyme was at 60 ºC compared to 80 ºC, and that the thermostability of immobilized L-ASNase on SILs is similar to that of free enzyme and there were no significant changes in the activities.

Zhang et al.[189] investigated the effect of the temperature on the activity of immobilized L-ASNase and concluded that the thermostability of the immobilized enzyme on the microparticles of the natural silk sericin protein is identical to that of free enzyme and there were no obvious changes in the activities. The optimum reaction temperature of immobilized L-ASNase was at 60ºC while that of free enzyme was at 50ºC. Even though the reaction temperature rose to 70ºC, their relative activities of immobilized enzyme was still about 60% while that of free L-ASNase completely lose. The immobilization of L-ASNase on these microparticles widened the optimum reaction temperature range of the enzyme. Moreover, Jia et al.[190] studied the thermostability of L-ASNase from *Bacillus subtilis* B11-06 by incubating at different temperatures for a certain time in pH 7.5. They reported that the enzyme showed maximum activity at 40ºC and retained about 14.7% of its residual activity after 2 h incubation in 50 °C and showed about 9.0% retention of activity after 2 h incubation in 60°C. The results of this work were similar to the found in Zhang et al.[189] study, in which the stability of free and immobilized L-ASNase showed maximum retained enzyme activity at 60°C. However, in this work, the activity of the free enzyme was not lost with the increase in temperature, remaining at levels similar to those obtained for the immobilized enzyme, which did not experience a significant loss of activity when the temperature was increased by 20ºC.

3.5 L-ASNase overactivity

From the results of L-ASNase activity obtained previously for the optimized conditions of immobilization onto the SILs, the enzyme overactivity in each material compared to activated silica (control) was studied (**Figure 21**).

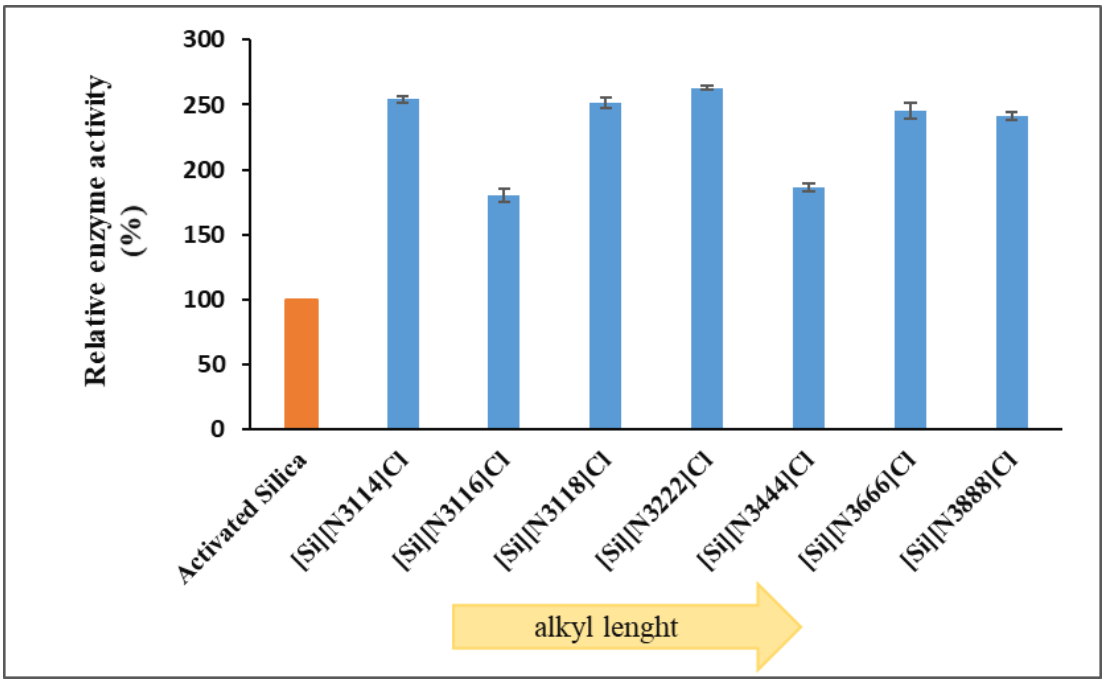

Figure 21: L-ASNase activity (%) obtained in each SILs. Activated silica was considered as control.

The results shown above demonstrate that in all SILs, L-ASNase has high levels of overactivity compared to the enzyme activity in the activated silica. For example, the best SIL according to the enzyme adsorption tests, **[Si][N$_{3222}$]Cl**, promote an L-ASNase overactivity with an increase up to 263% in relation to activated silica. All the other SILs presented enzyme activity values above 180%. As previously explained, and described in the literature, ILs often lead to improved process performance.[191]

Then, in order to verify the influence of the degree of functionalization of SILs in the activity of L-ASNase, tests were performed with [Si][N$_{3222}$]Cl. For this material, different degrees of functionalization were studied, through the synthesis of five materials with different number of moles of triethylamine: 0.007, 0.014, 0.036, 0.053 and 0.071 mol. In **Figure 22** is represented the relative enzyme activity as a function of the amount of the cation source (mol).

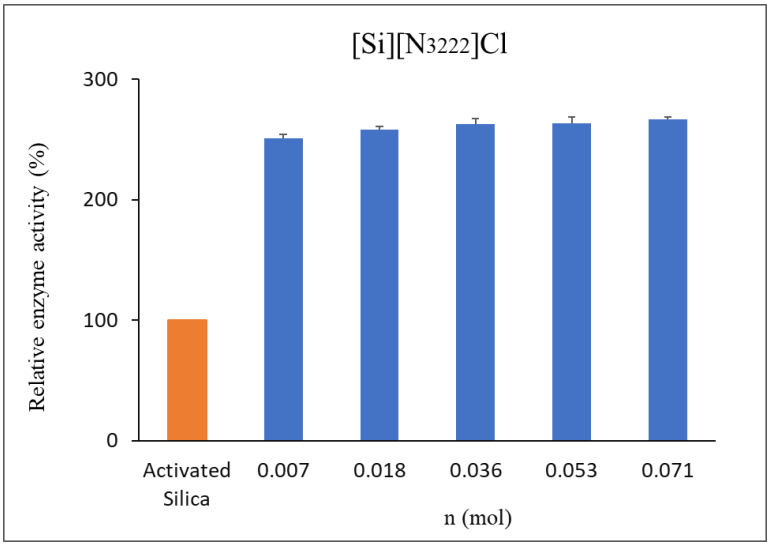

Figure 22: Relative enzyme activity (%) for [Si][N_{3222}]Cl with different degrees of functionalization.

Analysing **Figure 22**, it is understood that, although the increase in the degree of functionalization of [Si][N_{3222}]Cl, the reported values of L-ASNase overactivity remains almost constant. This may indicate that despite the increase in the amount of amine, the enzyme activity does not undergo significant changes.

In addition to the study of L-ASNase overactivity in [Si][N_{3222}]Cl under the previous conditions, the variation in IY and immobilized enzyme activity at different levels of triethylamine amount was also tested. The results are expressed in **Figure 23**.

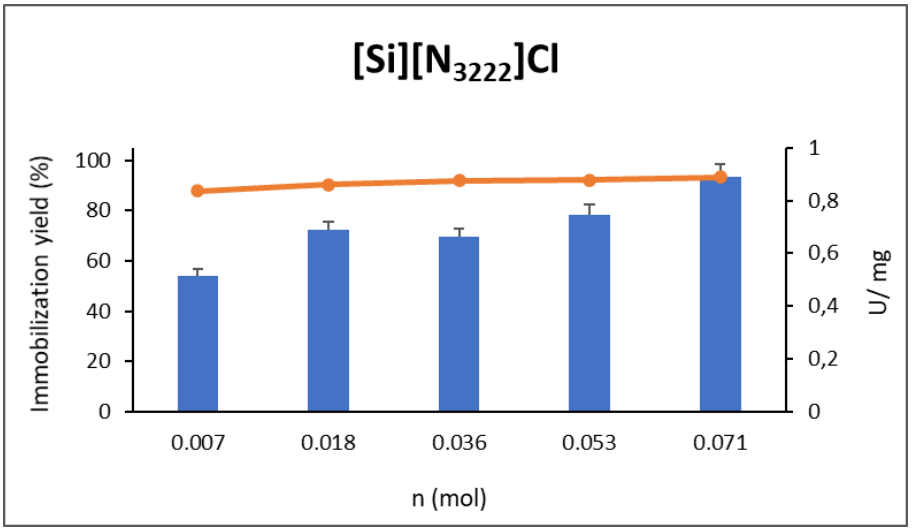

Figure 23: Immobilization yield (columns) and immobilized L-ASNase activity (symbols, line) at different amounts (n) of [Si][N_{3222}]Cl.

The results expressed in **Figure 23** are in agreement with those obtained previously, since the values of enzymatic activity do not vary significantly between each [Si][N_{3222}]Cl, and the lowest immobilization yield was found in the material with 0.007 mol of triethylamine.

3.6 Immobilized L-ASNase reuse

For the following assays on the commercial L-ASNase reuse, activated silica, free enzyme and the best and the worst SIL according to the enzyme adsorption test, **[Si][N_{3222}]Cl** and **[Si][N_{3116}]**, respectively, were used.

Regarding the recyclability of L-ASNase on these SILs and activated silica, the immobilized enzyme activity was determined in order to assess the ability of enzyme to remain active when immobilized on these materials. **Figure 24** represents the immobilized enzyme (%) in each cycle performed.

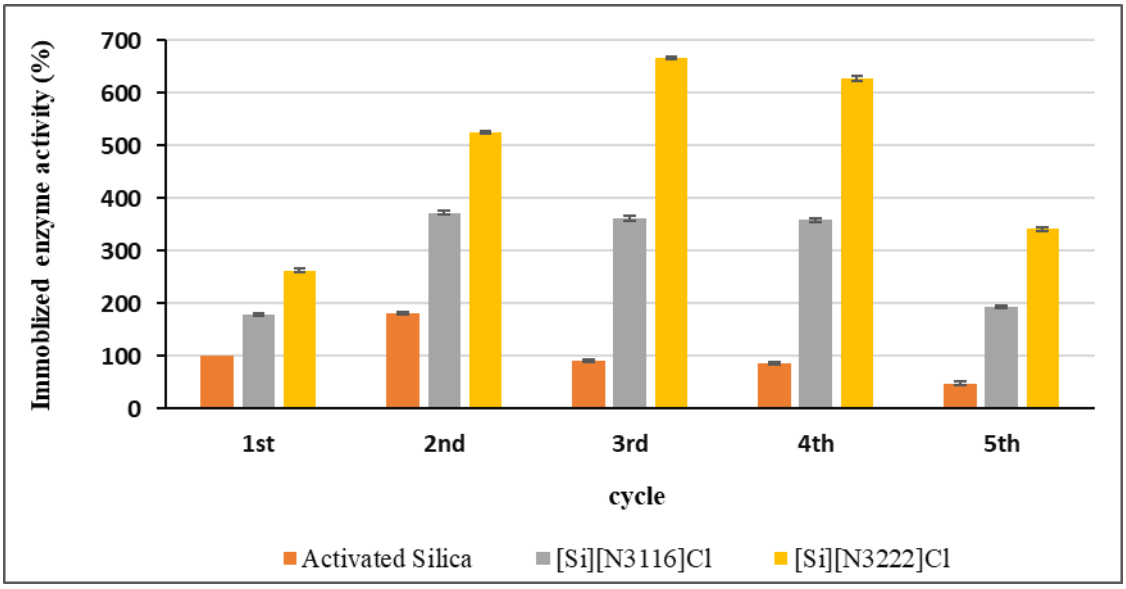

Figure 24: Relative immobilized enzyme activity (%) as function of the number of cycles performed by both SILs (**[**Si][N_{3222}]Cl and [Si][N_{3116}]Cl). Activated silica was considered as control.

The analysis of **Figure 24** demonstrates that the activity of immobilized commercial L-ASNase on [Si][N_{3222}]Cl and [Si][N_{3116}]Cl increased significantly after five consecutive uses, retaining above 600% and 300% of the initial activity compared to activated silica, respectively, up to four cycles. In contrast, the activity of immobilized L-ASNase on activated silica increased slightly after two cycles, but with increasing cycles there was a decrease in activity to about half of the initial after five uses. The increase in activity after three cycles of use of L-ASNase may be due to the fact that the immobilization procedure results in protein structures that are more rigid and have different specific chemical, biocatalytic, mechanical, and kinetic properties from the respective features of the native enzyme. This condition can lead to the improvement of a variety of enzyme features, such as activity.

The reusability of immobilized commercial L-ASNase in this work was compared with the results of another studies. For instance, Ulu et al.[192] described an immobilized L-ASNase on Ca-ALG/MWCNT that, after 5 cycles, retained only 58.7% of the initial activity. Ahmad et al.[193] reported an immobilized L-ASNase from *Bacillus licheniformis* which was immobilized by activated glutaraldehyde-carbon support, that retained its initial activity by 84.79% after 2 times repeated use. In both studies there was no high recyclability of L-ASNase as in this work.

Thus, it is concluded that once immobilized on SILs, L-ASNase presents a very high reusability, increasing its activity at high levels even with is reuse. In this case, the L-ASNase immobilization on the SILs improved the catalytic performance of L-ASNase. This effect suggest that the enzyme immobilized on SILs has some processing advantages over the free enzyme for significant industrial application. The successive loss of enzyme activity after 3 cycles of L-ASNase use might be mainly due to washing and centrifugation processes during repeating use.

3.7 Isotherms studies

The adsorption isotherms are fundamental to characterize the interactions between surfaces and proteins. In order to better understand how L-ASNase interacts with the SILs surface leading to the enzyme adsorption, the Langmuir and Freundlich adsorption isotherms were determined, whose results are shown in **Figure 25**. The adsorption isotherm parameters were obtained by non-linear fitting of Langmuir and Freundlich models to the experimental data, given by equations (5) and (6), respectively.

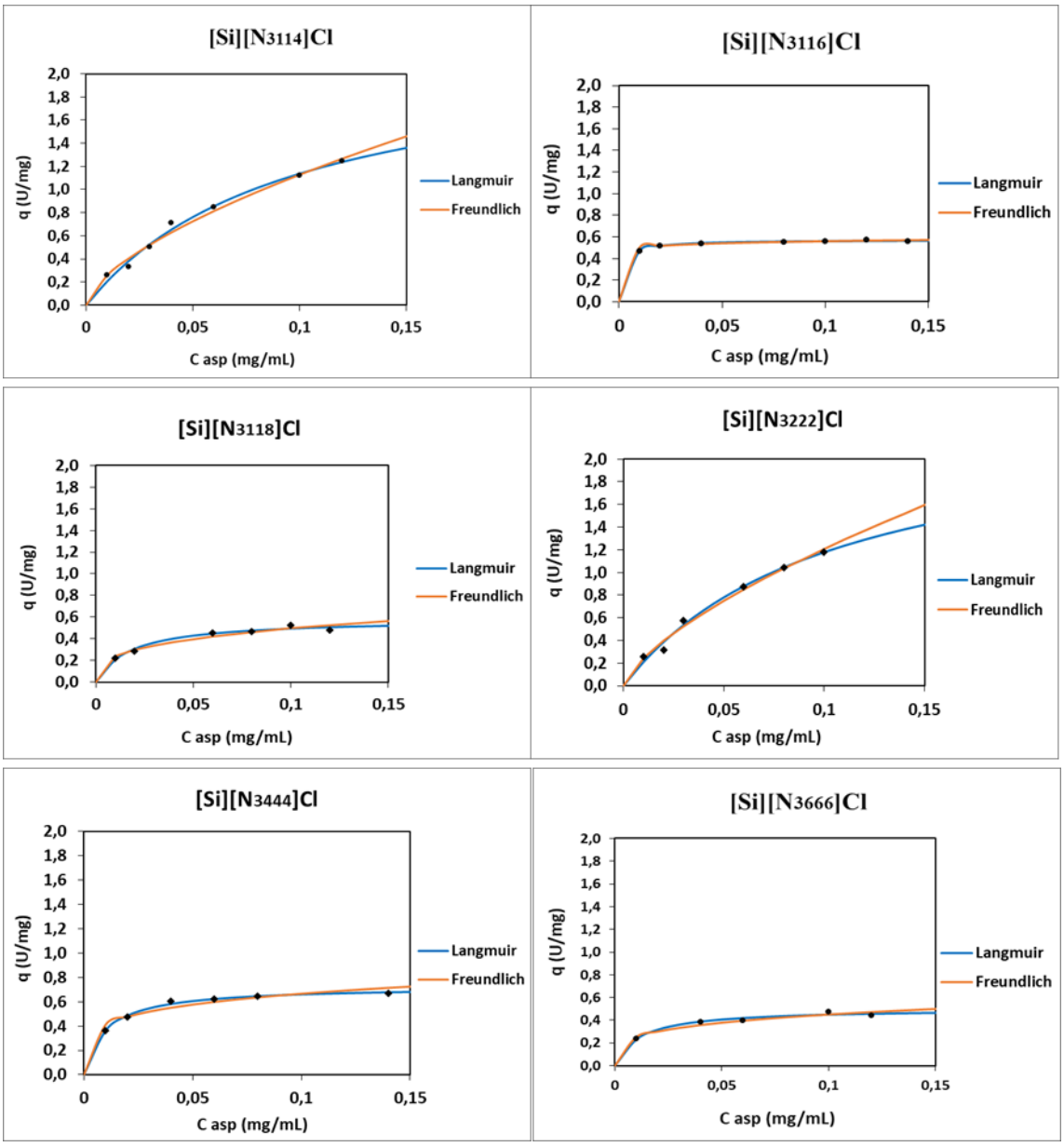

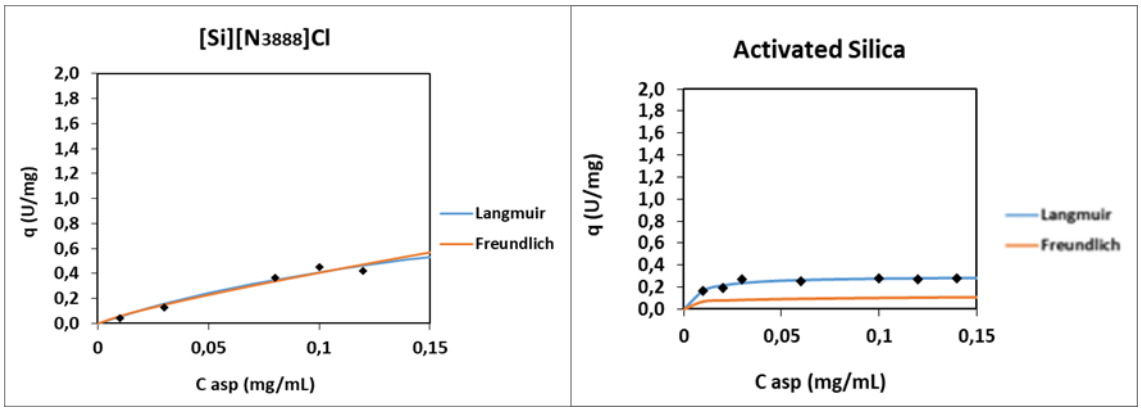

Figure 25: Langmuir (blue line) and Freundlich (orange line) isotherm models for the adsorption of L-ASNase onto SILs. Lines correspond to the fitting (nonlinear regression) of the experimental data (symbols). Experimental conditions: 10 mg of SIL, pH 8.0 and 60 min of contact time.

The respective detailed data corresponding to the experimental data fitting for all prepared SILs are given in **Table 14**.

Table 14: Langmuir and Freundlich parameters and their correlation coefficients for L-ASNase adsorption onto SILs.

SIL	Langmuir model			Freundlich model		
	q_{max} (U mg^{-1})	K (mL mg^{-1})	R^2	K_F	n	R^2
[Si][N_{3114}]Cl	2.232	10.38	0.9946	4.88	0.636	0.9920
[Si][N_{3116}]Cl	0.571	458.97	0.9997	0.65	0.063	0.9607
[Si][N_{3118}]Cl	0.578	56.32	0.9849	1.03	0.320	0.9711
[Si][N_{3222}]Cl	2.406	9.60	0.9943	5.88	0.688	0.9928
[Si][N_{3444}]Cl	0.725	100.69	0.9950	1.07	0.208	0.9437
[Si][N_{3666}]Cl	0.497	85.88	0.9819	0.81	0.252	0.9681
[Si][N_{3888}]Cl	1.348	4.37	0.9828	2.74	0.828	0.9774

Considering the correlation coefficient (R^2) obtained, the Langmuir model better describes the experimental equilibrium data, since $R^2_{Langmuir} > R^2_{Freundlich}$ for all SILs. The better correlation with Langmuir isotherm suggests a monolayer L-ASNase adsorption on the support surface, which indicates a homogeneous distribution of adsorption sites on the support surface. The Freundlich isotherm is characterized by an exponential distribution of heterogeneous active sites leading to a multilayer adsorption.[194] The lowest correlation coefficient observed in the Freundlich isotherm fitting shows that the formation of L-ASNase multilayers on the SILs probably does not occur.

According to the Langmuir isotherm, the SILs maximum adsorption capacity (q_{max}) for L-ASNase is 2.41 U mg^{-1} for **[Si][N_{3222}]Cl**, and the adsorption equilibrium constant (K), which defines the interactions strength between the enzyme and the surface of [Si][N_{3222}]Cl is 9.60 mL mg^{-1}.

3.8 Immobilization of L-ASNase from a cell extract preparation of *Bacillus subtilis*

The immobilization method was carried out using the L-ASNase from the cell extract of *Bacillus subtilis* produced as described previously (by another work of the research group). A cellular lysis was performed after the fermentation. The procedure was monitored before and after the L-ASNase extract adsorption onto **[Si][N_{3222}]Cl** by determining the total protein (A_{280}) and specific activity. Besides that, the purity of the commercial enzyme and the immobilized enzyme extract was checked by SDS-PAGE and HPLC. The conditions used, namely the L-ASNase concentration, pH and the contact time, were those optimized in the tests with the commercial enzyme. Before and after the immobilization, the following parameters were measured:

- total protein, in mg mL^{-1};
- total activity, in U mg^{-1};
- specific activity, in U mg^{-1}.

The protein concentration and enzyme activity were calculated by the methods described previously. For total protein, the absorbance of the samples was measured at 280 nm, and the protein concentration determined using the BSA calibration curve (**Figure 28** in Annex). The specific enzyme activity (U mg^{-1}), an important measure of enzyme purity, was calculated from these two parameters by equation (7).

The total protein, enzyme activity and specific activity of the L-ASNase from cell extract before and after the adsorption on [Si][N_{3222}]Cl are described in **Table 15**.

Table 15: Specific activity values obtained for the L-ASNase extract from *Bacillus subtilis* before and after adsorption of the enzyme on [Si][N_{3222}]Cl.

Sample	Total protein (mg mL^{-1})	Activity (U mL^{-1})	Specific activity (U mg^{-1})
L-ASNase extract (before adsorption)	79.20	90.84	1.15
Extracted L-ASNase (after adsorption)	30.97	47.38	1.53

Besides this, from **Table 15** it is possible to observe an increase in the specific activity of the enzyme and a decrease in the total protein content, which indicates that the support, [Si][N_{3222}]Cl, adsorbed the other proteins more, and it was possible to increase the purity after the immobilization of L-ASNase. Despite displaying less activity because part of the enzyme was adsorbed on the support, the purity of the supernatant raised significantly. Specifically, after the adsorption step, the specific activity of L-ASNase was increased from 1.15 to 1.53 U mg^{-1}, an enhance of about 33% of the specific activity in relation to the crude extract. Moorthy et al.[50] produced a L-ASNase from *Bacillus subtilis* DKMBT 10, and reported a specific activity of 0.10 U mg^{-1} for the crude extract. However, after the purification steps, which included ammonium sulphate and dialysis and ion exchange chromatography, obtained a specific activity of 1.12 U mg^{-1}. In another study, Chityala et al. related an increase of almost 280% in specific activity of a L-ASNase from *B. subtilis*

WB800N after the purification step by immobilized metal ion affinity chromatography (IMAC).[195] Furthermore, Jia et al. described a rise of around 290% in specific activity of a L-ASNase from *B. subtilis* B11-06 purified by a two-step procedure including ammonium sulfate fractionation and hydrophobic interaction chromatography.[196]

Thus, in this work it was achievable to improve the purity of the supernatant, increasing the specific activity by more than 30% compared to the initial extract with the adsorption of L-ASNase on [Si][N_{3222}]Cl, fulfilling the objective of this work. Comparing the results in literature with the ones from the present work, it is concluded that although in this work the method applied only includes the physical adsorption of L-ASNase onto the material, unlike the chromatographic techniques of other studies, the values of L-ASNase activity and total protein in the final supernatant were very promising, revealing the potential of using these materials in enzyme purification processes, such as the purification of L-ASNase.

The molecular weight of the extracted enzyme and impure proteins was determined by performing SDS-PAGE according to the method of Laemmli[197], through the protocol previously described. This technique has been widely used during protein purification and separation procedures for their quantification. Its main advantages are that it does not destroy the sample and is a quick method.[198] After the electrophoresis, protein bands were visualized by staining with Coomassie brilliant blue. The protein profile of L-ASNase samples is depicted in the SDS-PAGE represented in the **Figure 26**.

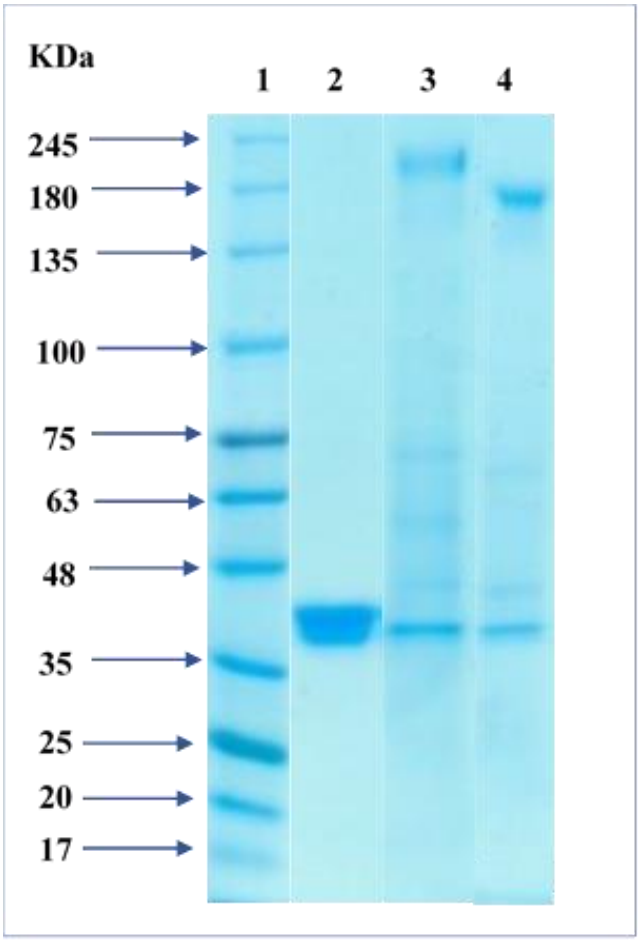

Figure 26: SDS-PAGE of the enzyme samples stained with Coomassie brilliant blue. Line 1: protein marker; Line 2: commercial L-ASNase from *E. coli*; Line 3: L-ASNase extract; Line 4: supernatant of L-ASNase extract after immobilization.

The molecular weight of the L-ASNase was estimated in comparison with standard molecular weight marker, with known molecular weight ranged from 10 to 250 kDa (**Figure 26**).

Based on the literature, it is known that the molecular native EC2 possess a molecular weight of 138-141 kDa and exist as a tetramer, consisting of four identical subunits each of 35.6 kDa.[26,199] The protein profile of commercial L-ASNase revealed only a single distinctive protein band of the L-ASNase subunit, with an apparent molecular weight of around 40 kDa, with the absence of contaminant proteins. Thus, it can be concluded that this band corresponds to the L-ASNase produced by *E. coli* and, as expected, this preparation

has a high purity. This result goes according the reported from Santos et al.[37], in which a clear band of the L-ASNase subunit was obtained (≈ 35 kDa) for the purification of periplasmatic L-ASNase from *E. coli* (EC2) by ATPS with 5 wt% [C_4mim][CH_3SO_3] as adjuvant without pre-purification.

Regarding the L-ASNase extract, is noted the presence of L-ASNase with a less intense band compared to that found in the commercial L-ASNase from *E. coli*. Besides that, the existence of other bands on the extract prove the presence of other proteins in this preparation. In contrast, the protein profile of supernatant of L-ASNase extract after immobilization demonstrated the presence of a thin band of L-ASNase, but the existence of other protein bands, in few quantities and less intense compared to the bands in the L-ASNase extract, conform to the specific activity values obtained.

Finally, the purity of the L-ASNase samples were checked by the SE-HPLC from **Figure 27**.

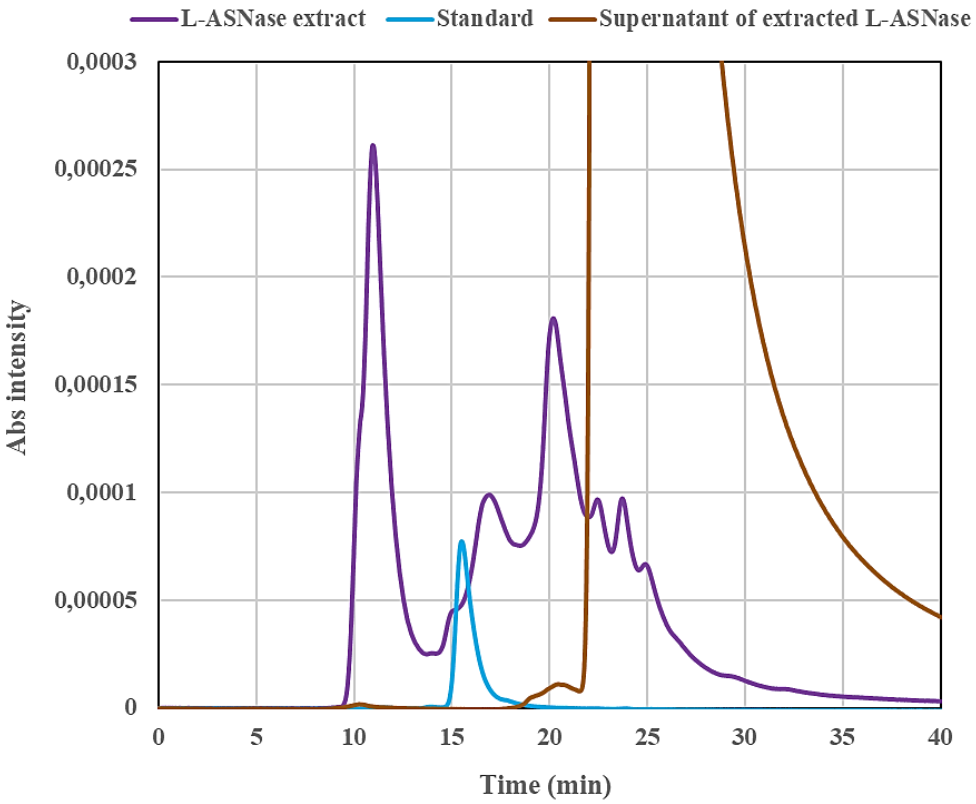

Figure 27: HPLC chromatogram of the samples of L-ASNase.

From the chromatogram above, it is possible to observe that standard L-ASNase (blue line) chromatogram revealed a single peak at a retention time of 15 min confirming that it was a pure preparation. This result agrees with that found in the SDS-PAGE. On the other hand, in the L-ASNase extract chromatogram (purple line) the second peak at a retention time of around 17 min corresponds to L-ASNase while all the other peaks are related to the presence of other proteins, such as the SDS-PAGE demonstrates by the presence of other bands in the protein profile of this preparation. Lastly, the supernatant of extracted L-ASNase chromatogram showed a very small peak at a retention time at 10 min and another peak at 20 min. The first peak corresponds to L-ASNase, which is visible in the SDS-PAGE as a thin band of this preparation. The last peak, the biggest peak, may be IL, which will have dispersed from the support and released into the supernatant. This hypothesis is explained by the profile and intensity of this peak, which is highly intense and has a retention time of more than 20 min. However, due to the experience in separation techniques of the research group in which this work is inserted, it was suggested that the analysis of L-ASNase samples by HPLC be repeated, in order to obtain a new chromatogram.

It is concluded from all these results that not all L-ASNase is immobilized on SIL, which is confirmed by the detection of the enzyme in the SDS-PAGE of the supernatant of enzyme extract after immobilization and by the analysis of the activity of L-ASNase after the adsorption. However, there is no agreement between some of the results obtained in the chromatogram and in the SDS-PAGE.

4. Conclusion and future work

To the best of knowledge, no scientific articles were found reporting the immobilization of L-ASNase using SILs materials. Considering all the noticed and discussed results from the characterization of SILs, it can conclude that the functionalization of silica with ILs proved to be successful and they pose as versatile and promising materials for adsorption of L-ASNase from aqueous solutions, but the extend of functionalization is low, so SILs with higher bonding amount should be synthesized to further improve their performance.

Firstly, the effects of L-ASNase concentration, pH and contact time of the enzyme with the substrate on the immobilization of commercial L-ASNase onto SILs were optimized. The parameter that revealed the most substantial influence on the immobilization effectiveness was the L-ASNase concentration. The highest IY and immobilized enzyme activity occurred with a concentration of ASNase of **6.0×10^{-1} mg mL^{-1}**, corresponding to the optimal concentration to perform the L-ASNase immobilization tests. The pH did not show a considerable effect on the IY within the range 5.0–8.0, with only a slight decrease with increasing pH. Though, the enzyme reaches the highest immobilized activity at pH **8.0**. The contact time between the L-ASNase and the SILs through the immobilization procedure influences the results, where short immobilization times may not allow the total enzyme adsorption. An IY above 80% was achieved after 120 min of contact, the longest time tested, for all SILs. However, it was for a time of **60 min** that the greatest activity of immobilized enzyme was obtained. It is concluded that the immobilization of commercial L-ASNase onto SILs was successfully achieved by adsorption. The best results with regard to the immobilized L-ASNase activity and IY were achieved with for a concentration of L-ASNase of 0.06 mg mL^{-1} at pH 8 during 60 min of contact time. Thus, these conditions were selected for all the experimental protocols.

Secondly, the adsorption capacity of the enzyme by the materials was evaluated, using the optimized conditions in the immobilization of L-ASNase. The isotherm model that best fitted the results was the Langmuir model with the best experimental q_{max}, 2.41 U mg^{-1} for **[Si][N_{3222}]Cl**. This SIL had the best adsorption capacity according to the tests performed, and and was used for the immobilization of L-ASNase from the cell extract. The determined adsorption isotherms allowed to conclude that there is monolayer adsorption of the L-ASNase on the SILs. Moreover, for all the SILs tested it was possible to observe an enzyme

overactivity with an increase in the enzyme recovery activity up to 263% in [Si][N_{3222}]Cl, and a high recyclability.

Regarding the extraction and purification of L-ASNase from the cell extract, after its adsorption onto [Si][N_{3222}]Cl a specific activity of 1.53 U mg^{-1} was reached in the supernatant, demonstrating an increase in the purity of the extract after the immobilization step. These results were corroborated by the SDS-PAGE analysis performed on the extract after the adsorption, which revealed the presence of a thin band of L-ASNase, but the existence of other protein bands, in few quantities and less intense compared to the bands in the non-immobilized extract.

For future work SILs with higher bonding amount should be synthesized and more adsorption experiments also be tested. After the adsorption step, the analysis of the supernatant in order to verify the presence of IL in the solution may be important. In addition, methods of desorption of L-ASNase like, for example, the used of EDTA, Ca (II) or pH/temperature changes may be performed. This step will allow the target biopharmaceutical recovery and the material reuse.

5. References

1. Brumano, L. P. & Vitor, F. Development of L-Asparaginase Biobetters : Current Research Status and Review of the Desirable Quality Profiles. *Front. Bioeng. Biotechnol*. **6**, 1–22 (2019).
2. Shakambari, G., Ashokkumar, B. & Varalakshmi, P. L-asparaginase - a promising biocatalyst for industrial and clinical applications. *Biocatal. Agric. Biotechnol.* **17**, 213-224 (2018).
3. Cachumba, M., Antunes, F., Peres, G., Brumano, L.P. & Santos, J.C. Santos. Current applications and different approaches for microbial l -asparaginase production. *Brazilian J. Microbiol.* 1–9 (2016).
4. Ulu, A., & Ates, B. Immobilization of l-Asparaginase on Carrier Materials: A Comprehensive Review. *Bioconjugate Chem.* **28**, 1598–1610 (2017).
5. Lang, S. Uber desamidierungim Tierkorper. *Beitrchem Physiol. Pathol* **5**, 321–345 (1904).
6. Kidd, J. G. Regression of transplanted lymphomas induced in vivo by means of normal guinea pig serum. I. Course of transplanted cancers of various kinds in mice and rats given guinea pig serum, horse serum, or rabbit serum. *J. Exp. Med.* **98**, 565–582 (1953).
7. Neuman, R. E. & Mccoy, T. A. Dual requirement of Walker carcinosarcoma 256 in vitro for asparagine and glutamine. *Science* **124**, 124–125 (1956).
8. Broome, J. D. Evidence that the L-asparaginase of guinea pig serum is responsible for its antilymphoma effects. I. Properties of the L-asparaginase of guinea pig serum in relation to those of the antilymphoma substance. *J. Exp. Med.* **118**, 99–120 (1963).
9. DeVita, V. T. J. & Chu, E. A history of cancer chemotherapy. *Cancer Res.* **68**, 8643–8653 (2008).
10. WHO | Model Lists of Essential Medicines (19th List). WHO at <https://www.who.int/medicines/publications/essentialmedicines/en/> [accessed: dec-2019].
11. Izadpanah, F., Homaei, A., Fernandes, P. & Javadpour, S. Marine microbial L-asparaginase: Biochemistry, molecular approaches and applications in tumor therapy and in food industry. *Microbiol. Res.* **208**, 99–112 (2018).
12. Del Casale, T., Sollitti, P. & Chesney, R. H. Cytoplasmic L-asparaginase: isolation of a defective strain and mapping of ansA. *J. Bacteriol.* **154**, 513–515 (1983).

13. Dijl, J. M. Van; Hecker, M. Bacillus Subtilis: From Soil Bacterium to Super-Secreting Cell Factory. *Microb. Cell Fact.* 1–6 (2013).
14. Borek, D.; Jaskólski, M. Sequence Analysis of Enzymes with Asparaginase Activity. *Acta Biochim. Pol.* **48**, 893–902 (2001).
15. Whitecar JP, Bodey GP, Harris JE, F. E. L-Asparaginase. *N Engl J Med.* **282**, 732–734 (1970).
16. Ebrahiminezhad, A.; Rasoul-Amini, S.; Ghasemi, Y. L-Asparaginase Production by Moderate Halophilic Bacteria Isolated from Maharloo Salt Lake. *Indian J. Microbiol.* **51**, 307–311 (2011).
17. Fisher, S. H.; Wray, L. V. Bacillus Subtilis 168 Contains Two Differentially Regulated Genes Encoding L-Asparaginase. *J. Bacteriol.* **184**, 2148–2154 (2002).
18. Yano, S.; Minato, R.; Thongsanit, J.; Tachiki, T.; Wakayama, M. Overexpression of Type I L-Asparaginase of Bacillus Subtilis in Escherichia Coli, Rapid Purification and Characterisation of Recombinant Type I L-Asparaginase. *Ann. Microbiol.* **58**, 711–716 (2008).
19. Verma, N., Kumar, K., Kaur, G. & Anand, S. L-Asparaginase: A Promising Chemotherapeutic Agent. *Crit. Rev. Biotechnol.* **27**, 45–62 (2007).
20. Ali, U. *et al.* L-asparaginase as a critical component to combat Acute Lymphoblastic Leukaemia (ALL): A novel approach to target ALL. *Eur. J. Pharmacol.* **771**, 199–210 (2016).
21. Batool, T., Makky, E. A., Jalal, M. & Yusoff, M. M. A Comprehensive Review on l-Asparaginase and Its Applications. *Appl. Biochem. Biotechnol.* **178**, 900–923 (2016).
22. Ramya, L. N., Doble, M., Rekha, V. P. B. & Pulicherla, K. K. L-asparaginase as potent anti-leukemic agent and its significance of having reduced glutaminase side activity for better treatment of acute lymphoblastic leukaemia. *Appl. Biochem. Biotechnol.* **167**, 2144–2159 (2012).
23. Kotzia, G. A. & Labrou, N. E. Engineering substrate specificity of E. carotovora l-asparaginase for the development of biosensor. *J. Mol. Catal. B Enzym.* **72**, 95–101 (2011).
24. Aghaiypour, K., Wlodawer, A. & Lubkowski, J. Structural basis for the activity and substrate specificity of Erwinia chrysanthemi L-asparaginase. *Biochemistry* **40**, 5655–5664 (2001).

25. Swain, A. L.; Jaskolski, M.; Housset, D.; Rao, J. K. M.; Wlodawer, A. Crystal Structure of Escherichia Coli L-Asparaginase, an Enzyme Used in Cancer Therapy. *Proc. Natl. Acad. Sci. U. S. A.* **90**, 1474–1478 (1993).
26. Kozak, M.; Jurga, S. A. Comparison between the Crystal and Solution Structures of Escherichia Coli Asparaginase II. *Acta biochimica Polonica.* **49**, 509-513 (2002).
27. Miller, H. K., Salser, J. S., Balis, M. E. Amino Acid Levels Following L-Asparagine Amidohydrolase (EC.3.5.1.1) Therapy. *Cancer Research*. **29**, 183–188 (1969).
28. Lopes, A. M. *et al.* Therapeutic l-asparaginase: upstream, downstream and beyond. *Crit. Rev. Biotechnol.* **37**, 82–99 (2017).
29. Deshpande, N., Choubey, P. & Agashe, M. Studies on optimization of growth parameters for L-asparaginase production by Streptomyces ginsengisoli. *ScientificWorldJournal.* **2014**, (2014).
30. Keating, M. J., Holmes, R., Lerner, S. & Ho, D. H. L-asparaginase and PEG asparaginase--past, present, and future. *Leuk. Lymphoma.* **10**, 153–157 (1993).
31. Belén, L. H. *et al.* A structural in silico analysis of the immunogenicity of L-asparaginase from Escherichia coli and Erwinia carotovora. *Biologicals.* **59**, 47–55 (2019).
32. Chen, S. H. Asparaginase Therapy in Pediatric Acute Lymphoblastic Leukemia: A Focus on the Mode of Drug Resistance. *Pediatr. Neonatol.* **56**, 287–293 (2015).
33. Zuo, S., Zhang, T., Jiang, B. & Mu, W. Recent research progress on microbial L-asparaginases. *Appl. Microbiol. Biotechnol.* **99**, 1069–1079 (2015).
34. Mishra, A. Production of l-asparaginase, an anticancer agent, from Aspergillus niger using agricultural waste in solid state fermentation. *Appl. Biochem. Biotechnol.* **135**, 33–42 (2006).
35. Pedreschi, F., Mariotti-Celis, M., Granby, K. & Risum, J. Acrylamide reduction in potato chips by using commercial asparaginase in combination with conventional blanching. *LWT - Food Sci. Technol.* **44**, 1473–1476 (2011).
36. Tundisi, L. L. *et al.* L-Asparaginase Purification. **2119**, (2016).
37. Santos, J. H. P. M. *et al.* In situ purification of periplasmatic L-asparaginase by aqueous two phase systems with ionic liquids (ILs) as adjuvants. *Journal of Chemical Technology & Biotechnology.* **93**, 1871-1880 (2017).
38. Vimal, A. & Kumar, A. Biotechnological production and practical application of L-

asparaginase enzyme. *Biotechnol. Genet. Eng. Rev.* **8725**, 1–22 (2017).

39. Wheelwright, S. M. The design of downstream processes for large-scale protein purification. *J. Biotechnol.* **11**, 89–102 (1989).
40. Wiriyawat, N. Strategies for Protein Purification. 1-165 (2010).
41. Zenatti, P. *et al.* Low Bioavailability and High Immunogenicity of a New Brand of E. coli L-Asparaginase with Active Host Contaminating Proteins. *EBioMedicine.* **30**, (2018).
42. Abd, H. H., Baky, E. & Baroty, G. S. El. Optimization of Growth Conditions for Purification and Production of L-Asparaginase by Spirulina maxima. *Evidence-Based Complementary and Alternative Medicine*. **2016**, (2016).
43. Zhu, J., Yan, X., Chen, H. & Wang, Z. In situ extraction of intracellular l -asparaginase using thermoseparating aqueous two-phase systems. *J. Chromatogr.* **1147**, 127–134 (2007).
44. Costa-Silva, T. A. *et al.* Critical overview of the main features and techniques used for the evaluation of the clinical applicability of L-asparaginase as a biopharmaceutical to treat blood cancer. *Blood Rev.* **43**, (2020).
45. Shakambari, G., Ashokkumar, B. & Varalakshmi, P. L-asparaginase – A promising biocatalyst for industrial and clinical applications. *Biocatal. Agric. Biotechnol.* **17**, 213–224 (2019).
46. Qin, M. & Zhao, F. L-asparaginase release from Escherichia coli cells with aqueous two-phase micellar systems. *Appl. Biochem. Biotechnol.* **110**, 11–21 (2003).
47. Mesas, J. M., Gil, J. A. & N, J. F. M. Characterization and partial purification of L-asparaginase from Corynebaeterium glutamicurn. *J Gen Microbiol.* **136**, 515-519 (1990).
48. El-Bessoumy, A. A., Sarhan, M. & Mansour, J. Production, isolation, and purification of L-asparaginase from Pseudomonas Aeruginosa 50071 using solid-state fermentation. *J. Biochem. Mol. Biol.* **37**, 387–393 (2004).
49. Kamble, V. P., Rao, R. S., Borkar, P. S., Khobragade, C. N. & Dawane, B. S. Purification of L-asparaginase from a bacteria Erwinia carotovora and effect of a dihydropyrimidine derivative on some of its kinetic parameters. *Indian J. Biochem. Biophys.* **43**, 391–394 (2006).
50. Vidhya Moorthy, Aishwarya Ramalingam, A. S. and R. T. S. Production, purification

and characterisation of extracellular L-asparaginase from a soil isolate of Bacillus sp. *African J. Microbiol. Res.* **4**, 1862–1867 (2010).

51. Amena S., Vishalakshi N., Prabhakar M., Dayanand A., L. K. Production, purification and characterization of l-asparaginase from Streptomyces gulbargensis. *Microbiol. Brazilian J.* **41**, 173–178 (2010).
52. Desai, S. S. & Hungund, B. S. Submerged fermentation, purification, and characterization of L-asparaginase from Streptomyces sp. isolated from soil. *J. Appl. Biol. Biotechnol.* **6**, 17–23 (2018).
53. Augusto Q. Pedro, J. A. P. C. and M. G. F. Immobilization of Ionic Liquids, Types of Materials, and Applications. *Springer Nat. Singapore Pte*. (2019).
54. Capizzi, R. L. Asparaginase revisited. *Leuk. Lymphoma.* **10**, 147–150 (1993).
55. Jacinto, M. J. *et al.* M13 bacteriophage purification using poly(ionic liquids) as alternative separation matrices. *J. Chromatogr.* **1532**, 246–250 (2018).
56. European Medicines Agency (2015). Assessment Report Spectrila. London: European Medicines Agency.
57. European Medicines Agency (2016). Assessment Report Oncaspar. London: European Medicines Agency.
58. Medicines Evaluation Board (2015). Public Assessmen Report Crisantaspase. London.
59. Shrivastava, A. *et al.* Recent Developments in L-asparaginase Discovery and Its Potential as Anticancer Agent. *Crit. Rev. Oncol. / Hematol.* (2015).
60. Völler, S., Pichlmeier, U., Zens, A. & Hempel, G. Pharmacokinetics of recombinant asparaginase in children with acute lymphoblastic leukemia. *Cancer Chemother. Pharmacol.* **81**, 305–314 (2018).
61. Islan, A., Martı, Y. N., Castro, G. R., Dura, N. & Bosio, V. E. Nanodevices for the immobilization of therapeutic enzymes. **8551**, 1–18 (2015).
62. Nguyen, H. H. & Kim, M. An Overview of Techniques in Enzyme Immobilization. *Appl. Sci. Converg. Technol.* **26**, 157–163 (2017).
63. Hettiarachchy, N. S., Feliz, D. J., Edwards, J. S. & Horax, R. *The use of immobilized enzymes to improve functionality*. *Proteins in Food Processing*. (2018).
64. Santos, J. C. S. dos, Barbosa, O., Ortiz, C., Berenguer-Murcia, A., Rodrigues, R. C., & Fernandez-Lafuente, R. Importance of the Support Properties for Immobilization

or Purification of Enzymes. *ChemCatChem.* **7**, 2413–2432 (2015).

65. Homaei, A. A., Sariri, R., Vianello, F., & Stevanato, R. Enzyme immobilization: an update. *J. Chem. Biol.* **6**, 185–205 (2013).
66. Singh, A., Negi, M. S., Dubey, A., Kumar, V., & Verma, A. K. Methods of Enzyme Immobilization and Its Applications in Food Industry. *Enzym. Food Technol.* 103–124 (2018).
67. Tran, D. N., & Balkus, K. J. Perspective of Recent Progress in Immobilization of Enzymes. *ACS Catal.* **1**, 956–968 (2011).
68. M J Poznansky, M Shandling, M A Salkie, J F Elliott, E. L. Advantages in the use of L-asparaginase-albumin polymer as an antitumor agent. *Cancer Res.* **42**, 1020–5 (1982).
69. Uren, J. R., Hargis, B. J., and Beardsley, P. Immunological and pharmacological characterization of poly-DLalanyl modified Erwinia carofoyora L-Asparaginase. *Cancer Res.* **42**, 4068−4071 (1982).
70. Wileman, T. E., Foster, R. L., and Elliott, P. N. C. Soluble asparaginase-dextran conjugates show increased circulatory persistence and lowered antigen reactivity. *J. Pharm. Pharmacol.* **38**, 264−271 (1986).
71. Qian, G., Zhou, J., Ma, J., Wang, D., and He, B. Immobilization of E-coli L-asparaginase on chitosan microsphere. *Chem. J.* **17**, 1147–1150 (1996).
72. Balcao, V. M., Mateo, C., Fernandez-Lafuente, R., Malcata, F. X. & and Guisan, J. M. Structural and functional stabilization of Lasparaginase via multi-subunit immobilization onto highly activated supports. *Biotechnol. Prog.* **17**, 537−542 (2001).
73. Vina, I., Karsakevich, A., and Bekers, M. Stabilization of anti-leukemic enzyme L-asparaginase by immobilization on polysaccharide levan. *J. Mol. Catal. B Enzym.* **11**, 551−558 (2001).
74. Amena, S., Lingappa, K., Vishalakshi, N., Prabhakar, M. & Dayanand, A. Immobilization and Characterization of L-Asparaginase from Streptomyces gulbargensis. *J. Pure Appl. Microbiol.* **4**, 623–628 (2010).
75. Wang, B., and Cao, Y. Purified silk fibroin-Lasparaginase bioconjugates show increased thermostability and resistance to trypsin digestion. *Eng. Life Sci.* **11**, 44−51 (2011).
76. Zhang, Y. Q., Zhou, W. L., Shen, W. D., Chen, Y. H., Zha, X. M. & Shirai, K., and

Kiguchi, K. Synthesis, characterization and immunogenicity of silk fibroin-L-asparaginase bioconjugates. *J. Biotechnol.* **120**, 315−326 (2005).

77. Ashrafi, H., Amini, M., Mohammadi-Samani, S., Ghasemi, Y., Azadi, A., Tabandeh, M. R., Kamali-Sarvestani, E., and D. & S. Nanostructure L-asparaginase-fatty acid bioconjugate: synthesis, preformulation study and biological assessment. *Int. J. Biol. Macromol.* **62**, 180−187 (2013).
78. Labrou, N. E., and Muharram, M. M. Biochemical characterization and immobilization of Erwinia carotovora Lasparaginase in a microplate for high-throughput biosensing of Lasparagine. *Enzym. Microb. Technol.* **92**, 86−93 (2016).
79. Soares, A. L., Guimaraes, G. M., Polakiewicz, B., de M. & Pitombo, R. N., and Abrahao-Neto, J. Effects of polyethylene glycol attachment on physicochemical and biological stability of E. coli L-asparaginase. *Int. J. Pharm.* **237**, 163−170 (2002).
80. Mori, T., Tosa, T., and Chibata, I. Preparation and properties of asparaginase entrapped in the lattice of polyacrylamide gel. *Cancer Res.* **34**, 3066−3068 (1974).
81. Almendral, M. J., Porras, M. J., Alonso, A., Baez, M. D., A. & Alonso, C. Spectrophotometric determination of L-asparagine by flow-injection analysis using L-asparaginase immobilized on an epoxy resin. *Anal. Chim.* **308**, 170−177 (1995).
82. Erdogan, A., Koytepe, S., Ates, B., Yilmaz, I., and Seckin, T. Preparation of the L-asparaginase-based biosensor with polyimide membrane electrode for monitoring L-asparagine levels in leukemia. *Int. J. Polym. Mater.* **63**, 909−917 (2014).
83. Teodor, E., Litescu, S. C., Lazar, V., and Somoghi, R. Hydrogel-magnetic nanoparticles with immobilized L-asparaginase for biomedical applications. *J. Mater. Sci. Mater. Med.* **20**, 1307−1314 (2009).
84. Ghosh, S., Chaganti, S. R., and Prakasham, R. S. Polyaniline nanofiber as a novel immobilization matrix for the antileukemia enzyme L-asparaginase. *J. Mol. Catal. B Enzym.* **74**, 132− 137 (2012).
85. Raquel O. Cristóvão, Mafalda R. Almeida, Maria A. Barros, João C. F. Nunes, Rui A. R. Boaventura, José M. Loureiro, Joaquim L. Faria, Márcia C. Neves, Mara G. Freire, Valéria C. Ebinuma-Santos, A. P. M. T. and C. G. S. Development and characterization of a novel L-asparaginase/MWNT nanobioconjugate. *RSC Adv.* **10**, 31205–31213 (2020).
86. C. Sundaramoorthu, R. Rajakumari, A. DharamsiI, K. V. Production and

immobilization of L-Asparaginase from marine source. *Int. J. Pharm. Pharm. Sci.* **4**, 229–232 (2012).

87. El-Sayed, S. T., Fyiad, A. A., and Gamal-Eldeen, A. M. Immobilization, properties and anti-tumor activity of l-asparaginase of vicia faba and phaseoulus vulgaris seeds. *Aust. J. Basic Appl.* **6**, 785−794 (2012).
88. Maysa E- Moharam, A. M. G.-E. and S. T. E. Production, Immobilization and Anti-tumor Activity of LAsparaginase of Bacillus sp R36. *J. Am. Sci.* **6**, 131–140 (2010).
89. Francois, J., and Fortier, G. Immobilization of Lasparaginase into a biocompatible poly(ethylene glycol)-albumin hydrogel 0.1. preparation and in vitro characterization. *Biotechnol. Appl. Biochem.* **23**, 221–226 (1996).
90. Francois, J., Durso, E. M., and Fortier, G. Immobilization of L-asparaginase into a biocompatible poly(ethylene glycol)-albumin hydrogel: evaluation of performance in vivo. *Biotechnol. Appl. Biochem.* **26**, 203−212 (1997).
91. Youssef, M. M., and Al-Omair, M. A. Cloning, purification, characterization and immobilization of L-asparaginase II from E. coli W3110. *Asian J. Biochem.* **3**, 337−350 (2008).
92. Jesionowski, T., Zdarta, J. & Krajewska, B. Enzyme immobilization by adsorption: A review. *Adsorption* **20**, 801–821 (2014).
93. Liu, H., Wu, X., Sun, J. & Chen, S. Stimulation of Laccase Biocatalysis in Ionic Liquids: A Review on Recent Progress. *Curr. Protein Pept. Sci.* **19**, (2017).
94. WHO | Cancer. WHO at <http://www.who.int/cancer/en/> [accessed: dec-2019].
95. Nowell, P. C. The clonal evolution of tumor cell populations. *Science.* **194**, 23–28 (1976).
96. Vogelstein, B. *et al.* Cancer genome landscapes. *Science* **339**, 1546–1558 (2013).
97. Omran, A. R. The epidemiologic transition: a theory of the epidemiology of population change. *Milbank Q.* **83**, 731–757 (2005).
98. CANCER | Cancer at <https://www.cancer.org/cancer/acute-lymphocytic-leukemia/about/what-is-all/> [accessed: dec-2019].
99. Terwilliger, T. & Abdul-Hay, M. Acute lymphoblastic leukemia: a comprehensive review and 2017 update. *Blood Cancer J.* **7**, 577–577 (2017).
100. Nguyen, H. A. *et al.* A Novel L -Asparaginase with low L -Glutaminase Coactivity Is Highly Efficacious against Both T- and B-cell Acute Lymphoblastic Leukemias In

Vivo. 1549–1561 (2018).

101. Bray, F. *et al.* Global cancer statistics 2018: GLOBOCAN estimates of incidence and mortality worldwide for 36 cancers in 185 countries. *CA. Cancer J. Clin.* **68**, 394–424 (2018).
102. Appel, I. M., van Kessel-Bakvis, C., Stigter, R. & Pieters, R. Influence of two different regimens of concomitant treatment with asparaginase and dexamethasone on hemostasis in childhood acute lymphoblastic leukemia. *Leukemia.* **21**, 2377–2380 (2007).
103. Berg, H. Asparaginase revisited. *Leuk Lymphoma.* **52**, 168–178 (2011).
104. Gerson, S. L., Caimi, P. F., William, B. M. & Creger, R. J. Pharmacology and Molecular Mechanisms of Antineoplastic Agents for Hematologic Malignancies. *Hematology: Basic Principles and Practice.* 849-912 (2018).
105. MSH | International Medical Products Price Guide. WHO at <http://mshpriceguide.org/en/single-drug-information/?DMFId=70&searchYear=2015> [accessed: jan-2020].
106. Knott, S. R. V *et al.* Asparagine bioavailability governs metastasis in a model of breast cancer. *Nature.* **554**, 378–381 (2018).
107. W C Dolowy, D Henson, J Cornet, H. S. Toxic and Antineoplastic Effects of L-asparaginase. Study of Mice With Lymphoma and Normal Monkeys and Report on a Child With Leukemia. *Cancer.* **19**, 1813–1819 (1966).
108. H E Wade, R Elsworth, D Herbert, J Keppie, K. S. A New L-asparaginase With Antitumour Activity? *Lancet.* **2**, 776–777 (1968).
109. Y Kamisaki, H Wada, T Yagura, A Matsushima, Y. I. Reduction in Immunogenicity and Clearance Rate of Escherichia Coli L-asparaginase by Modification With Monomethoxypolyethylene Glycol. *J Pharmacol Exp Ther.* **216**, 410–414 (1981).
110. Thandeeswaran, M. *et al.* Screening and production of anticarcinogenic enzyme from escherichia coli ctls20: l - asparaginase. *Int. J. Pharm. Pharm. Sci.* **8**, (2016).
111. Starkova, J., Hermanova, I., Hlozkova, K., Hararova, A. & Trka, J. Altered Metabolism of Leukemic Cells : New Therapeutic Opportunity. *International Review of Cell and Molecular Biology*. **336,** 93-147 (2018).
112. Lomelino, C. L., Andring, J. T., McKenna, R. & Kilberg, M. S. Asparagine synthetase: Function, structure, and role in disease. *J. Biol. Chem.* **292**, 19952–19958

(2017).

113. Narta, U. K., Kanwar, S. S. & Azmi, W. Pharmacological and clinical evaluation of L-asparaginase in the treatment of leukemia. *Crit. Rev. Oncol. Hematol.* **61**, 208–221 (2007).
114. Mitchell, L., Hoogendoorn, H., Giles, A. R., Vegh, P. & Andrew, M. Increased Endogenous Thrombin Generation in Children With Acute Lymphoblastic Leukemia: Risk of Thrombotic Complications in L'Asparaginase-Induced Antithrombin I11 Deficiency. *Blood.* **83**, 386–391 (1994).
115. Nowak-Göttl, U. *et al.* Enhanced thrombin generation, P-von willebrand factor, P-fibrin D-dimer and P-plasminogen activator inhibitor 1: Predictive for venous thrombosis in asparaginase-treated children. *Fibrinolysis.* **8**, 63–65 (1994).
116. Rizzari, C. *et al.* L-asparagine depletion and L-asparaginase activity in children with acute lymphoblastic leukemia receiving i.m. or i.v. Erwinia C. or E. coli L-asparaginase as first exposure. *Ann. Oncol. Off. J. Eur. Soc. Med. Oncol.* **11**, 189–193 (2000).
117. Mohan Kumar, N. S., Shimray, C. A., Indrani, D. & Manonmani, H. K. Reduction of Acrylamide Formation in Sweet Bread with l-Asparaginase Treatment. *Food Bioprocess Technol.* **7**, 741–748 (2014).
118. Javier, J.; Cachumba, M.; Antonio, F.; Antunes, F.; Fernando, G.; Peres, D.; Brumano, L. P.; César, J.; Santos, D.; Silvério, S. . et al. Current Applications and Different Approaches for Microbial l -Asparaginase Production. *Brazilian J. Microbiol.* **47**, 77–85 (2016).
119. Krishnapura, P. R., Belur, P. D. & Subramanya, S. A critical review on properties and applications of microbial l-asparaginases. *Critical Reviews in Microbiology.* **42**, 720–737 (2016).
120. Xu, F.; Elmore, J. S. The Use of Asparaginase to Reduce Acrylamide Levels in Cooked Food. *Food Chem.* **210**, 163–171 (2016).
121. Hedegaard, R. V; Frandsen, H.; Skibsted, L. H. Kinetics of Formation of Acrylamide and Schiff Base Intermediates from Asparagine and Glucose. *Food Chem.* **108**, 917–925 (2008).
122. Gökmen, V., & Palazoğlu, T. K. Acrylamide Formation in Foods during Thermal Processing with a Focus on Frying. *Food Bioprocess Technol.* **1**, 35–42. (2007).

123. Vinci, R., Mestdagh, F. & Meulenaer, B. Acrylamide formation in fried potato products – Present and future, a critical review on mitigation strategies. *Food Chem.* **133**, 1138–1154 (2012).
124. Ciesarov, Z; Marková, L. Improvement of Cereal Product Safety by Enzymatic Way of Acrylamide Mitigation. *Chech J. Food Sci.* **27**, 1–3 (2009).
125. Singh, H. R.; Jha, S. K. Microbial L-Asparaginase: Present and Future Prospective. *Int. J. Innov. Res. Sci. Eng. Technol.* **2**, 7031–7051 (2013).
126. Zubavichus, Y.; Fuchs, O.; Weinhardt, L.; Heske, C.; Umbach, E.; Denlinger, J. D.; Grunze, M. Soft X-Ray-Induced Decomposition of Amino Acids: An XPS, Mass Spectrometry, and NEXAFS Study. *Radiat. Res.* **161**, 346–358 (2004).
127. Tagami, S.; Matsuda, K. An Enzymatic Method for the Kinetic Measurement of L-Asparaginase Activity and L-Asparagine with an Ammonia Gas-Sensing Electrode. *Chem. Pharm. Bull.* **38**, 153–155 (1990).
128. Verma, N.; Kumar, K.; Kaur, G.; Anand, S. *E. Coli* K-12 Asparaginase-Based Asparagine Biosensor for Leukemia. *Artif Cells Blood Substit Immobil Biotechnol.* **35**, 449-456 (2007).
129. Verma, N.; Bansal, M.; Kumar, S. Whole Cell Based Miniaturized Fiber Optic Biosensor to Monitor L-Asparagine. *Adv Appl Sci Res.* **3**, 809–814 (2012).
130. Zhang, S., Zhang, J., Zhang, Y. & Deng, Y. Nano confined Ionic Liquids. *Chem. Rev.* **117**, 6755-6833 (2017)
131. Zhao, H. Enzymatic polymerization to polyesters in nonaqueous solvents. *Methods Enzymol.* **627**, 1–21 (2019).
132. Fehrmann, R., Haumann, M. & Riisager, A. Supported Ionic Liquids: Fundamentals and Applications, Introduction. 1–9 (2014).
133. Riisager, A., Fehrmann, R., Haumann, M. & Wasserscheid, P. Supported ionic liquids: versatile reaction and separation media. **40**, 91–102 (2006).
134. Vidal, L., Riekkola, M. & Canals, A. Ionic liquid-modified materials for solid-phase extraction and separation : A review. *Anal. Chim. Acta.* **715**, 19–41 (2012).
135. Skoda-földes, R. The Use of Supported Acidic Ionic Liquids in Organic Synthesis. *Molecules*. **19**, 8840–8884 (2014).
136. Seddon, K. R. Ionic Liquids for Clean Technology. *J. Chem. Technol. Biotechnol.* **68**, 351–356 (1997).

137. Erbeldinger, M., Mesiano, A. J. & Russell, A. J. Enzymatic Catalysis of Formation of Z -Aspartame in Ionic Liquid - An Alternative to Enzymatic Catalysis in Organic Solvents. **6**, 1129–1131 (2000).
138. Sheldon, R. Catalytic reactions in ionic liquids. *Chemical Communications.* 2399–2407 (2001).
139. Zhang, P., Wu, T. & Han, B. Preparation of Catalytic Materials Using Ionic Liquids as the Media and Functional Components. *Adv. Mater.* **26**, 6810–6827 (2014).
140. Scholten, J. D., Leal, B. C. & Dupont, J. Transition Metal Nanoparticle Catalysis in Ionic Liquids. *ACS Catal.* **2**, 184–200 (2012).
141. Han, X. & Armstrong, D. W. Ionic Liquids in Separations. *Acc. Chem. Res.* **40**, 1079–1086 (2007).
142. Zhang, X., Zhang, F., Luo, G., Yang, S. & Wang, D. Extraction and Separation of Phycocyanin from Spirulina using Aqueous Two-Phase Systems of Ionic Liquid and Salt. *J. Food Nutr. Res.* **3**, 15–19 (2019).
143. Sun, X., Luo, H. & Dai, S. Ionic Liquids-Based Extraction: A Promising Strategy for the Advanced Nuclear Fuel Cycle. *Chem. Rev.* **112**, 2100–2128 (2012).
144. Asefa, T. & Tao, Z. Biocompatibility of Mesoporous Silica Nanoparticles. (2012).
145. Zhou, H. *et al.* Immobilizing Penicillin G Acylase Using Silica-Supported Ionic Liquids: The Effects of Ionic Liquid Loadings. (2012).
146. Campisciano, V., Giacalone, F. & Gruttadauria, M. Supported Ionic Liquids : A Versatile and Useful Class of Materials. *The Chemical Record*. **17**, 1–22 (2017).
147. Meijboom, R., Haumann, M. & Thomas, E. M. Synthetic Methodologies for Supported Ionic Liquid Materials. 75–93 (2014).
148. Garc, E., Lozano, P. & Luis, S. V. Biocatalytic Processes Based on Supported Ionic Liquids. 351–367 (2014).
149. Giacalone, F. & Gruttadauria, M. Covalently Supported Ionic Liquid Phases : An Advanced Class of Recyclable Catalytic Systems. *ChemCatChem*. **8**, 664–684 (2016).
150. Zhang, H. *et al.* An ionic liquid-magnetic graphene composite for magnet dispersive solid-phase extraction of triazine herbicides in surface water followed by high performance liquid chromatography. *Analyst.* **143**, 175–181 (2017).
151. Almeida, H. F. D., Neves, M. C., Trindade, T., Marrucho, I. M. & Freire, G. Supported ionic liquids as efficient materials to remove non-steroidal anti-inflammatory drugs

from aqueous media (experimental part). *Chem. Eng. J.* (2019).

152. Kumar, A. *et al.* Unique structured SiO_2 microparticles with carbon nanotube-derived mesopores as an efficient support for enzyme immobilization Department of Biological Sciences and KI for the BioCentury , Korea Advanced Institute of. *Chem. Eng. J.* (2018).
153. Marwani, H. M. & Bakhsh, E. M. Selective adsorption of 4-chlorophenol based on silica-ionic liquid composite developed by sol – gel process. **326**, 794–802 (2017).
154. Wanigasekara, E. *et al.* Bonded ionic liquid polymeric material for solid-phase microextraction GC analysis. 511–524 (2010).
155. Fontanals, N., Borrull, F. & Marce, R. M. Ionic liquids in solid-phase extraction. **41**, 15–26 (2012).
156. Moniruzzaman, M., Kamiya, N. & Goto, M. Activation and stabilization of enzymes in ionic liquids. *Org. Biomol. Chem.* **8**, 2887–2899 (2010).
157. Xin, B., Jia, C. & Li, X. Supported Ionic Liquids: Efficient and Reusable Green Media in Organic Catalytic Chemistry. 616–628 (2016).
158. Vishal KUMAR, Upendra SHARMA, Praveen Kumar VERMA, Neeraj KUMAR, and B. S. Silica-Supported Boric Acid with Ionic Liquid : A Novel Recyclable Catalytic System for One-Pot Three-Component Mannich Reaction. **59**, (2011).
159. Singh, R. K., Tiwari, M. K., Singh, R., Haw, J.-R., & Lee, J.-K. Immobilization of l-arabinitol dehydrogenase on aldehyde-functionalized silicon oxide nanoparticles for L -xylulose production. *Appl. Microbiol. Biotechnol.* **98**, 1095–1104 (2013).
160. Magri A, Soler MF, Lopes AM, et al. A critical analysis of L-asparaginase activity quantification methods—colorimetric methods versus high-performance liquid chromatography. *Anal Bioanal Chem.* **410**, 6985–6990 (2018).
161. Molins-Legua C, Meseguer-Lloret S, Moliner-Martinez Y, C.-F. P. A guide for selecting the most appropriate method for ammonium determination in water analysis. *TrAC - Trends Anal Chem.* **25**, 282–290 (2006).
162. Khushoo A, Pal Y, Singh BN, M. K. Extracellular expression and single step purification of recombinant Escherichia coli l-asparaginase II. *Protein Expr Purif.* **38**, 29–36 (2004).
163. Ruthven, D. M. Adsorption and Diffusion. *Springer Berlin Heidelb.* **7**, 1–43 (2008).
164. Ahmed, M. B., Zhou, J. L., Ngo, H. H. & Guo, W. Adsorptive removal of antibiotics

from water and wastewater: Progress and challenges. *Sci. Total Environ.* **532**, 112–126 (2015).

165. Ho, Y. S. & McKay, G. Pseudo-second order model for sorption processes. *Process Biochem.* **34**, 451–465 (1999).
166. Mckay, G. The Adsorption of basic dye onto silica from aqueous solution-solid diffusion model. *Chem. Eng. Sci.* **39**, 129–138 (1984).
167. Tong, Y., McNamara, P. J. & Mayer, B. K. Adsorption of organic micropollutants onto biochar: a review of relevant kinetics, mechanisms and equilibrium. *Environ. Sci. Water Res. Technol.* **5**, 821–838 (2019).
168. Foo, K. Y. & Hameed, B. H. Insights into the modeling of adsorption isotherm systems. *Chem. Eng. J.* **156**, 2–10 (2010).
169. Redlich, O. & Peterson, D. L. A Useful Adsorption Isotherm. *J. Phys. Chem.* **63**, 1024 (1959).
170. Jossens, L., Prausnitz, J. M., Fritz, W., Schlünder, E. U. & Myers, A. L. Thermodynamics of multi-solute adsorption from dilute aqueous solutions. *Chem. Eng. Sci.* **33**, 1097–1106 (1978).
171. Liu B., Cao S., Deng X., Li S., L. R. Adsorption behavior of protein onto siloxane microspheres. *Appl. Surf. Sci.* **252**, 7830–7836 (2006).
172. Lima, É. C., Adebayo, M. A. & Machado, F. M. Carbon Nanomaterials as Adsorbents for Environmental and Biological Applications. *Springer Int. Publ.* 33–69 (2015).
173. Langmuir, I. The adsorption of gases on plane surfaces of glass, mica and platinum. *J. Am. Chem. Soc.* **40**, 1361–1403 (1918).
174. Haghseresht, F. & Lu, G. Q. Adsorption Characteristics of Phenolic Compounds onto Coal-Reject-Derived Adsorbents. *Energy & Fuels.* **12**, 1100–1107 (1998).
175. Khodaie, M., Ghasemi, N., Moradi, B. & Rahimi, M. Removal of Methylene Blue from Wastewater by Adsorption onto $ZnCl_2$ Activated Corn Husk Carbon Equilibrium Studies. *J. Chem.* 1–6 (2013).
176. Andrade J. D., V. R. Protein adsorption at polymer surfaces. *Abstr. Pap. Am. Chem. Soc.* **185**, 189 (1983).
177. Simonian, M. H. & Smith, J. A. Quantitation of proteins. (2006).
178. Wang, Z., Zhu, Y., Chen, H., Wu, H. Ye, C. Fabrication of three functionalized silica adsorbents: Impact of co-immobilization of imidazole, phenyl and long-chain alkyl

groups on bisphenol A adsorption from high salt aqueous solutions. *Journal of the Taiwan Institute of Chemical*. **86**, 120–132 (2018).

179. Nie, L., Lu, J., Zhang, W., He, A. & Yao, S. Ionic liquid-modified silica gel as adsorbents for adsorption and separation of water-soluble phenolic acids from Salvia militiorrhiza Bunge. *Sep. Purif. Technol.* **155**, 2–12 (2015).
180. Jiang, Q., Zhao, W., Qiu, H. & Zhang, S. Silica-Based Phenyl and Octyl Bifunctional Imidazolium as a New Mixed-Mode Stationary Phase for Reversed-Phase and Anion-Exchange Chromatography. *Chromatographia.* **79**, 1437–1443 (2016).
181. Menéndez, J. A., Illán-Gómez, M. J., y León, C. A. L. & Radovic, L. R. On the difference between the isoelectric point and the point of zero charge of carbons. *Carbon N. Y.* **33**, 1655–1657 (1995).
182. Zhang, W., Feng, X., Alula, Y. & Yao, S. Bionic multi-tentacled ionic liquid-modified silica gel for adsorption and separation of polyphenols from green tea (Camellia sinensis) leaves. *Food Chem.* **230**, 637–648 (2017).
183. Kosmulski, M. pH-dependent surface charging and points of zero charge II. Update. *J. Colloid Interface Sci.* **275**, 214–224 (2004).
184. S. M. Kumar and K. Selvam. Isolation and purification of high efficiency L-asparaginase by quantitative preparative continuous-elution SDS PAGE electrophoresis. *J Microb. Biochem Technol.* **3**, 73–83 (2011).
185. A. Haroun, H. Ahmed, A.-T. Mossa, S. M. and E. A. Production, characterization and immobilization of Aspergillus versicolor L-asparaginase onto multi-walled carbon nanotubes. *Biointerface Res. Appl. Chem.* **10**, 5733–5740 (2020).
186. Ulu, A., Karaman, M., Yapıcı, F., Naz, M., Sayın, S., Saygılı, E. İ., & Ateş, B. The Carboxylated Multi-walled Carbon Nanotubes/l-Asparaginase Doped Calcium-Alginate Beads: Structural and Biocatalytic Characterization. *Catal. Letters.* (2019).
187. Kumar S, Dasu VV, P. K. Studies on pH and thermal stability of novel purified L-asparaginase from Pectobacterium carotovorum MTCC 1428. *Microbiology*. **80**, 355–362 (2011).
188. Stecher, A. L., de Deus, P. M., Polikarpov, I. & Abrahao-Neto, J. Stability of L-asparaginase: an enzyme used in leukemia treatment. *Pharm Acta Helv*. **74**, 1–9 (1999).

189. Yu-QingZhang, Mei-LinTao, Wei-DeShen, Yu-Zhen Zhou, Yue Ding, Yan Ma, W.-L. Z. Immobilization of l-asparaginase on the microparticles of the natural silk sericin protein and its characters. *Biomaterials.* **25**, 3751–3759 (2004).
190. Jia M, Xu M, He B, R. Z. Cloning, expression and characterization of L-asparaginase from a newly isolated *Bacillus subtilis* B11- 06. *J Agric Food Chem.* **61**, 9248–9434 (2013).
191. Park, S. & Kazlauskas, R. J. Biocatalysis in ionic liquids - Advantages beyond green technology. *Curr. Opin. Biotechnol.* **14**, 432–437 (2003).
192. A Ulu, M Karaman, F Yapıcı, M Naz, S Sayın, Eİ Saygılı, B. A. The Carboxylated Multi-walled Carbon Nanotubes/l-Asparaginase Doped Calcium-Alginate Beads: Structural and Biocatalytic Characterization. *Catal. Letters.* **150**, 1679–1691 (2020).
193. Ahmad, A., Patta, A. M., and Natsır, H. Purification and immobilization of L-Asparaginase enzyme from the thermophilic bacteria bacillus licheniformis Strain HSA3−1a. *Int. J. Pharm. Bio Sci.* **4**, 274−280 (2013).
194. F. Eba, S. Gueu, A. Eya'A-Mvongbote, J. A. Ondo, B. K. Yao, J. Ndong Nlo, R. K. B. Evaluation of the absorption capacity of the natural clay from Bikougou (Gabon) to remove Mn(II) from aqueous solution. *Int. J. Eng. Sci. Technol.* **2**, 5001–5016 (2010).
195. Chityala, S., Venkata Dasu, V., Ahmad, J. & Prakasham, R. S. High yield expression of novel glutaminase free l-asparaginase II of Pectobacterium carotovorum MTCC 1428 in Bacillus subtilis WB800N. *Bioprocess Biosyst. Eng.* **38**, 2271–2284 (2015).
196. Jia, M., Xu, M., He, B. & Rao, Z. Cloning, expression, and characterization of L-asparaginase from a newly isolated Bacillus subtilis B11-06. *J. Agric. Food Chem.* **61**, 9428–9434 (2013).
197. Laemmli, U. K. Cleavage of structural proteins during the assembly of the head of bacteriophage T4. *Nat.* **227**, 680–685 (1970).
198. Jeremy M Berg, John L Tymoczko, and L. S. Biochemistry. (2002).
199. M P Jennings and I R Beacham. Analysis of the Escherichia coli gene encoding L-asparaginase II, ansB, and its regulation by cyclic AMP receptor and FNR proteins. *J Bacteriol.* **172**, 1491–1498 (1990).

6. Annex

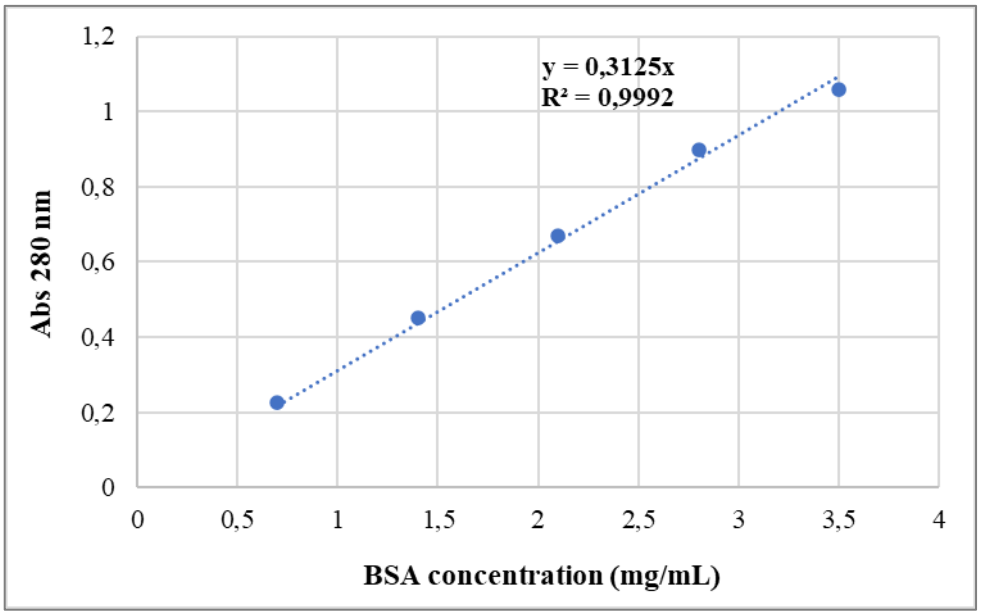

Figure 28: BSA calibration curve.